University of Groningen

Translational PKPD modeling in schizophrenia

Johnson, Martin

Translational PKPD Modeling in Schizophrenia

Predicting Human Receptor Occupancy

rijksuniversiteit
groningen

Translational PKPD Modeling in Schizophrenia
Predicting Human Receptor Occupancy

Proefschrift

ter verkrijging van het doctoraat in de
Wiskunde en Natuurwetenschappen
aan de Rijksuniversiteit Groningen
op gezag van de
Rector Magnificus, dr. E. Sterken,
in het openbaar te verdedigen op
vrijdag 15 juni 2012
om 11.00 uur

door

Martin Gnanamuthu Johnson
geboren op 4 oktober 1977
te Nagercoil, India

Faith is permitting ourselves to be seized by the things we do not see
– Martin Luther

Contents

Schizophrenia, D$_2$ Receptor Occupancy and Translational Modeling

General Introduction
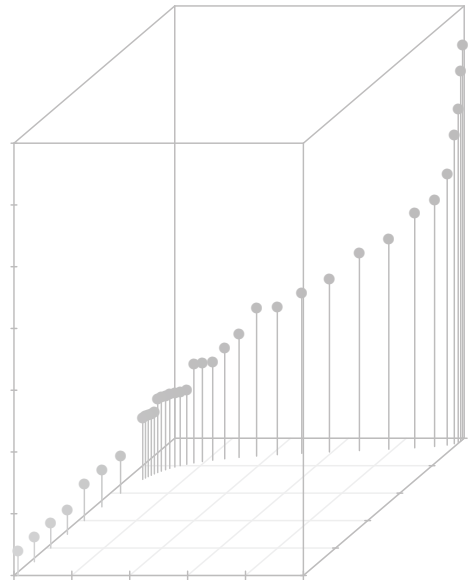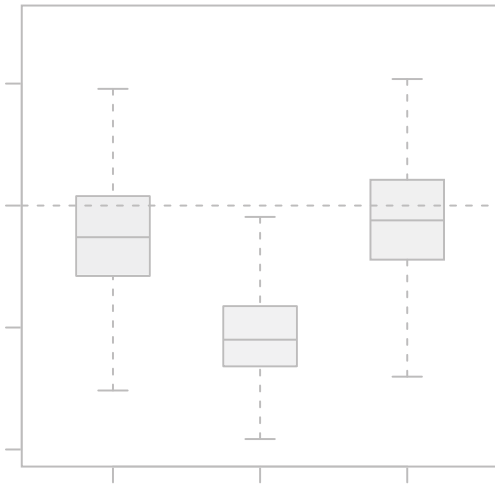
The aim of this thesis was to use pharmacokinetic and pharmacodynamic modeling tools to predict the target receptor occupancy of antipsychotic drugs for the treatment of schizophrenia. In this introduction, an overview about schizophrenia, translational modeling concepts and translational modeling in schizophrenia is presented.

Schizophrenia

Schizophrenia is a lifelong and often devastating psychiatric disorder of which the first symptoms often are recognized in late adolescence or early adulthood. The disease rarely occurs before adolescence or after the age of 40 years (1). The risk of developing schizophrenia is less than 1% in the general population. Schizophrenia is defined by characteristic but nonspecific disturbances in the form and content of thought, perception, cognition, emotion, sense of self, volition, social relationships, and psychomotor behavior (2). The etiology of schizophrenia remains unclear to date. Although the fundamental pathology of schizophrenia remains ambiguous, it has been hypothesized that an excessive level of striatal dopamine (3), which can be caused by several factors, is responsible for the development of psychotic symptoms. A developmental cascade leading to schizophrenia involves several factors action on early neuronal development stage to late adolescence (Figure 1.1) (4). Dopamine dysregulation appears to be the final step in this complex developmental cascade.
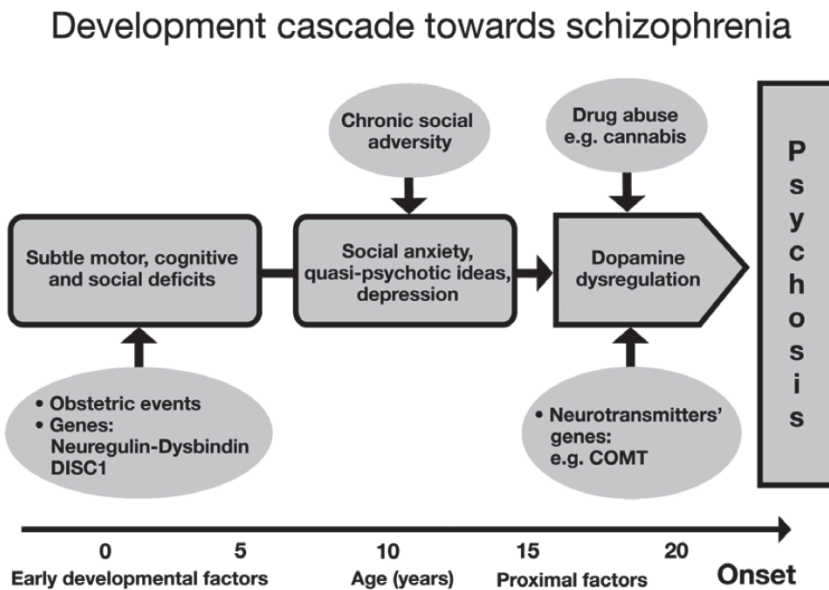
Figure 1.1: *Aetiological model of schizophrenia (Figure is reused with permission from reference 4).*
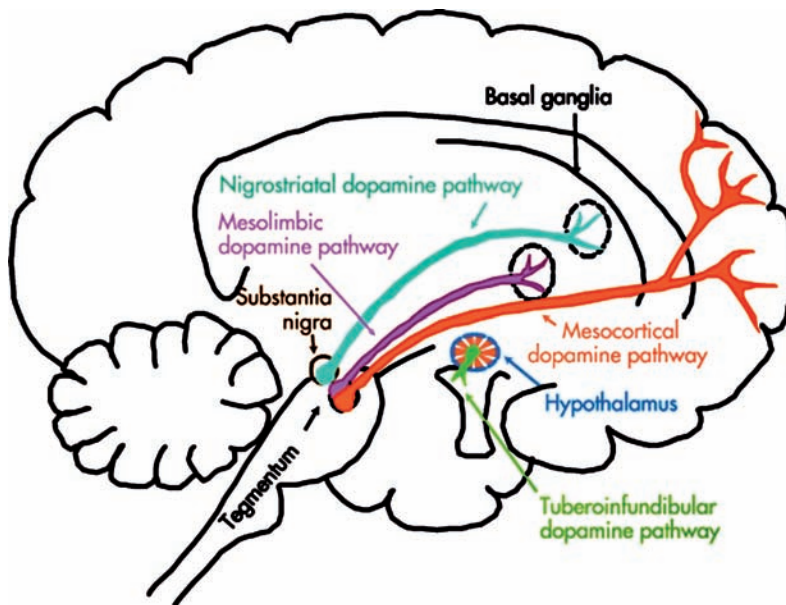
Figure 1.2: *Dopaminergic pathways of the brain. Each colored line represents each dopaminergic pathway.*

It was postulated that an early developmental insult to mesocortical dopamine system would reduce the dopamine function (hypodopaminergia) in this system and which in turn would lead to dopamine elevation (hyperdopaminergia) in mesolimbic dopamine system (5). In addition, the complex physiological function of dopamine, acting through different dopaminergic pathways with unique activities in each of them, makes the aetiology of this disease even more complicated.

Dopamine Pathways and their Functions

In the brain, four dopamine pathways play a role in the pathophysiology of schizo-phrenia as well as in the therapeutic effects and side effects of antipsychotic agents that are designed to block the dopamine D_2 receptor (Figure 1.2 and Table 1.1).

Table 1.1: Dopaminergic Pathways in schizophrenia	
Pathways and Functions	Dopamine antagonism
Mesolimbic Pathway Controls emotion and sensations of pleasure Hyperactivity in this pathway is seems to be responsible for psychosis.	Reduction of positive symptoms
Mesocortical Pathway Controls cognitive function Hypoactivity in this pathway may be responsible for the negative and cognitive symptoms of schizophrenia.	Worsening negative and cognitive symptoms
Nigrostriatal Pathway Controls movements	Extrapyramidal symptoms, akathisia, dystonia and tardive dyskinesia
Tuberoinfundibular Pathway Controls prolactin release	Hyperprolactinemia and sexual dysfunction

Hypotheses of Schizophrenia

The Dopamine Hypothesis

The onset and course of schizophrenia has been hypothesized to result from dysregulation in the dopamine-mediated neurotransmission (6). The Dopamine hypothesis mainly relies on the observation that the clinical antipsychotic potency of current drugs is in direct relation to their affinity to the D_2 receptors (7).

A developmentally specific dysfunction in the dopaminergic innervation of the prefrontal cortex (PFC) leads to the hypodopaminergic activity in mesocortical pathway and causes negative and cognitive symptoms of schizophrenia. This functional deficit in dopamine neurotransmission in the PFC would increase subcortical dopamine turnover (8). This leads to the hyperdopaminergic activity in other dopaminergic pathways (in the subcortical region) and causes positive symptoms of schizophrenia. Thus, this hypothesis incorporates an explanation for positive and negative symptoms. However, the new generation of antipsychotic drugs have affinity for multiple receptors and showed antipsychotic efficacy with less affinity towards D_2 receptors (9).

The Glutamate Hypothesis

Several studies have reported the involvement of the glutamatergic system (2, 10, 11) in schizophrenia pathogenesis. Glutamate appears to play an important role in regulating the dopamine release. The interactions between the glutamatergic and the

1

dopaminergic systems may be highly significant in the aetiology and pathophysiology of schizophrenia (11). The glutamate hypothesis of schizophrenia proposes that neurodevelopmental abnormalities in glutamate synapse formation result in the hypofunction of N-Methyl-D-aspartate (NMDA) receptors and thereby an abnormal dopamine activity which is associated with the symptoms of schizophrenia. Noncompetitive NMDA antagonists like phencyclindine (PCP) and ketamine were reported to (re)produce psychotic conditions, which are very similar to the positive and negative symptoms of schizophrenia, including hallucinations and delusions. This observation directed towards the hypofunctionality of the NMDA receptor in schizophrenia patients. Several studies have shown that NMDA hypofunction can lead to alterations in dopamine-related phenomena similar to those observed in schizophrenia, namely, subcortical dopamine excess and cortical D_1 receptor upregulation (11, 13).

Though pathophysiology of schizophrenia is explained based on different hypotheses, it is clear that all these hypotheses funnel into the abnormal dopamine activity. Hence, D_2 receptor antagonism is being the basis for the drug therapy in schizophrenia.
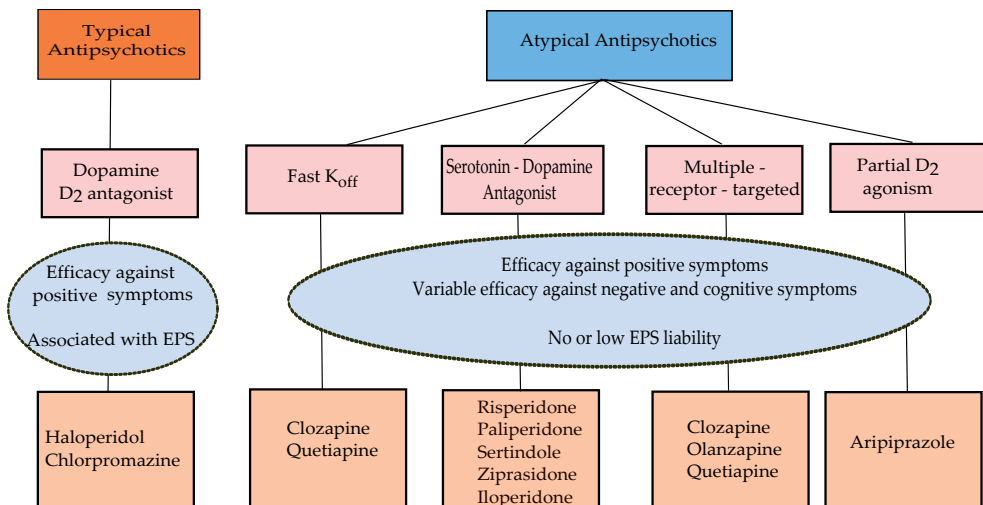
Figure 1.3: *Classification of antipsychotic drugs.*

Antipsychotics – Mechanism of Action

Antipsychotic drugs are classified as typical (or conventional) antipsychotics and atypical (or new generation) antipsychotics based on their mechanism of action (Figure 1.3)

Typical or Conventional Antipsychotics

By the 1970s, it was widely recognized that the key pharmacological property of all neuroleptics with antipsychotic properties was their ability to block dopamine D_2 receptors, specifically in the mesolimbic dopamine pathway. The hyperactivity of dopamine in this pathway was postulated to cause the positive symptoms. These typical antipsychotics bind to the D_2 receptors throughout the brain and block them. This results in a hypofunction of the dopamine system in all dopamine pathways, which causes apart from the antipsychotic effects also the side effects, e.g. extrapyramidal symptoms (EPS).

Atypical Antipsychotics

A reduction of excessive dopaminergic neurotransmission in the mesolimbic brain regions without blocking dopamine transmission in the nigrostriatal projections is the characteristic of atypical antipsychotics. Low or less EPS and lack of sustained prolactin elevation are the essential features of atypicality.

Fast "K_{off}" antipsychotics

All antipsychotics block dopamine D_2 receptors, but some dissociate from the receptors more quickly than others (Figure 1.4). The rate of dissociation from the receptor is characterized by the rate constant k_{off}.

It had been demonstrated that slow k_{off} antipsychotic agents (e.g. haloperidol) have been associated with EPS and prolactin elevation, whereas the fast k_{off} antipsychotic agents (e.g., clozapine, quetiapine) are known to be free of EPS and prolactin elevation. Kapur *et al* showed that antipsychotic agents may differ as much as almost a thousand-fold in the rate at which they dissociate from the D_2 receptor and it is the k_{off} that determines how quickly the antipsychotic drug will respond to the dynamic interaction between dopamine and D_2 receptors in the synapse (14). Thus, a fast k_{off} at the D_2 receptor may contribute to the atypicality of antipsychotics (15). However,

1
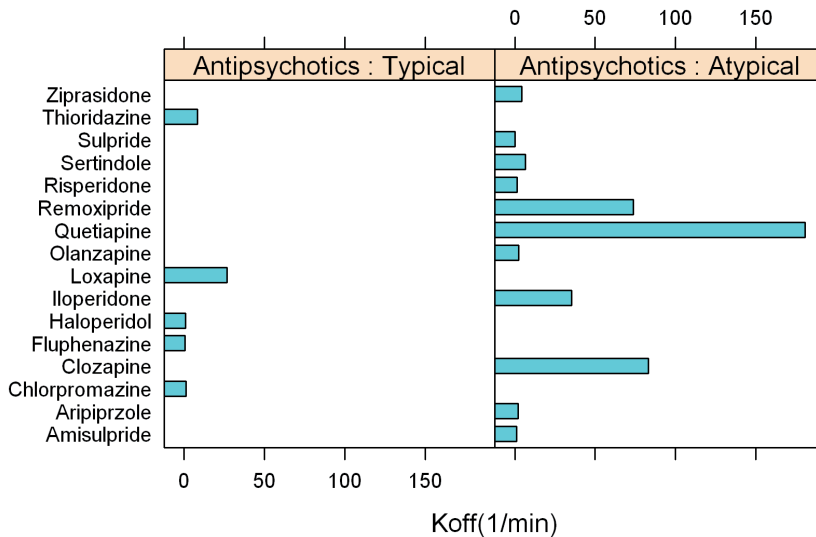
Figure 1.4: *K_{off} values of different antipsychotics.*

it is noteworthy that not all the atypical antipsychotics have a fast dissociation from the receptor (Figure 1.4).

Hence, it is clear that atypicality of an antipsychotic depends not only on the dissociation rate constant of the drug from the receptor (k_{off}).

Serotonin – Dopamine antagonists

This class of atypical antipsychotics is characterized by relatively weak affinities for dopamine D_2 receptors and high affinities for serotonin 5-HT_{2A} receptors. The high affinity for 5-HT_{2A} receptors seems to play a role in the low EPS side effects on atypical antipsychotic treatment. The combination of D_2 and 5-HT_{2A} antagonism may increase dopamine levels in the prefrontal cortex and alleviate the cognitive dysfunction. In the nigrostriatal pathway, serotonin-dopamine antagonists play a dual role by inducing the release of dopamine via 5-HT_{2A} antagonism. The released dopamine competes with the drug for the D_2 receptor and reverses the blockade of the D_2 receptor. As D_2 receptor blockade is reversed, serotonin-dopamine antagonists cause little or no EPS. Since there are few 5-HT_{2A} receptors in the other brain regions (for e.g. mesolimbic pathway), antipsychotic actions are preserved.

Multiple-receptor-target antipsychotics ('Magic shotgun')

Most of the common central nervous system disorders — such as depression, bipolar disorder and schizophrenia — seem to be polygenic in origin. Hence, it was proposed that designing non-selective drugs ('magic shotguns') that interact with several molecular targets would lead to new and more effective medications for schizophrenia.

The prominent example for this class of atypical antipsychotics is clozapine. Clozapine, has a low affinity to some of the dopamine (D_1, D_2, D_3 and D_5) receptors and has a high affinity for a number of serotonin ($5\text{-}HT_{2A}$, $5\text{-}HT_{2C}$, $5\text{-}HT_6$, $5\text{-}HT_7$), dopamine D_4, muscarinic (M_1, M_2, M_3, M_4, M_5), adrenergic (Alpha$_1$ and Alpha$_2$) and other biogenic amine receptors (16). The atypilcality of clozapine was determined by the absence of EPS and clozapine showed superiority in treating schizophrenia. Clozapine is thought to normalize glutamatergic and dopaminergic neurotransmission in schizophrenia, thereby ameliorating symptoms, via complex interactions with a large number of molecular targets (16).

Despite of these superior antipsychotic effects, clozapine was voluntarily withdrawn from the treatment of schizophrenia due to the agranulocytosis side effect. Health authorities in most countries approved its use only for treatment-resistant schizophrenia with regular hematological monitoring to detect granulocytopenia. Other atypical antipsychotics including quetiapine and olanzapine also have appreciable affinities for other receptors (16).

Partial agonists

Partial agonist offer clinical efficacy with a diminished liability for producing side effects. The atypical antipsychotic aripiprazole has the pharmacologic mechanism of action as a partial agonist at dopamine D_2 receptors, providing antipsychotic efficacy without significant EPS. For partial agonists, the effective receptor blockade is lower than the receptor occupancy by a proportion reflecting the amount of intrinsic agonist activity (17). Hence, even a high D_2RO (95%) may not induce EPS or elevate prolactin levels. Moreover, aripiprazole has a robust pharmacological profile at several serotonin ($5\text{-}HT_{1A}$, $5\text{-}HT_{2A}$, $5\text{-}HT_{2C}$, $5\text{-}HT_7$) and dopamine (D_2, D_3, D_4) receptors (16). So although aripiprazole is clearly a functionally selective partial agonist, its complex pharmacology precludes us from concluding that its beneficial actions in schizophrenia are due solely to partial agonism of D_2 receptors (16). It is more likely that the balance of partial agonism and antagonism at a multiplicity of receptors is responsible for its efficacy in schizophrenia and related disorders. Other recently developed partial $D_{2/3}$ agonists did not show a significant efficacy over other drugs (16).

Dopamine D$_2$ Blockade and Treatment Of Schizophrenia

1

Several arguments can be mentioned to support the hypothesis that the therapeutic effects and side effects of antipsychotic drugs are closely related to their dopamine D$_2$ receptor occupancy.

- Several studies suggest that blockade of 65% to 80% of D$_2$ receptors is the key to antipsychotic efficacy for both conventional neuroleptics and atypical antipsychotics (7). However, some antipsychotics, for example clozapine, show antipsychotic activity at a lower receptor blockade (20-67%) than other antipsychotics (7). Aripiprazole, an atypical antipsychotic, has been shown to be a partial agonist on the D$_2$ receptors (18). Hence for aripiprazole a higher degree of D$_2$ receptor occupancy may be required for antipsychotic efficacy.
- Drugs devoid of D$_2$ antagonism and with high 5-HT$_{2A}$ occupancy did not show any antipsychotic activity (19).
- Investigational drugs that acting as non-D$_2$ dopamine antagonists in schizophrenia showed inferior efficacy results in clinical studies (16).
- Animal studies suggested that blockade of D$_2$ receptor is required for efficacy (20, 21).
- Dopamine D$_2$ receptor occupancy (D$_2$RO) higher than 80% increases the risk of adverse effects such as extra pyramidal symptoms (22, 24).
- Additionally, D$_2$RO is also connected to prolactin elevation, a side effect of antipsychotic treatment. Prolactin elevation is closely associated with D$_2$RO higher than 70% (25, 26).

Thus, D$_2$RO plays a crucial role in schizophrenia drug discovery, drug development and therapy. In general, target occupancy is important both in early drug discovery, where accurate knowledge of the degree of occupancy could help to determine the suitability of a drug candidate for further development, and later in the drug development process, when target site occupancy measurements can guide dosing selection (27). Hence, it is essential to predict D$_2$RO in humans during the early drug discovery phase to expedite the drug development process.

Translational PKPD Modeling

In general the effect of a drug is a result of the interplay of the drug distribution to the site of action and the complex cascade of dynamic pharmacological processes or responses. PKPD models describe the complex relationship between drug exposure, and the pharmacological effect.

In a human system, it is often not possible to obtain information on the exposure to the drug at the site of drug action and it is sometimes impossible to obtain information on the time course of pharmacodynamic markers. However it is possible to measure the drug concentration at the site of action in animals. Understanding the exposure-effect relationship in animals using PKPD modeling tools may allow translating this relationship from one species to other using appropriate scaling factors and human specific information on PK and receptor binding. Lepist and Jusko proposed a method for the scaling of pharmacodynamic parameters across species using a relatively simple physiological model (28). With an assumption of pharmacodynamic marker or similar drug-receptor interaction for the pathological conditions between animals and human, it is can be hypothesized that the structural PKPD models developed on the basis of data obtained from lower species are applicable to humans (29).

Moreover, the mechanism-based PKPD modeling approaches which have the unique capacity to explicitly make a distinction between drug-specific and biological system-specific parameters. Drug-specific parameters describe the interaction between the drug and the biological system in terms of target affinity and target activation, whereas system-specific parameters describe the response of the biological system (Figure 1.5). The distinction between drug-specific and biological system-specific parameters is crucial for predicting drug effects in humans accurately.

Danhof *et al* (30) proposed that the values of drug-specific parameters such as target affinity are likely to be identical between species and between individuals. This
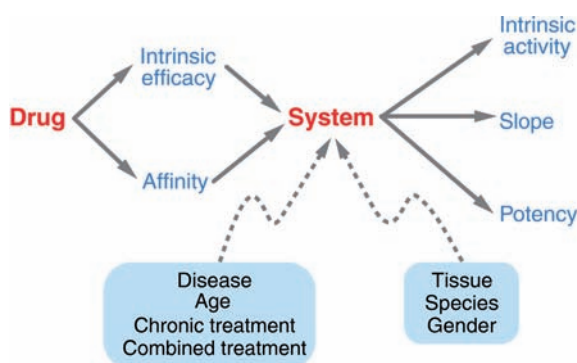
Figure 1.5: *Components of mechanism-based pharmacokinetic–pharmacodynamic (PKPD) models. (Figure is reused with permission from reference 42)*
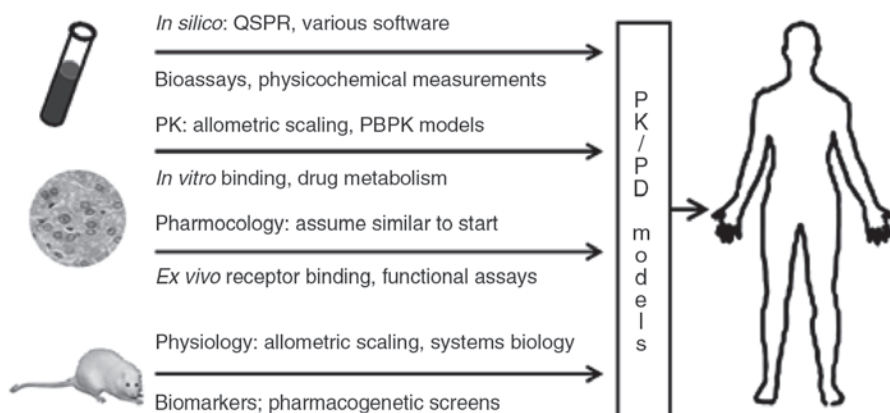
Figure 1.6: *Components of mechanism-based pharmacokinetic–pharmacodynamic (PKPD) models for translation of animal data to human clinical pharmacology. Predictive techniques (above the arrows) can be improved by selective measurements (below the arrows). PBPK – physiology-based PK; QSPR-quantitative structure–PKPD relationship. (Figure is reused with permission from reference 33).*

would imply that binding rate constants estimated in animals could be used in human to extrapolate the pharmacodynamics from rat to human.

However, several other studies showed differences in receptor affinity between species (31). Notwithstanding divergent reports on the species independence of drug-specific parameters, an integration of allometric principles, *in vitro* information, and a physiological basis to PKPD modeling would increase the potential to translate effects from rat to human (29, 32, 33). Hence, translational PKPD modeling can be defined (Mager and Jusko) as the integration of *in silico*, *in vitro*, and *in vivo* preclinical data with mechanism-based models to anticipate the effects of new drugs in humans and across different levels of biological organization (Figure 1.6) (34).

Translational PKPD modeling tools are increasingly used in drug development to improve the predictability of clinical efficacy by providing insight on the likely PKPD relationship for drugs in development to facilitate decisions with respect to the dose and dosing regimen for clinical trials (33, 35, 36). Interspecies scaling has been successfully applied to scale pharmacodynamic effects like hypothermic and cortisol responses to buspirone and flesinoxan treatment; the effect on reticulocytes,

red blood cells and hemoglobin levels of erythropoietin and the antinociceptive and respiratory depressant effects of buprenorphine (29, 32, 37).

Translational Models in CNS active drugs

The main objective of PKPD modeling is to elicit the relationship between drug exposure (preferably at the site of action) and effect of the drug. As stated before, in central nervous system (CNS) disorders it is seldom possible to measure drug concentrations in the human brain. In addition, in schizophrenia drug development it is not often possible to repeatedly measure the pharmacodynamic markers (e.g. target occupancy) in patients due to the experimental constraints. However, measuring drug concentration at the site of action (or target organ) and a repeated measurement of pharmacodynamic marker (e.g. target occupancy) is possible in animals. Hence, understanding the complex target site distribution and target site binding in animals using PKPD modeling tools would be of value in predicting these relationships to humans.

Target site distribution and translational PKPD modeling

The distribution of a drug to the site of action is an important determinant in the time course and intensity of drug effects in CNS drug therapy. Drug distribution to the brain is characterized by both passive diffusion and active efflux by transporters present at the luminal surface of the blood-brain-barrier (BBB). So, the drug concentration at the site of action may be different from the concentration in the plasma compartment. It is reported that drugs that are P-gp substrates in rats are likely to also be P-gp substrates in higher species (38). Nevertheless, translating the target site kinetics for CNS active drugs from rat to human would require proper understanding of drug transport at the BBB of both species taking into account differential expression and functionality of drug transporters (39) and structural differences of BBB between species (40). This involves physiology-based pharmacokinetic (PBPK) modeling concepts for interspecies scaling because in PBPK modeling the system has to be represented in a physiologically realistic manner using species-specific data on tissue structure, volume and the associated blood flows. Target site distribution of several CNS active drugs was successfully described using the combination of physiology and mechanism-based PKPD approaches, for drugs such as opoids, antipsychotics and serotonin reuptake inhibitors. Liu *et al* (41) proposed a hybrid physiology-based model to explain the brain kinetics of several CNS active drugs.

In conclusion, one of the challenging tasks for the inter-species translation of drug distribution to brain is the translation of passive permeability and active transport between species. Once developed, such a model might be used to predict the target site (brain) distribution of drugs in human.

1

Target binding and translational PKPD modeling

The ultimate effect of drug-target binding and activation depends on target affinity and intrinsic efficacy and receptor expression and transduction processes (42). PKPD modeling approaches for target binding and activation are based on the concepts of the receptor theory. Receptor theory defines that target affinity and intrinsic efficacy are drug-specific properties, whereas receptor expression and the transduction process are dependent on the biological system. As stated earlier, this distinction of drug-specific and system-specific properties is essential for translational modeling.

In translational modeling, these drug-specific properties can often be predicted on the basis of *in vitro* bioassays. Furthermore, the values of drug-specific pharmacodynamic parameters (target affinity) are often identical between species. System-specific parameters vary between species and scaling of system-specific parameters remains challenging. However, simple allometric principles have been successfully applied to extrapolate biological system-specific parameters from rat to human. The mechanism-based PKPD concepts were applied with success in animal to human extrapolation of the pharmacodynamics of semi-synthetic μ opioid receptor agonists, selective serotonin 5-HT$_{1A}$ receptor agonists and gamma-aminobutyric acid receptor agonists (42).

In conclusion, a successful implementation of a translational framework to predict clinical outcome or biomarker responses (e.g. D$_2$RO in schizophrenia) in clinical situations will have an impact on the drug development process. Thus, translational models hold the key to expedite the selection of lead compounds, the selection of first-in-human dose and the design of clinical trials. Translational PKPD modeling has the potential to integrate information across species and to direct effective drug development.

Translational PKPD Modeling in Schizophrenia

The research described in this thesis work was performed within the framework of the Dutch Top Institute Pharma project: Mechanism-based PKPD modeling (http://www.tipharma.com). This platform involves leading pharmaceutical companies worldwide, and academic institutes from The Netherlands. This program focuses on the development and application of novel mechanism-based PKPD modeling concepts to describe the processes on the path between plasma concentration and effect that can be employed for extrapolation and prediction of treatment effects in drug development.

Translational PKPD modeling in schizophrenia is one of the projects of within this platform with an overall objective of developing a general PKPD model framework
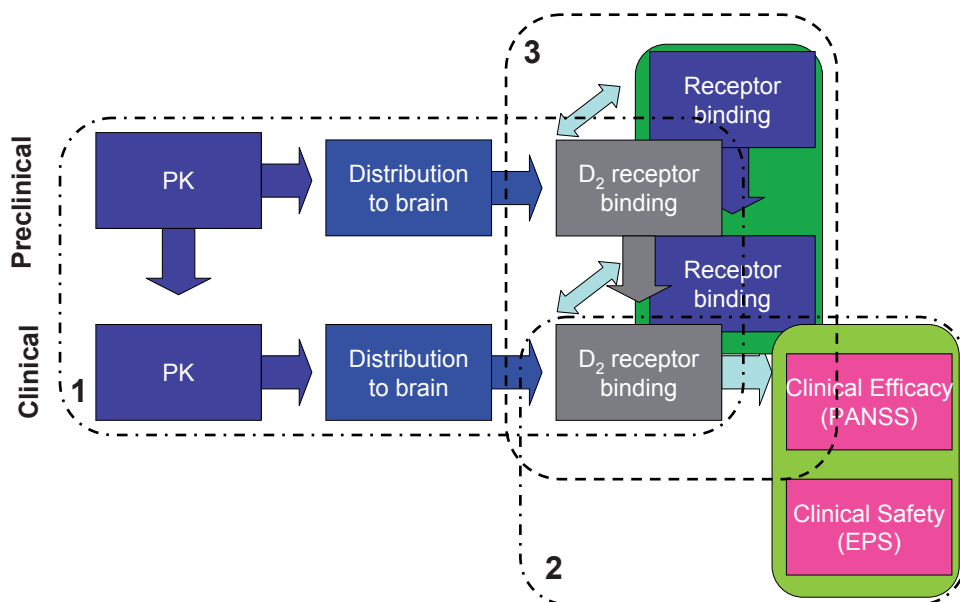
Figure 1.7: *Translational PKPD modeling in schizophrenia.*

that integrates receptor-binding data across species and clinical data (both efficacy and safety) across compounds and that can be used to optimize drug development strategies for future compounds in schizophrenia. This project comprised three parts (Figure 1.7).

1. Prediction of receptor occupancy in human using *in vitro* and preclinical information
2. Linking receptor occupancy of antipsychotics to efficacy and safety
3. Extrapolation of the translation concepts developed in the project to other receptor subtypes

This thesis is concerned with part 1 and 3 of the overall project.

The aim of the research described in thesis was to develop a generic mecha-nistic pharmacokinetic and pharmacodynamic (PKPD) modeling framework that scales in vitro and preclinical in vivo information to the human situation. This thesis is focused on drugs used to treat schizophrenia.

References

1. Crimson ML, Argo TR, Buckley PF. Schizophrenia. In: DiPiro JT, Talbert RL, Yee GC, Matzke GR, Wells BG, Posey LM, editors. Pharmacotherapy: A pathophysiologic approach. Seventh ed. Newyork: McGraw Hill; 2008. p. 1099-122.
2. Miyamoto S, LaMantia AS, Duncan GE, Sullivan P, Gilmore JH, Lieberman JA. Recent advances in the neurobiology of schizophrenia. Mol Interv 2003;3(1):27-39.
3. Laruelle M, bi-Dargham A. Dopamine as the wind of the psychotic fire: new evidence from brain imaging studies. J Psychopharmacol 1999 Dec;13(4):358-71.
   (4) Di Forti M, Lappin JM, Murray RM. Risk factors for schizophrenia – All roads lead to dopamine. European Neuropsychopharmacology 2007 Mar;17:S101-S107.
5. Fischer BA, Kirkpatrick B, arpenter WT. The Neurobiology of Negative Symptoms and the Deficit Syndrome. In: Lajtha A, Javitt DC, Kantrowitz JT, editors. Handbook of Neurochemistry and Molecular Neurobiology. 3rd Edition ed. 2009. p. 507-24.
6. Duncan GE, Sheitman BB, Lieberman JA. An integrated view of pathophysiological models of schizophrenia. Brain Research Reviews 1999 Apr;29(2-3):250-64.
7. Seeman P, Van Tol HH. Dopamine receptor pharmacology. Trends Pharmacol Sci 1994;15(7):264-70.
8. Kapur S, Remington G. Serotonin-dopamine interaction and its relevance to schizophrenia. Am J Psychiatry 1996;153(4):466-76.
9. Horacek J, Bubenikova-Valesova V, Kopecek M, Palenicek T, Dockery C, Mohr P, et al. Mechanism of action of atypical antipsychotic drugs and the neurobiology of schizophrenia. CNS Drugs 2006;20(5):389-409.
10. Whitton PS. Glutamatergic control over brain dopamine release in vivo and in vitro. Neurosci Biobehav Rev 1997;21(4):481-8.
11. Laruelle M, Kegeles LS, Abi-Dargham A. Glutamate, dopamine, and schizophrenia: from pathophysiology to treatment. Ann N Y Acad Sci 2003;1003:138-58.
12. Abi-Dargham A, Moore H. Prefrontal DA transmission at D1 receptors and the pathology of schizophrenia. Neuroscientist 2003;9(5):404-16.
13. Narendran R, Frankle WG, Keefe R, Gil R, Martinez D, Slifstein M, et al. Altered prefrontal dopaminergic function in chronic recreational ketamine users. Am J Psychiatry 2005;162(12):2352-9.
14. Kapur S, Seeman P. Antipsychotic agents differ in how fast they come off the dopamine D2 receptors. Implications for atypical antipsychotic action. J Psychiatry Neurosci 2000 Mar;25(2):161-6.
15. Kapur S, Seeman P. Does fast dissociation from the dopamine d(2) receptor explain the action of atypical antipsychotics?: A new hypothesis. Am J Psychiatry 2001 Mar;158(3):360-9.
16. Roth BL, Sheffler DJ, Kroeze WK. Magic shotguns versus magic bullets: selectively nonselective drugs for mood disorders and schizophrenia. Nature Reviews Drug Discovery 2004 Apr;3(4):353-9.

17. Reynolds GP. Receptor mechanisms in the treatment of schizohrenia. Journal of Psychopharmacology 2004 Sep;18(3):340-5.

18. Biojone C, Casarotto PC, Resstel LB, Zangrossi H, Jr., Guimares FS, Moreira FA. Anti-aversive effects of the atypical antipsychotic, aripiprazole, in animal models of anxiety. J Psychopharmacol 2010 Aug 10;Epub ahead of print Aug 10.

19. Truffinet P, Tamminga CA, Fabre LF, Meltzer HY, Riviere ME, Papillon-Downey C. Placebo-controlled study of the D-4/5-HT2A antagonist fananserin in the treatment of schizophrenia. American Journal of Psychiatry 1999 Mar;156(3):419-25.

20. Wadenberg MLG. Conditioned Avoidance Response in the Development of New Antipsychotics. Current Pharmaceutical Design 2010 Jan;16(3):358-70.

21. Wadenberg MLG, Soliman A, VanderSpek SC, Kapur S. Dopamine D-2 receptor occupancy is a common mechanism underlying animal models of antipsychotics and their clinical effects. Neuropsychopharmacology 2001 Nov;25(5):633-41.

22. Farde L, Nordstrom AL, Wiesel FA, Pauli S, Halldin C, Sedvall G. Positron Emission Tomographic Analysis of Central D1-Dopamine and D2-Dopamine Receptor Occupancy in Patients Treated with Classical Neuroleptics and Clozapine – Relation to Extrapyramidal Side-Effects. Arch Gen Psychiatry 1992 Jul;49(7):538-44.

23. Nordstrom AL, Farde L, Wiesel FA, Forslund K, Pauli S, Halldin C, et al. Central D2-Dopamine Receptor Occupancy in Relation to Antipsychotic Drug Effects – A Double-Blind Pet Study of Schizophrenic-Patients. Biol Psychiatry 1993 Feb 15;33(4):227-35.

24. Kapur S, Zipursky R, Jones C, Remington G, Houle S. Relationship between dopamine D-2 occupancy, clinical response, and side effects: A double-blind PET study of first-episode schizophrenia. American Journal of Psychiatry 2000 Apr;157(4):514-20.

25. Turrone P, Kapur S, Seeman MV, Flint AJ. Elevation of prolactin levels by atypical antipsychotics. American Journal of Psychiatry 2002 Jan;159(1):133-5.

26. Kapur S, Roy P, Daskalakis J, Remington G, Zipursky R. Increased dopamine D-2 receptor occupancy and elevated prolactin level associated with addition of haloperidol to clozapine. American Journal of Psychiatry 2001 Feb;158(2):311-4.

27. Grimwood S, Hartig PR. Target site occupancy: emerging generalizations from clinical and preclinical studies. Pharmacol Ther 2009 Jun;122(3):281-301.

28. Lepist EI, Jusko WJ. Modeling and allometric scaling of s(+)-ketoprofen pharmacokinetics and pharmacodynamics: a retrospective analysis. J Vet Pharmacol Ther 2004 Aug;27(4):211-8.

29. Zuideveld KP, Van der Graaf PH, Peletier LA, Danhof M. Allometric scaling of pharmacodynamic responses: application to 5-Ht1A receptor mediated responses from rat to man. Pharm Res 2007 Nov;24(11):2031-9.

30. Danhof M, de Lange EC, la Pasqua OE, Ploeger BA, Voskuyl RA. Mechanism-based pharmacokinetic-pharmacodynamic (PK-PD) modeling in translational drug research. Trends Pharmacol Sci 2008 Apr;29(4):186-91.

31. Chien JY, Friedrich S, Heathman MA, de Alwis DP, Sinha V. Pharmacokinetics/Pharmacodynamics and the stages of drug development: role of modeling and simulation. AAPS J 2005 Oct 7;7(3):E544-E559.

32. Woo S, Jusko WJ. Interspecies comparisons of pharmacokinetics and pharmacodynamics of recombinant human erythropoietin. Drug Metab Dispos 2007 Sep;35(9):1672-8.

33. Agoram BM, Martin SW, Van der Graaf PH. The role of mechanism-based pharmacokinetic-pharmacodynamic (PK-PD) modelling in translational research of biologics. Drug Discov Today 2007 Dec;12(23-24):1018-24.

34. Mager DE, Jusko WJ. Development of translational pharmacokinetic-pharmacodynamic models. Clinical Pharmacology & Therapeutics 2008 Jun;83(6):909-12.

35. Chang C, Byon W, Lu Y, Jacobsen LK, Badura LL, Sawant-Basak A, et al. Quantitative PK-PD model-based translational pharmacology of a novel kappa opioid receptor antagonist between rats and humans. AAPS J 2011;13(4):565-75.

36. Bursi R, Erdemli G, Campbell R, Hutmacher MM, Kerbusch T, Spanswick D, et al. Translational PK-PD modelling of molecular target modulation for the AMPA receptor positive allosteric modulator Org 26576. Psychopharmacology (Berl) 2011 Dec;218(4):713-24.

37. Yassen A, Olofsen E, Kan J, Dahan A, Danhof M. Animal-to-human extrapolation of the pharmacokinetic and pharmacodynamic properties of buprenorphine. Clin Pharmacokinet 2007;46(5):433-47.

38. Syvanen S, Lindhe O, Palner M, Kornum BR, Rahman O, Langstrom B, et al. Species Differences in Blood-Brain Barrier Transport of Three Positron Emission Tomography Radioligands with Emphasis on P-Glycoprotein Transport. Drug Metab Disposition 2009 Mar;37(3):635-43.

39. Uchida Y, Ohtsuki S, Katsukura Y, Ikeda C, Suzuki T, Kamiie J, et al. Quantitative targeted absolute proteomics of human blood-brain barrier transporters and receptors. J Neurochem 2011 Apr;117(2):333-45.

40. Westerhout J, Danhof M, de Lange EC. Preclinical prediction of human brain target site concentrations: considerations in extrapolating to the clinical setting. J Pharm Sci 2011;100(9):3577-93.

41. Liu X, Smith BJ, Chen C, Callegari E, Becker SL, Chen X, et al. Use of a physiologically based pharmacokinetic model to study the time to reach brain equilibrium: an experimental analysis of the role of blood-brain barrier permeability, plasma protein binding, and brain tissue binding. J Pharmacol Exp Ther 2005 Jun;313(3):1254-62.

42. Danhof M, de Jongh J, De Lange ECM, la Pasqua O, Ploeger BA, Voskuyl RA. Mechanism-based pharmacokinetic-pharmacodynamic modeling: Biophase distribution, receptor theory, and dynamical systems analysis. Annual Review of Pharmacology and Toxicology 2007;47:357-400.

Scope and Outline
of the Present Thesis
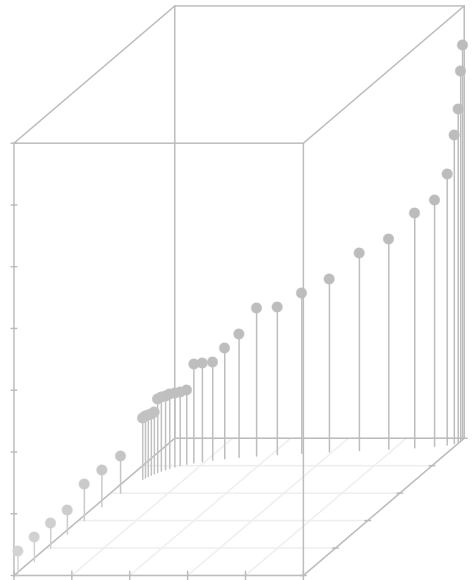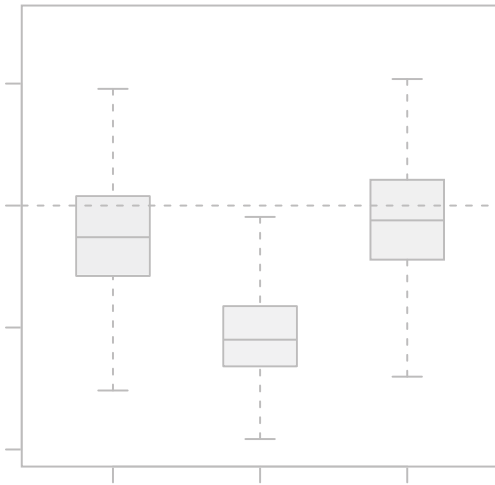
The research described in this thesis was aimed to develop a generic mechanistic pharmacokinetic and pharmacodynamic (PKPD) modeling framework that scales *in vitro and preclinical in vivo* information to the human situation and was focused on schizophrenia drug development.

Schizophrenia is a severe and disabling disorder, associated with marked social and occupational dysfunction, tenfold increase in suicidal risk, intensive use of healthcare resources, and poor prognosis (1). Although the fundamental pathology of schizophrenia remains ambiguous, it has been hypothesized that an excessive level of striatal dopamine, which can be caused by several factors, is responsible for development of psychotic symptoms (2). It is now widely accepted that dopamine and the dopamine D_2 receptor in the brain play a central role in schizophrenia (2, 3). As a result, dopamine D_2 receptor occupancy (D_2RO) can be used as a potential biomarker for the clinical outcome of schizophrenia therapy (4). D_2RO is measured by positron emission tomography (PET) in clinical studies and by both radio-ligand binding and PET studies in preclinical studies (5, 10). Moreover, drug-receptor interaction is also measured in *in vitro* experiments using receptor-bearing tissue or a cloned receptor system (10). Drug-receptor interaction is a dynamic process, which is described by association and dissociation rates. The rate constants of association and dissociation help to understand drug action in living systems. However, the *in vivo* association and dissociation rates of drugs to and from the receptors may be influenced by a number of conditions (11). The distribution of the drug to the receptor across the blood-brain-barrier (BBB) via passive diffusion and with active efflux may exert additional constraints on the drug-receptor binding process (12). The influence of this complex transport process on receptor binding is not yet elucidated. The new generation of antipsychotic drugs has affinity for multiple receptors and shows antipsychotic efficacy with less affinity towards D_2 receptors (13). Hence, extension of this framework to other receptor types would increase utility of this work.

For antipsychotic drugs, catalepsy in rats and extra-pyramidal side effects (EPS) in human are caused by excessive D_2RO (>80%)(8). Even though a clear relationship between D_2RO and side effects exists, the relationship between catalepsy and EPS is lacking. Hence, the information on catalepsy in rats is not yet utilized in human dose projections.

PKPD modeling is an excellent tool not only to characterize the time course of drug effects but also to separate drug-specific and system-specific factors contributing to the pharmacodynamics of a drug (14). Therefore it is hypothesized that a mechanism-based PKPD model framework would allow to integrate data from receptor binding studies, and to translate to clinical receptor occupancy, efficacy and safety parameters.

In the development of this translational framework, PKPD modeling and simulation were applied at different levels: i) describing drug distribution to brain, ii)

2

characterizing drug binding to the D_2 receptor, iii) predicting human D_2RO using *in vitro* and preclinical *in vivo* information and iv) linking D_2RO with side effects. This is described in the following four chapters.

Chapter 3: Drug transport to the brain is a complex process involving different transport mechanism and the subsequent drug binding to receptor is a dynamic process. Since this model is intended for translational purposes, we developed a physiology-based pharmacokinetic and pharmacodynamic (PBPKPD) model to characterize the drug distribution into the brain and to explain the kinetics of the binding of the drug to its receptor using association and dissociation rate constants for the atypical antipsychotic olanzapine in rats.

Chapter 4: The aim of this chapter is to develop a PKPD model describing D_2RO for the atypical antipsychotics risperidone and paliperidone in rats using the hybrid physiology-based PKPD model structure obtained by using olanzapine in rats (chapter 3). This model takes into account the distribution of a drug in the brain and association and dissociation kinetics at the D_2 receptors. Risperidone and paliperidone are atypical antipsychotics with high affinity for D_2 and $5\text{-}HT_{2A}$ receptors. Risperidone is metabolized to paliperidone and both drugs show similar binding properties and clinical profile. Therefore, to properly describe receptor occupancy of risperidone and eventually its clinical effect, it is necessary to take into account the formation of paliperidone, its distribution to brain and its binding to receptors. Therefore, we extended the previously published model for olanzapine to incorporate metabolite formation, brain kinetics and receptor binding. Also, since both risperidone and paliperidone are known P-glycoprotein (P-gp) substrates, we included an active efflux process at the brain-blood barrier. We also investigated whether binding to $5\text{-}HT_{2A}$ receptors influence PK and PD of both drugs.

Chapter 5: The objective of this chapter is to explore different approaches to predict human striatal D_2RO of antipsychotics using the previously developed translational PBPKPD model structure. This model allows for the integration and scaling of information from *in vitro* and preclinical *in vivo* data to the human situation. We also attempted to combine different approaches to determine the minimal amount of information required to predict human D_2RO using this translational framework. Since atypical antipsychotics also bind to other receptors in the brain, we also used the extended model structure which accounts for $5\text{-}HT_{2A}$ binding to predict human $5\text{-}HT_{2A}RO$.

Chapter 6: The relationship between the different outcome parameters used to assess the side effects in preclinical and clinical studies is not elucidated yet. Hence, we used PKPD tools to relate D_2RO and catalepsy in rats and subsequently we compared the D_2RO-catalepsy relationship in rats with the D_2RO-EPS relationship in humans in a quantitative manner. Furthermore, we aimed at a model structure that can

predict the severity of catalepsy for other antipsychotics. These tools and approaches might help to predict the incidence of EPS and other side effects and thereby accelerate the drug development process.

Chapter 7: In this chapter, we discuss the need of PKPD modeling concepts in the development of translational framework. The discussion is focused on the challenges and limitations involved in the translational modeling of receptor occupancy. In addition, we discuss the possibilities of using this framework for other therapeutic indications.

Chapter 8: presents the final summarizing discussion.

References

1. Crimson ML, Argo TR, Buckley PF. Schizophrenia. In: DiPiro JT, Talbert RL, Yee GC, Matzke GR, Wells BG, Posey LM, editors. Pharmacotherapy: A pathophysiologic approach. Seventh ed. Newyork: McGraw Hill; 2008. p. 1099-122.
2. Murray RM, Lappin J, Di FM. Schizophrenia: from developmental deviance to dopamine dysregulation. Eur Neuropsychopharmacol 2008 Aug;18 Suppl 3:S129-S134.
3. Howes OD, Kapur S. The Dopamine Hypothesis of Schizophrenia: Version III - The Final Common Pathway. 2009;35(3):549-62.
4. de Greef R, Maloney A, Olsson-Gisleskog P, Schoemaker J, Panagides J. Dopamine D(2) Occupancy as a Biomarker for Antipsychotics: Quantifying the Relationship with Efficacy and Extrapyramidal Symptoms. Aaps Journal 2011 Mar;13(1):121-30.
5. Kapur S, Zipursky RB, Remington G, Jones C, DaSilva J, Wilson AA, et al. 5-HT2 and D2 receptor occupancy of olanzapine in schizophrenia: a PET investigation. Am J Psychiatry 1998;155(7):921-8.
6. Nordstrom AL, Farde L, Nyberg S, Karlsson P, Halldin C, Sedvall G. D-1, D-2, and 5-Ht2 Receptor Occupancy in Relation to Clozapine Serum Concentration - A Pet Study of Schizophrenic-Patients. American Journal of Psychiatry 1995 Oct;152(10):1444-9.
7. Gefvert O, Lundberg T, Wieselgren IM, Bergstrom M, Langstrom B, Wiesel FA, et al. D-2 and 5HT(2A) receptor occupancy of different doses of quetiapine in schizophrenia: a PET study. 2001;11(2):105-10.
8. Kapur S, Remington G, Jones C, Wilson A, DaSilva J, Houle S, et al. High levels of dopamine D-2 receptor occupancy with low-dose haloperidol treatment: A PET study. American Journal of Psychiatry 1996 Jul;153(7):948-50.
9. Knauer CS, Campbell JE, Galvan B, Bowman C, Osgood S, Buist S, et al. Validation of a rat in vivo [3H] M100907 binding assay to determine a translatable measure of 5-HT2A receptor occupancy. 2008;591(1-3):136-41.
10. Kapur S, Seeman P. Antipsychotic agents differ in how fast they come off the dopamine D2 receptors. Implications for atypical antipsychotic action. J Psychiatry Neurosci 2000 Mar;25(2):161-6.

11. Kapur S. Receptor Occupancy by Antipsychotics - Concepts and Findings. Neurotransmitter Receptors in Actions of Antipsychotic Medications. CRC Press; 2000. p. 163-76.
12. De Lange ECM, Ravenstijn PGM, Groenendaal D, van Steeg TJ. Toward the prediction of CNS drug-effect profiles in physiological and pathological conditions using microdialysis and mechanism-based pharmacokinetic-pharmacodynamic modeling. Aaps Journal 2005;7(3):E532-E543.
13. Horacek J, Bubenikova-Valesova V, Kopecek M, Palenicek T, Dockery C, Mohr P, et al. Mechanism of action of atypical antipsychotic drugs and the neurobiology of schizophrenia. CNS Drugs 2006;20(5):389-409.
14. Danhof M, de Jongh J, De Lange ECM, la Pasqua O, Ploeger BA, Voskuyl RA. Mechanism-based pharmacokinetic-pharmacodynamic modeling: Biophase distribution, receptor theory, and dynamical systems analysis. Annual Review of Pharmacology and Toxicology 2007;47:357-400.

2

Mechanism-based Pharmacokinetic-Pharmacodynamic Modeling of the Dopamine D$_2$ Receptor Occupancy of Olanzapine in Rats

Martin Johnson[1], Magdalena Kozielska[1],
Venkatesh Pilla Reddy[1], An Vermeulen[2],
Cheryl Li[3], Sarah Grimwood[3], Rik de Greef[4],
Geny M.M. Groothuis[1], Meindert Danhof[5]
and Johannes H. Proost[1]

[1] *Dept. of Pharmacokinetics, Toxicology and Targeting, University of Groningen, The Netherlands*
[2] *Advanced PKPD Modeling and Simulation, Janssen Research and Development, a division of Janssen Pharmaceutica NV, Beerse, Belgium*
[3] *Worldwide Research & Development, Pfizer, Inc., Groton, CT, USA*
[4] *Clinical PK-PD, Pharmacokinetics, Pharmacodynamics & Drug Metabolism, Merck Sharp & Dohme, Oss, The Netherlands*
[5] *Division of Pharmacology, Leiden-Amsterdam Center for Drug Research, Leiden, The Netherlands*

Abstract

Purpose A mechanism-based pharmacokinetic-pharmacodynamic model was developed to predict the time course of dopamine D_2 receptor occupancy (D_2RO) in rat striatum following administration of olanzapine, an atypical antipsychotic drug.

Methods A population approach was utilized to quantify both the pharmacokinetics and pharmacodynamics of olanzapine in rats using the exposure (plasma and brain concentration) and D_2RO profile obtained experimentally at various doses (0.01-40 mg/kg) administered by different routes. A two-compartment pharmacokinetic model was used to describe the plasma pharmacokinetic profile. A hybrid physiology- and mechanism-based model was developed to characterize the D_2 receptor binding in the striatum and was fitted sequentially to the data. The parameters were estimated using nonlinear mixed-effects modeling.

Results Plasma, brain concentration profiles and time course of D_2RO were well described by the model and the validity of the proposed model is supported by a good agreement between the estimated association and dissociation rate constants, and the *in vitro* values from literature.

Conclusion This model includes both receptor binding kinetics and pharmacokinetics as the basis for the prediction of the D_2RO in rats. Moreover, this modeling framework can be applied to scale the *in vitro* and preclinical information to clinical receptor occupancy.

Introduction

Schizophrenia is a lifelong and often devastating, psychiatric disorder which often begins in late adolescence or early adulthood (1). Although the fundamental pathology of schizophrenia remain ambiguous, it has been hypothesized that an excessive level of striatal dopamine, which can be caused by several factors, is responsible for development of psychotic symptoms (2). This is also supported by the elevation of dopamine release in naïve patients following an acute amphetamine challenge (3). Preclinical and clinical studies suggest that blockade of dopamine-2 receptors (D_2 receptors) is the key pharmacological component to the antipsychotic efficacy of both the typical and the newer atypical antipsychotics (4, 5). However, the degree of D_2 receptor antagonism required for an antipsychotic efficacy is still unclear. Some antipsychotics, for example clozapine, show antipsychotic activity at a lower receptor blockade (20-67%) than other antipsychotics (6). Aripiprazole, an atypical antipsychotic, has been shown to be a partial agonist on the D_2 receptors (7). Kapur *et al* (8) reported that the rate of dissociation of antipsychotics from the D_2 receptors drives their efficacy and safety. These studies show that little is known about the degree of target occupancy and the role of the dynamic interactions between the drugs and the receptor in schizophrenia treatment. Moreover, the importance and influence of the distribution to the target site on the receptor binding is not yet elucidated and it is known that some antipsychotics, e.g. risperidone and its active metabolite paliperidone, are P-gp substrates and that therefore their transport into brain involves a complex process of active and passive transport (9). In addition, one of the other challenges in schizophrenia drug discovery and development is scaling and extrapolating the dopamine-2 receptor occupancy (D_2RO) obtained in preclinical studies to the clinical situation in a quantitative manner.

Hence, there is a need for a tool in the drug discovery process to characterize both penetration of the candidate compound into the brain (target site distribution) and the degree of D_2RO, which could also support the scaling of D_2RO from rat to human. It is essential to have sufficient information about the cascade of processes (distribution to and in the brain, receptor occupancy as a net result of association and dissociation) to generate such a tool. In schizophrenia drug discovery research, the information available to study the drug distribution into brain and the time course of D_2RO is rather sparse. Brain concentration and D_2RO are usually measured at the terminal time point, unless a labor-intensive microdialysis technique is used. Standard radioligand binding study protocols provide limited data with respect to brain exposure and receptor binding obtained at only one time point from one animal.

Pharmacokinetic and pharmacodynamic (PKPD) modeling tools are extensively used to characterize the process between drug administration and its effect. In the

last two decades, population-based approaches are being utilized to integrate the available sparse information from different resources to study the underlying PKPD processes. These approaches provide population mean parameter estimates and allow partition into inter-individual and intra-individual variability. Mechanism-based pharmacokinetic–pharmacodynamic models integrated with population approaches were used to characterize and predict the time course of pharmacodynamic responses in rats and human (10, 11). These models parameterize biophase equilibration kinetics and receptor association– dissociation kinetics to describe the drug binding to receptors. The important feature of these mechanistic models is their ability to distinguish the system- and drug- specific parameters, which has been proven to be useful in the extrapolation of treatment effects from rat to human. Moreover, these PKPD models when combined with physiological parameters have the ability to predict human PKPD properties using prior information from *in vitro* and preclinical studies (12).

In the present analysis, PKPD tools were utilized to describe the brain distribution and D_2RO of olanzapine, an atypical antipsychotic drug which is a dopamine D_2 receptor antagonist and which has been proven to have antipsychotic effects in the treatment of patients with schizophrenia (13).

Hence, a mechanism-based population PKPD model was developed to describe the time course of D_2RO of olanzapine, with emphasis on the modeling of receptor association/dissociation kinetics. This model can be utilized in the future to translate the *in vitro* and preclinical information to D_2RO in humans.

Methods

Data Management

This work was performed within the framework of the Dutch Top Institute Pharma project: Mechanism-based population PKPD modeling (http://www.tipharma.com). This mechanism-based population PKPD modeling platform involves leading pharmaceutical companies from worldwide and academic institutes from The Netherlands. The data used for this analysis were contributed by the pharmaceutical companies who are the members of this mechanism-based population PKPD platform. The data was anonimized, except the modeler was aware that the data was sourced from three industrial partners: Janssen Research and Development, Belgium, *Merck* Sharp and Dohme Limited – The Netherlands and Pfizer Global Research and Development – USA. The dataset included plasma and brain exposure data of olanzapine and its D_2RO measured at different time intervals from 12 different studies, which consisted of 283 rats of either the Wistar or Sprague-Dawley strain. The experimental

Table 3.1: Brief description of the studies that were used in this analysis

Study Number	Dose in mg/kg (min-max)	Number of animals	Type of Observations	Route of administration	observation time points (h)	Mode of D_2RO measurement
1	0.03	18	PC	IP	0.25, 0.5,1,1.5,2,4	NA
2	0.3-30	15	PC, BC, RO	IP	1	In vivo binding
3	0.01-10	28	PC	IP	1	NA
4	0.01-30	32	PC	IP	1	NA
5	3	20	PC, BC, RO	IP	0.25, 0.5, 1,1.5,2	In vivo binding
6a	0.01-30	26	PC, BC, RO	IP	1	In vivo binding
6b	0.01-30	22	PC, RO	IP	1	In vivo binding
7	3	20	PC, BC, RO	SC	0.5,1,2,4,6	In vivo binding
8	0.32 & 20	30	PC, BC, RO	SC	0.5,1,2,4,8	Ex vivo binding
9	0.04-40	18	RO	SC	1	In vivo binding
10	2.5	15	RO	SC	0.25,0.5,2,4, 6	In vivo binding
11	0.01-40	33	RO	SC	2	Ex vivo binding
12	2.5	3	PC	IV	0.12,0.33,1,2,4,8, 24	NA

PC – Plasma Concentration; BC – Total Brain Concentration; RO – Dopamine D2 Receptor occupancy; IP – intraperitoneal; SC – subcutaneous; IV – Intravenous; NA – not applicable; min – minimum dose used in the study; max – maximum dose used in the study; *In vivo* binding and *ex vivo* binding studies were performed using [3H]raclopride and [125I]sulpiride as the radioligand, respectively.

procedures for the plasma sample collection, brain dissection, tissue homogeniza-tion, and D_2RO measurements were similar across the different study sites and these procedures were published elsewhere (4, 14). Exposure and occupancy information was obtained following the administration of olanzapine by either intraperitoneal, subcutaneous or intravenous route in a wide range of single doses (0.01 to 40 mg/kg body weight). More details about the studies and data are depicted in Table 3.1.

3

Modeling Tools

A population based approach was employed to utilize all the relevant information in order to obtain population parameter estimates along with both the inter-animal and residual variability. All the parameter estimations were performed with the nonlinear mixed effects modeling software NONMEM (version VI level 2.0) (15). Log-transformed plasma and brain olanzapine concentrations were used for the data analysis, and concentrations below the limit of quantification were excluded from this analysis.

The inter-animal variability on the parameters was modeled according to:

$$Pi = \theta * \exp(\eta i)$$

in which Pi is the estimate of parameter P for the ith animal, θ the population estimate for parameter P and $\exp(\eta i)$ the inter-animal random deviation of Pi from P. The values of ηi are assumed to be normally distributed with mean zero and variance ω_i^2. Inter-animal variability is expressed as per cent coefficient of variation which is the square root of $\omega_i^2 *100$.

The adequacy of the PK model was assessed on the basis of goodness-of-fit plots, parameter correlations and precision in parameter estimates. An additional struc-tural parameter or inter-animal variability (IAV) was included in the model if the resulting change in objective function value (OFV) was >6.64 (p<0.01). Different types of residual error models (proportional, additive, combined proportional and additive) were tested. Based on the visual inspection of the diagnostic plots, a pro-portional error model was proposed to describe residual error in the plasma and brain drug concentration, as $\ln(Yobs_{ij}) = \ln(Ypred_{ij}) + \varepsilon_{ij}$ in which $Yobs_{ij}$ is the jth observed concentration in the ith animal, $Ypred_{ij}$ is the predicted concentration. An additive term was used to account for the unexplained variability in D_2RO as $Yobs_{ij} = Ypred_{ij} + \varepsilon_{ij}$, in which $Yobs_{ij}$ is the jth observed D_2RO in the ith animal, $Ypred_{ij}$ is the predicted D_2RO. The residual random variable (ε_{ij}) was assumed to be normally distributed with mean zero and variance σ^2. The residual error describes the error terms which remain unexplained and refers to, for example, dosing inaccuracies, as-say and experimental error (e.g., error in recording sampling times) and structural model misspecifications.

During the analysis, Census (16) integrated with Xpose (R package) (17) was used for NONMEM run management and also for making different types of diagnostic plots, which were used in the model selection process.

Population Pharmacokinetic Analysis

To determine the basic structural pharmacokinetic model for olanzapine, one- and two-compartment models were tested. Population pharmacokinetic values of olanzapine were estimated using the first-order conditional estimation method (FOCE). This model was implemented by user-defined differential equations using the ADVAN 9 subroutine in NONMEM. Using this routine, the parameters systemic clearance (CL in L/h/kg), volume of the central compartment (V_1 in L/kg), volume of the peripheral compartment (V_2 in L/kg), inter-compartmental clearance (Q in L/h/kg), and bioavailability for intraperitoneal (F_{IP}) and subcutaneous (F_{SC}) routes of administration were estimated.

Hybrid Physiology-based Pharmacokinetic-Pharmacodynamic Model

A mechanism- and physiology-based PKPD model was developed and evaluated for its usefulness in describing the time course of brain concentration and D_2RO. A four compartment hybrid physiology-based pharmacokinetic and pharmacodynamic (PBPKPD) model was sequentially linked to the plasma population pharmacokinetic model to describe the concentration-time profile of olanzapine in brain and the binding to D_2-receptors in striatum, which consists of brain-vascular, brain-extravascular, striatum-free and striatum- bound compartments (Figure 3.1). Following administration, olanzapine is transported from the plasma compartment to the brain-vascular compartment; this process is assumed to be influenced only by the cerebral blood flow. Only the unbound olanzapine in this intravascular compartment crosses the blood-brain barrier (BBB) and is transported into the brain-extravascular compartment, which is governed by the brain-extravascular clearance (CL_{bev}). Furthermore, olanzapine is transported from the brain-extravascular compartment to the striatum compartment where it can reversibly bind to the dopamine receptor complex (Figure 3.1). The receptor association and dissociation processes were described using k_{on} as the receptor association rate constant ($nM^{-1}h^{-1}$), k_{off} as the receptor dissociation rate constant (h^{-1}), and the Dopamine D_2 receptor density (B_{max}) in rat striatum. The volumes of brain-vascular (V_{bv}) and brain-extravascular (V_{bev}) compartments were assumed to be equal to the physiological values in the rat: 0.00024 L/kg and 0.00656 L/kg, respectively (18).

The clearance from the brain-vascular compartment (CL_{bv}) was assumed to be equal to the cerebral blood flow in rats, which is 0.312 L/h/kg (18). The brain-extravascular and striatum-free compartments were assumed to be equilibrated rapidly. This was achieved by fixing the clearance between brain-extravascular and striatum-free compartments (CL_{st}) to a high value. The unbound fraction of olanzapine in plasma (fu_{plasma}) and brain
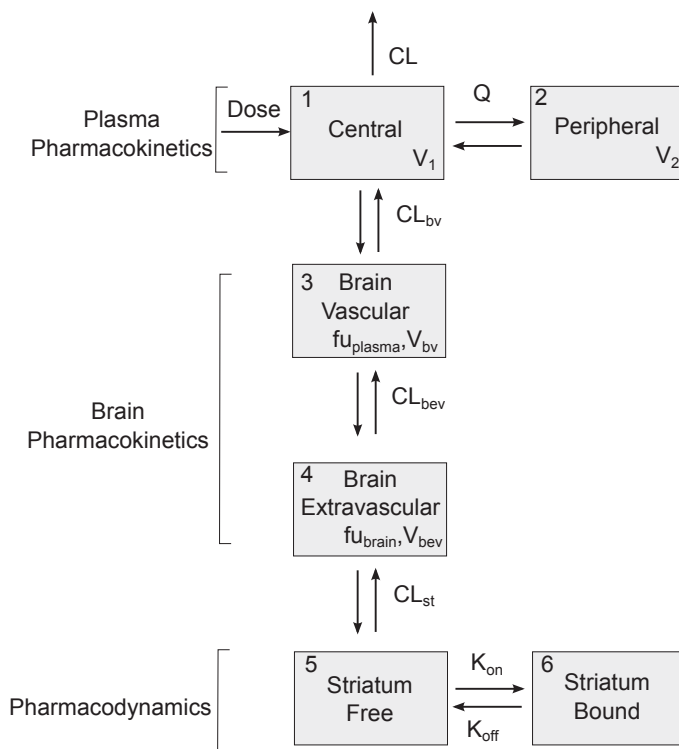
Figure 3.1: *A schematic representation of the PBPKPD model. The model incorporates different processes to explain the time course of D$_2$RO. The plasma pharmacokinetics describe the disposition of the drug in the plasma, the brain pharmacokinetics describe the processes involved in the transport of drug from plasma to brain, and the striatum compartment explains the drug binding to receptors through the binding constants.*

(fu$_{brain}$) were fixed to the values obtained from literature: 0.23 and 0.034, respectively (19). The brain-extravascular clearance (CL$_{bev}$), the binding parameters (kd and k$_{off}$) and the B$_{max}$ were estimated by fitting the PBPKPD model to the experimentally obtained brain concentrations and dopamine receptor occupancy data. Kd, (an equilibrium constant) and k$_{off}$ were estimated from the model and k$_{on}$ was derived as k$_{on}$=k$_{off}$/Kd. During this analysis, the plasma pharmacokinetic parameters were fixed to the parameter estimates obtained from the population pharmacokinetic analysis. This model was implemented through user-defined differential equations in the ADVAN 9 subroutine in NONMEM and differential equations related to this processes are provided in Appendix 1.

This model was based on the following assumptions: (1) Cerebrospinal fluid flow does not significantly influence the brain disposition, and (2) Plasma pharmacokinetics are not affected by brain disposition. The latter assumption allows the plasma concentration-time profile to be described by a conventional two-compartment model, independent of the brain distribution. In addition, it allows a separate analysis of the plasma concentration data to the population pharmacokinetic model.

During model development, it was observed that the model was not able to estimate B_{max}. So this parameter was assumed to be 48 nM, calculated as the maximum concentration of olanzapine bound to this receptor (20).

Due to the scarcity of data, no inter-animal variability was assumed in the PBPKPD model. *In vivo* and *ex vivo* binding studies were performed to measure the D_2RO in rats. So, it was also attempted to estimate separate binding constants for each *in vivo* and *ex vivo* studies. Moreover, an active efflux parameter was added in the model to check for the influence of active drug transport across the BBB.

Sensitivity Analysis

The objective of this analysis was to develop a stable mechanism- and physiology-based PKPD model that could be supported by the data used in the analysis and with a minimum number of parameters to be estimated. Hence, it was decided to perform a sensitivity analysis so that the model could be reduced by removing parameters, which have little or no influence on the model outputs. Hence, the pharmacodynamic parameters Kd (derived as k_{off}/k_{on}), k_{off}, k_{on} and B_{max} were perturbed to determine their influence on the D_2RO. A series of simulations were conducted with differing parameter values, which were varied 5- and 10-fold on the lower and higher side of the base value (model parameter estimate). Each simulation was conducted by altering one parameter at a time and fixing all remaining parameter values. The outputs considered for the parameter sensitivity analysis were the simulated D_2RO-time profiles with respect to the altered pharmacodynamic parameter. All simulations were performed using R (version 2.10). Primarily, 3 mg/kg dose was selected for this analysis, as this is the intermediate dose in the available dataset. Subsequently, a lower and higher dose levels to 3 mg/kg dose were also included in this analysis. D_2RO profiles were generated over a 24-hour time interval.

Model Evaluation

The bootstrap resampling technique and stochastic simulation and estimation (SSE) were used as model evaluation tools to check the stability and adequacy of the model, respectively. In the bootstrap resampling technique, bootstrap replicates are generated by sampling randomly from the original data set with replacement. One thousand replicate data sets were obtained using the bootstrap option in the software

package Perl Speaks NONMEM (PsN, version 3.2.4) (21). This resampling was strati-fied based on the three dose levels (low, medium and high). Low, medium and high dose levels included the doses ranges from 0.01 to 0.63 mg/kg, 1 to 3 mg/kg and 10 to 40 mg/kg, respectively. Parameter estimates for each of the re-sampled data sets were obtained by fitting the final model using NONMEM. Finally, median and 90% confidence intervals of all model parameters were calculated and the medians of the bootstrap estimates were compared with parameter values obtained from the original dataset. Furthermore, a simulation-based evaluation was performed using the SSE option as implemented in PsN. Briefly, the final PBPKPD model was used to both stimulate 1000 datasets and subsequently estimate PKPD parameters from these simulated datasets. The accuracy in parameter estimation was assessed from the bias as calculated below.

For instance, bias is calculated for k_{off} as

$$\text{Bias (\%)} = (\text{Median }(k_{off\text{-}i\,(1..n)}) - \text{True } k_{off}) / \text{True } k_{off} * 100\%$$

where, $k_{off\text{-}i}$ is the population mean k_{off} for the ith simulated dataset, n is the number of simulations, True k_{off} is the value which was used for the simulation.

Predictive check for D_2RO

A predictive check was performed to determine whether the final PBPKPD model provides an adequate description of D_2RO. One thousand datasets were simulated from the final PBPKPD parameter estimates to compare the distribution of simulated D_2RO with the observed D_2RO. The median, lower (5%) and upper (95%) quantiles of the simulated D_2RO were calculated for a time period between 0 and 360 min after olanzapine administration.

Application of the Rat PBPKPD model

Rat PBPKPD model structure was integrated with available population pharma-cokinetic parameters from human plasma concentration-time data, *in vitro* binding constants, fraction unbound in human plasma (22), and human brain physiologi-cal information (23) to predict the human D_2RO of olanzapine. All the parameters which were used for the simulations, are tabulated in Table 3.2. Distribution of olan-zapine across the BBB surrogated with permeability surface area product (PS) was calculated as a product of *in vitro* apparent membrane permeability (Papp, which is 15.7 $*10^{-6}$ cm/s) (19) value and human brain endothelial surface area (20 m^2) (24). One thousand human D_2RO- time curves were simulated for 10 mg/day and 20 mg/day dose levels, administered orally. Inter-individual variability (IIV) in the plasma population pharmacokinetic parameters was accounted in these simulations. The ob-served human D_2RO was taken from the published literature domain (25,26). These

Table 3.2: Population pharmacokinetic parameters, passive membrane permeability, physiological parameters and *in vitro* binding values used for the simulations

Parameter	Values used in human D$_2$RO Simulations	Source
CL/F (L/h)	19.5 (58)*	(25)
V/F (L)	1150 (75)*	(25)
Ka (h^{-1})	0.600 (32)*	(25)
k$_{off}$ (h^{-1})	2.34	(35)
Kd (nM)	5.10 [#]	(38)
fraction unbound in plasma	0.0700	(22)
fraction unbound in brain	0.034	(19)
Human cerebral blood flow (L/h)	36.0	(24)
Human brain extravascular volume (L)	1.4	(23)
Human brain vascular volume (L)	0.150	(23)
CL$_{bev}$ (L/h)	11.3	**

CL/F clearance; Ka absorption rate constant; V/F central volume of distribution;
* Population mean (Inter-Individual variability as %CV)
** Calculated as Papp* human brain endothelial surface area
[#] *In vitro* Ki value assumed as Kd

Table 3.3: Population pharmacokinetic parameter estimates from the original data set and resulting from 1000 bootstrap replicates for V1, CL, V2, Q with 90% confidence interval (CI)

Parameter	Original dataset (%RSE)	Median of 1000 bootstrap replicates	90% CI from Non-parametric bootstrap
V1(L/kg)	4.22 (9)	4.17	3.61-4.93
CL (L/h/kg)	3.21 (9)	3.12	2.74-3.65
V2 (L/h/kg)	2.23 (14)	2.23	1.87-2.87
Q (L/h/kg)	1.70 (30)	1.67	1.19-2.92
F$_{IP}$	0.636 (12)	0.633	0.538-0.771
Inter-animal variability			
IAV-CL (%CV)	56 (19)	55	47-66
IAV-F1 (%CV)	87 (18)	87	73-98
Residual variability			
Proportional Error	0.141 (7)	0.130	0.073-0.159

%RSE = Relative standard error as obtained from the COVARIANCE option of NONMEM
IAV = Inter-animal variability calculated as $100 \times \sqrt{\omega^2}$, where ω^2 is the variance term

observed values were measured at steady-state conditions after varying treatment duration across different studies. Hence, the simulations were made at steady-state conditions, which were achieved within 2 weeks of drug treatment. Berkeley Madonna (version 8.3.18, Berkeley Madonna Inc, University of California, USA) was used in this simulation study. The predictive power of this translational approach was determined by comparing the simulations with observed human D_2RO.

Results

Population Plasma Pharmacokinetics
A two-compartment model best described the plasma pharmacokinetics of olanzapine. The appropriateness of the two-compartment over the one-compartment model was based on the visual comparison of goodness-of-fit (GOF) plots and the lower objective function. Population pharmacokinetic parameter estimates are given in Table 3.3. The observed and population predicted concentration of olanzapine is depicted in Figure 3.2.

All structural pharmacokinetic parameters were estimated precisely with acceptable relative standard error (RSE) which varied between 9% and 30%. The absorption rate constant was not estimable due to lack of information on early time points for both the intraperitoneal and the subcutaneous routes of administration and hence it was assumed that olanzapine was administered directly into the central compartment. A relative bioavailability was estimated for the intraperitoneal route of administration. The bioavailability for the subcutaneous route of administration was estimated to be close to 1. Indeed, fixing this parameter improved the model convergence with a successful covariance step, so the bioavailability for the subcutaneous route of administration was assumed to be complete for further modeling. Estimation of inter-animal variability was possible only for CL and F_{IP} and was estimated as 56% and 87%, respectively. No trend or pattern was observed in the conditional weighted residual diagnostics versus time and in the population predictions versus time, which demonstrates that this model adequately describes the time course of olanzapine plasma concentration (Figures. 3.2 and 3.3).

Hybrid Physiology-Based PKPD model
Initially, a PBPKPD model was developed, which included the effect of binding to the receptor on the free drug concentrations at the receptor binding sites (Figure 3.1). Parameter estimates that were obtained using this model are tabulated (Table 3.4). Later, a sensitivity analysis was performed to identify whether the model could be reduced by removing any parameters that were not influencing the model output(s).

Plasma Pharmacokinetics
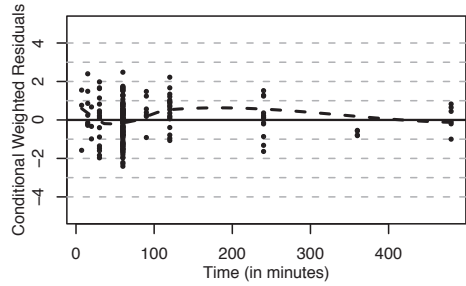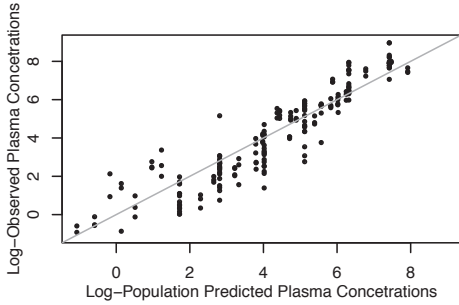
Brain Pharmacokinetics
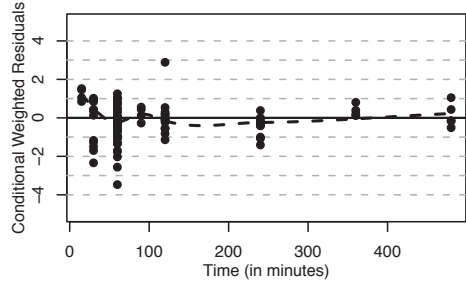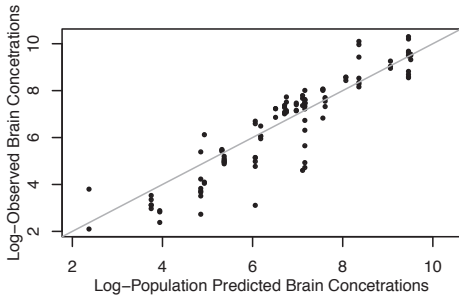
Dopamine D$_2$ receptor occupancy
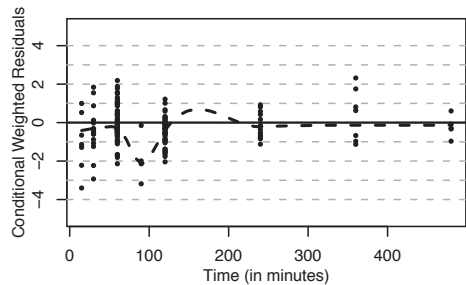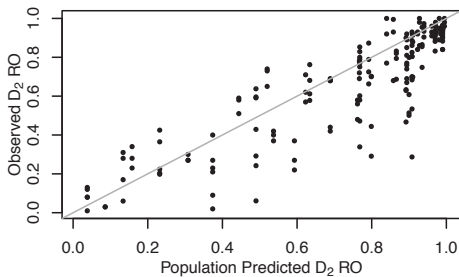
Figure 3.2: *Goodness-of-fit plots for the final PBPKPD model. Depicted are scatter plots of the observed olanzapine concentrations or D$_2$RO vs. population predictions and scatter plots of the population conditional weighted residuals vs. time.*
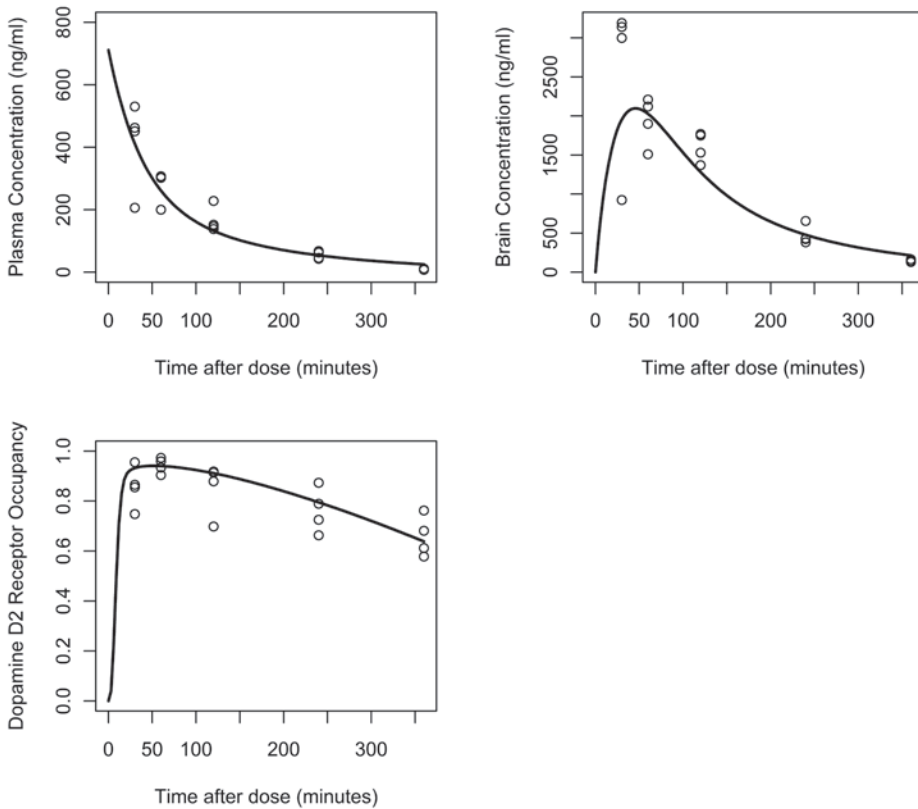
Figure 3.3: *Observed and predicted olanzapine concentrations and D₂RO vs. time. Open circles represent the observed olanzapine concentrations or D₂RO and the solid line represent the population predictions for 3 mg/kg dose of olanzapine administered subcutaneously.*

The simulated D_2RO profiles (model outcome) following variations in Kd, k_{on}, k_{off} and B_{max} for a dose of 3 mg/kg are shown in Figure 3.4. This sensitivity analysis clearly showed that B_{max} did not influence the model output when perturbed to different values, whereas perturbations of the values Kd, k_{on} and k_{off} all affected the D_2RO to some extent. This sensitivity analysis was also performed using lower and higher dose levels, which resulted in similar observations to those at the 3 mg/kg dose level. As little or no influence of the parameter B_{max} was shown at any of the doses, a reduced model with an alternative assumption was proposed as described in Figure 3.5. Briefly, this model assumes that binding to dopamine receptors does not affect the brain concentration significantly and thereby allows to drop the striatum free compartment from

Parameter	Full Model (FM)	Reduced Model (RM)	% difference
	Population Mean (%RSE)	Population Mean (%RSE)	
CL_{bev} (L/h/kg)	0.433 (16)	0.394 (15)	-10
Kd (nM)	14.6 (7)	14.7 (8)	<1
k_{off} (h^{-1})	3.04 (24)	2.62 (24)	-16
k_{on} (nM^{-1} h^{-1})[*]	0.208	0.178	-17
Proportional error (BC)	0.479 (6)	0.479 (6)	<1
Additive Error (D_2RO)	0.136 (5)	0.136 (5)	<1

Table 3.4: Population brain pharmacokinetic and pharmacodynamic parameter estimates from full and reduced PBPKPD model

%RSE = Relative standard error as obtained from the COVARIANCE option in NONMEM
[*]k_{on} derived as k_{off}/Kd
% difference calculated as,100-(Parameter estimate- RM*100/ Parameter estimate-FM)
BC = Brain Concentration
D_2RO = Dopamine D_2 receptor occupancy

the full model. In other words, it is assumed that a relatively low fraction of the drug in the brain extra-vascular compartment binds to the dopamine receptor. Further, this reduced model was subjected to model evaluation. The parameter estimates obtained from this model were close to the earlier model with B_{max} (Table 3.4) indicating that the reduced model is equivalent to the full model. There were no significant parameter correlations (R>0.95) reported in the NONMEM output between any of the PKPD model parameters, indicating the uniqueness of the parameter estimates obtained from the reduced model. Information about the brain concentration levels was limited to one observation per animal, which leaves no opportunity to estimate both inter- and intra-individual variability for brain clearance. No trend or pattern was observed in the conditional weighted residual diagnostics versus time and in the population predictions versus time which demonstrates that this model adequately describes the time course of olanzapine brain concentration and D_2RO (Figs. 3.2 and 3.3). Different sources of the data and data scarcity explain the high residual variability of the brain concentrations.

Model evaluation

Population Plasma Pharmacokinetic Model
In the bootstrap analysis of the population plasma pharmacokinetic model, all the replicates were minimized successfully. The population estimates as well as the

residual error of this model are in close agreement with the median values as depicted in Table 3.3. Difference in the estimated parameters from the final model between the original observed plasma data and the combined bootstrap replicates was <3% for all the parameter estimates.
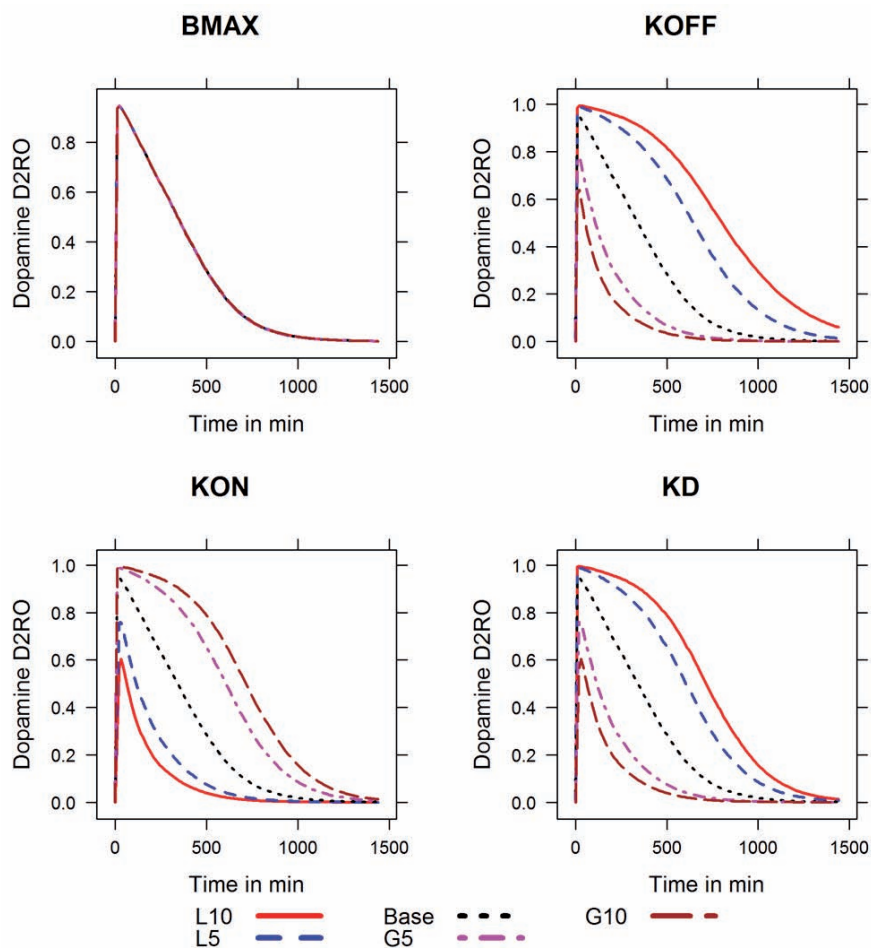
Figure 3.4: *Simulated drug concentration-time profiles for perturbations in different pharmacodynamic parameters at the 3 mg/kg dose level. The values were perturbed 5- and 10-fold at the higher and lower end of the base value. The fold variations are denoted by numerals corresponding to the extent of variation. The perturbations at the lower end of the base parameter values are denoted by the letter L and at the higher end by the letter G. For example, L10 indicates a value 10-fold lower than the base value of the parameter. This nomenclature is adapted from reference 27.*
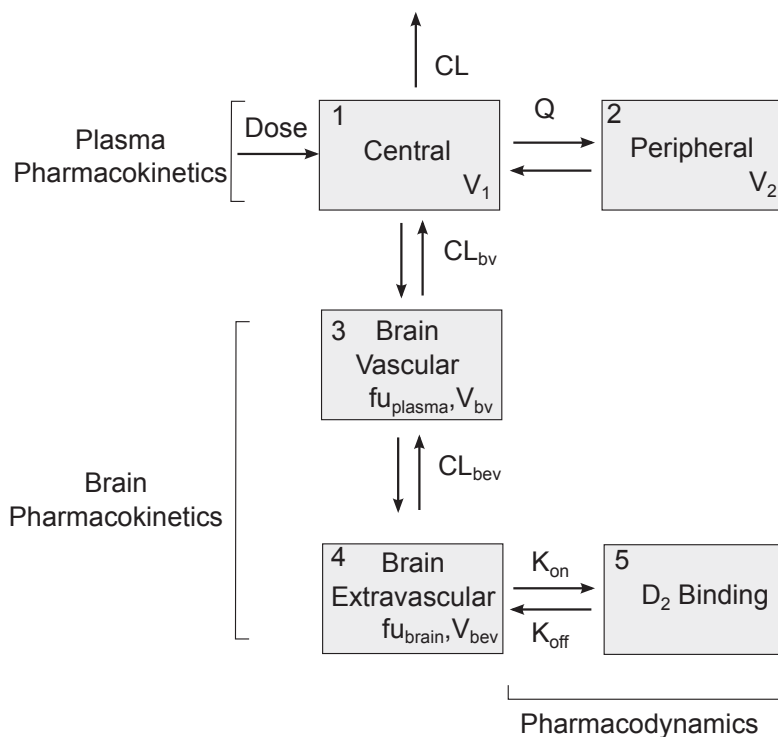
Figure 3.5: *The reduced model incorporates different processes to explain the time course of D₂RO. This model excluded the non-influential parameter Bₘₐₓ from the full model. This reduced model is based on the assumption that binding to dopamine receptors does not affect the free drug concentration in the brain.*

Hybrid physiology-based pharmacokinetic-pharmacodynamic model
In the bootstrap analysis, 960 out of 1000 bootstrap replicates minimized successfully. The population estimates as well as the residual error terms of the final model are in close agreement with the median values of the 960 successful bootstrap replicates. The median bootstrap estimates and 90% non-parametric bootstrap confidence intervals are depicted in Table 3.5. In figure 3.6, the distribution of the PKPD parameter estimates from the 1000 simulated datasets is displayed as a histogram. 955 out of 1000 simulated datasets minimized successfully. The bias for CL_{bev}, Kd, k_{off} was 2.2, 0.7, and 0.5%, respectively. The bias for the residual variability on brain concentration and D₂RO was -0.2 and -0.7%, respectively.

3

Table 3.5: Population brain pharmacokinetic and pharmacodynamic parameter estimates from the original data set and resulting median 1000 bootstrap replicates with 90% confidence interval for the Reduced Model

Parameter	Original dataset (%RSE)	940 bootstrap replicates (n=940)	95%CI from Non-parametric bootstrap
CL_{bev} (L/h/kg)	0.394 (15)	0.398	0.276-0.648
Kd (nM)	14.7 (8)	14.6	12.2-17.7
k_{off} (h^{-1})	2.62 (24)	2.64	1.58-6.36
Proportional error (BC)	0.479 (6)	0.470	0.380-0.560
Additive Error (D_2RO)	0.136 (5)	0.141	0.121-0.152

%RSE = Relative standard error as obtained from the COVARIANCE option in NONMEM
BC = Brain Concentration
D_2RO = Dopamine D_2 receptor occupancy
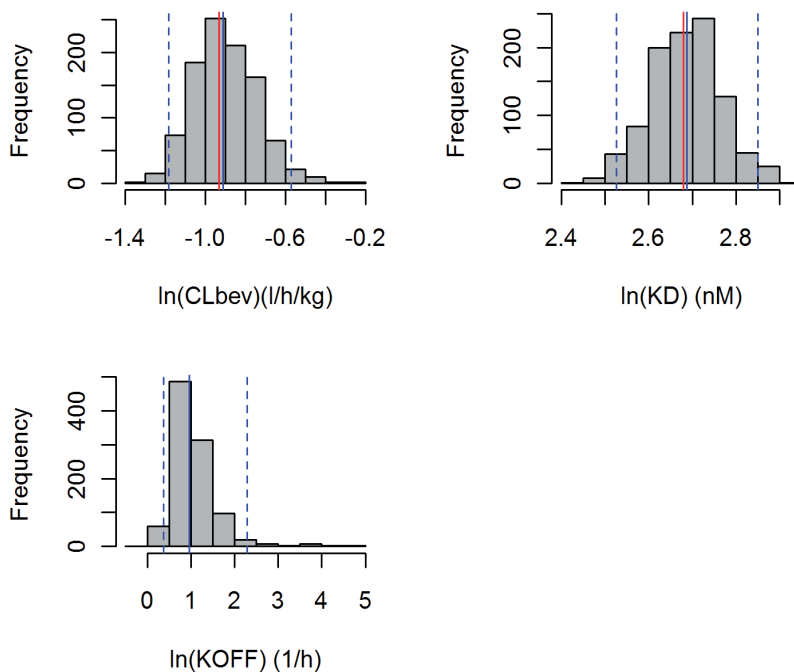
Figure 3.6: *Histograms of CL_{bev}, Kd, and k_{off} (in logarithmic scale) based on the 1000 stochastic simulations and estimations. Median values are plotted with blue solid lines and overlaid with the true parameter estimates (red solid lines). The blue dotted lines represent the 25th and 975th values of 1000 parameter estimates.*

Predictive check for D$_2$RO

The result of the predictive check for D$_2$RO is depicted in Figure 3.7. More than 80% of the observed olanzapine D$_2$RO are within the range of the simulated upper (95%) and lower (5%) quantiles of the simulated D$_2$RO.

Application of the Rat PBPKPD model

This hybrid PBPKPD model structure, using available human pharmacokinetic model parameters, *in vitro* permeability and binding data, predicted the human D$_2$RO for olanzapine at both 10 mg/day and 20 mg/day dose levels well. The result of these simulations is depicted in Figure 3.8.
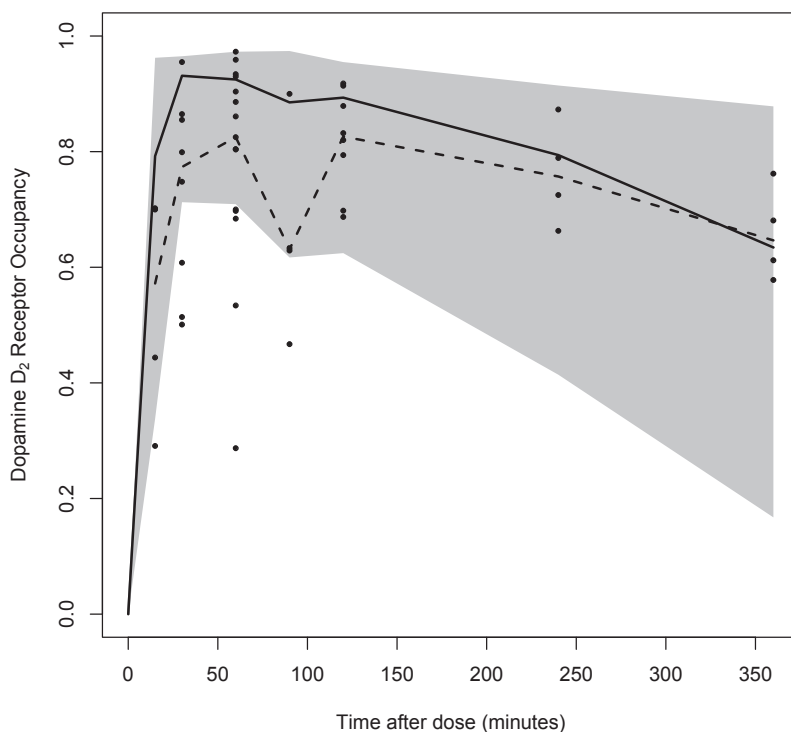
Figure 3.7: *Predictive check of the PBPKPD model for D$_2$RO after olanzapine administration, at 3 mg/kg dose. A number of 1000 data sets were simulated from the final PBPKPD parameter estimates. Depicted are the observed D$_2$RO (dots) and the shaded area represent the upper (95%) and lower (5%) quantile of the simulated D$_2$RO. Median of the simulated D$_2$RO are represented as solid line and median of the observed D$_2$RO are represented as dashed line.*
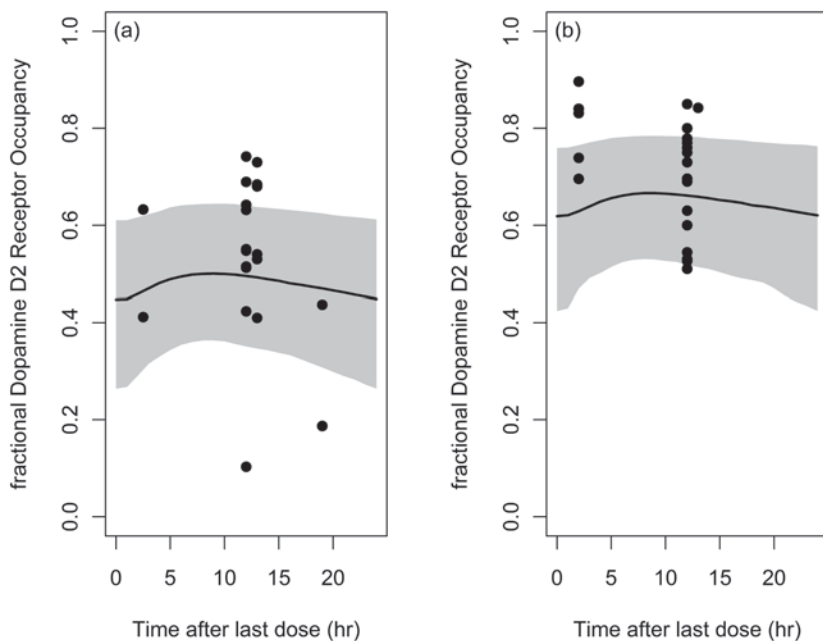
Figure 3.8: *Observed and predicted steady-state D_2 receptor occupancy in humans after oral administration of 10 mg/day (a) or 20 mg/day (b) of olanzapine. Simulations were performed using the rat PBPKPD model structure integrated with in vitro apparent permeability and in vitro binding information (Table V). Depicted are the observed D_2RO (dots) and the shaded area represent the 95% prediction limits of the simulated D_2RO. The medians of the simulated D_2RO are represented as a solid line.*

Discussion

This work aimed at developing a mechanism- and physiology-based PKPD model for olanzapine, which takes into account the barriers in drug transport to the brain and describes the association and dissociation kinetics of the drug to the D_2-receptor. The mechanistic nature and population basis of this model could provide a reliable tool for translating D_2RO between species that may support future drug discovery efforts, both specifically in the development of antipsychotics as more generally in the development of drug targeting other receptors in the brain.

A population approach is utilized here to integrate sparse data from a range of experimental sources to estimate the PKPD parameters. Plasma pharmacokinetics was fitted well using a two-compartment classical pharmacokinetic model. There were

only 3 rats with a full plasma concentration-time profile after intravenous olanzapine administration and during the modeling exercise, it was observed that bioavailability of olanzapine administered through the subcutaneous route was close to one with low inter-animal variability. Hence, to stabilize and increase the F_{IP} parameter precision, it was assumed that olanzapine administered by the subcutaneous route had a bioavailability of 100%. However, high variability in F_{IP} was estimated, which may reflect dosing inaccuracies or a variable first-pass effect. There are some deviations in the observed and population-predicted olanzapine concentrations, which could potentially be explained by covariates. Nevertheless, a covariate analysis was not performed due to lack of information on the individual characteristics of the animals. Possible sources of this variability were differences in the analytical methodologies which were used to measure the plasma concentration. In addition, the study sites where studies were performed (three different pharmaceutical companies) could also be a source of variation. However, no covariate relations were graphically observed between different study sites and pharmacokinetic parameters. Finally, population PK model evaluation demonstrated the accuracy and precision of the developed population PK model. This population pharmacokinetic model was utilized as a driving force for the brain PBPKPD model.

Target-site distribution might be complex for drugs acting on targets in organs protected by specific barriers (e.g. the brain), so a detailed characterization of these barriers is required to be included in the brain PBPKPD for meaningful concentration- and effect relationships. Drug distribution across the BBB was previously described by several pharmacokinetic models, which utilized the drug levels from extracellular fluid of brain to model the drug transport across the BBB (28-30). These models explained both the passive and active drug transport across the BBB in a quantitative manner. The objective of this study was to make a PKPD model structure, to explain the drug transport of antipsychotics across the BBB and the time course of D_2RO, which later can be utilized for translating PKPD information from rat to human. It is expected that these PKPD models when combined with physiological basis have the ability to predict human PKPD properties using prior information from *in vitro* and preclinical studies. So, this PBPKPD model was developed on a physiology basis including brain-vascular and brain-extravascular compartments to describe the brain pharmacokinetics and striatum compartments to explain the binding to dopamine D_2 receptors. This physiology basis is expected to enable this model structure to utilize the *in vitro* permeability and any efflux related information as a surrogate to explain drug transport across the brain in humans. Additionally, the observed brain drug concentrations were obtained from the whole brain homogenates, which represent the drug in both vascular and extravascular compartments of the brain. The brain-vascular and brain-extravascular compartment structure enables

this PBPKPD model to adapt this type of brain drug concentration data without any correction. This PBPKPD model adequately described both the brain concentration and D_2RO. The brain pharmacokinetic parameter CL_{bev} describes the passive transport of olanzapine across the blood brain barrier. It has been reported that olanzapine is a substrate for the BBB drug transporter P-glycoprotein (P-gp) in mice (31). Therefore, an active efflux parameter was added in the model to account for the active transport of olanzapine across the BBB. However, this additional parameter did not improve the model fit and consequently this additional parameter was not retained in the final model. Moreover, there are ambiguous reports about the active transport of olanzapine across the BBB in different species from both *in vivo* and *in vitro* studies (32-34). A significant influence of lag-time between drug exposure and D_2RO is expected for antipsychotic compounds and seen in the data. This model identifies both brain distribution (transfer across BBB) and binding kinetics (k_{on} and k_{off}) as determinants of this time delay on effect. A simulation based analysis also showed that both these components are essential to explain this time delay process (not shown).

The limited information on the brain concentrations (one observation per animal) did not allow separating the inter-animal and residual variability. Hence, no inter-animal variability for brain pharmacokinetics was estimated and this resulted in a high residual variability (48%) for the brain concentrations. In addition to the possible sources that were discussed earlier, different surgical procedures, brain dissections and extraction procedures could also cause high residual variability.

The pharmacodynamic parameters were estimated by incorporating a binding model to the brain pharmacokinetic model. This modeling exercise was started with the assumption that the binding to the dopamine receptor did affect the free drug concentration in the receptor vicinity, which included the parameter for maximum binding capacity (as B_{max}) in the model. Later, sensitivity analysis showed that the value of the parameter B_{max} hardly affected the model output. This observation could be either due to the model structure or to the limited information about this parameter. Hence, in the final model it was assumed that binding to D_2 receptors did not affect the free drug concentration in the receptor vicinity. Nevertheless, this model still holds its mechanistic nature by characterizing the time course of D_2RO on the basis of receptor association and dissociation kinetics. It has been demonstrated that antipsychotics differ in their k_{off} (dissociation) rate, which may determine the efficacy and safety of the antipsychotics (35). Hence, the current population PKPD model for olanzapine is proposed, which allows the separate characterization of the kinetics of target site distribution and the receptor association and dissociation kinetics as determinants of the time course of the dopamine D_2RO. This model, as implemented in NONMEM, was able to estimate Kd and k_{off} with acceptable RSE of 8 and 24%, respectively. Kd and k_{off} were estimated using the D_2RO data from both *in vivo* and

ex vivo binding studies. However, when it was attempted to estimate separate values of Kd and k_{off} for *in vivo* and *ex vivo* binding studies, this resulted in imprecise k_{off} estimates. Zasadny *et al* (36) found a significant correlation in the D_2RO measured using *ex vivo* binding and *in vivo* imaging techniques in rats. Hence, it is agreeable to estimate single values of Kd and k_{off} using the D_2RO from both *ex vivo* and *in vivo* studies. The validity of the proposed model is supported by the good agreement between the estimated pharmacodynamic parameters and the *in vitro* k_{off} (2.34 h^{-1}) and Ki (17 nM) values in rats (35, 37).

The model evaluation tools indicated that some parameters (CL_{bev} and k_{off}) had wide bootstrap confidence intervals. These wide bootstrap confidence intervals could be due to scattered and unbalanced information available from our dataset, which consists of D_2RO information from a wide range of doses (Table 3.1). So the bootstrap procedure could resample unrealistic datasets with very limited information to estimate the PKPD parameters, resulting in wide confidence intervals. However, the median bootstrap parameter estimates are close to the model parameter estimates, which indicates that this model could still be accepted with confidence. Moreover, the results of the predictive check for D_2RO showed that most of the observed D_2RO at 3 mg/kg dose levels were within the 5th and 95th percentiles of the simulated values. So, this model described the observed D_2RO reasonably well. However, the median of the simulated values were not in close agreement with the median of the observed data (Figure 3.6). This could be due to the limited and unbalanced amount of D_2RO observations available at each time points.

This proposed PBPKPD model is intended to be utilized in a translational framework to scale pharmacokinetic and pharmacodynamic information from rats to human. So, this general translational framework was based on a mechanism-based approach which accounts for the different processes involved in the transport of drug to brain. Moreover, this mechanism- and physiology-based PKPD model separates the drug specific properties, which describe the interaction between the drug and the biological system (target affinity, occupancy), and system specific properties, which describe the functioning of the biological system. Further, the utility of this proposed PBPKPD model was tested for its ability to predict the human dopamine D_2 receptor occupancy. These simulations were based on *in vitro* k_{off} values obtained from rat studies (35), *in vitro* human D_2 receptor binding values (38) and calculated surrogate (for example, PS) for the drug transport across BBB. Danhof *et al* (39) proposed that the values of drug-specific parameters such as target affinity are likely to be identical between species and individuals. This would imply that the binding rate constants estimated in rats can be used in human as well to extrapolate the pharmacodynamics from rat to human. However, several other studies showed differences in receptor affinity and protein binding between species (40). Notwithstanding divergent reports

on the species independence of drug-specific parameters, an integration of allometric principles (41-43), *in vitro* information, and a physiological basis to PKPD modeling would increase the prospective of translating effects from rat to human. The human D_2RO predictions at both dose levels are acceptable as 24 out of 39 observed values are within the 95% prediction limits. The predictions might improve further by considering the inclusion of allometric principles and *in vitro in vivo* correlations. Some antipsychotics, e.g. risperidone and its active metabolite paliperidone, have been extensively studied as P-gp substrates, and, therefore their transport into and from brain involve a complex process of active and passive transport (9). This model structure, with few modifications, will also allow to extend this approach for other drugs with active transport across the BBB.

Hence, this proposed PBPKPD model, which accounts for the barriers in drug transport and describes the association and dissociation kinetics, may be a useful tool to extrapolate the D_2RO of antipsychotics from rat to human.

Acknowledgements

Abbreviations

bBB	blood-brain barrier
B_{max}	dopamine D_2 receptor density
CB	concentration of olanzapine bound to receptor
CEV	concentration in extravascular brain compartment
CL	systemic clearance
CL_{bev}	brain-extravascular clearance
CL_{bv}	brain-vascular clearance
D_2RO	Dopamine D_2 Receptor Occupancy
FOCE	First Order Conditional Estimation method
fu_{plasma}	unbound fraction in plasma
fu_{brain}	unbound fraction in brain
GOF	Goodness of Fit plots
F_{IP}	bioavailability for intraperitoneal route of administration
F_{SC}	bioavailability for subcutaneous route of administration

IAV	inter-animal variability
k_{on}	receptor association rate constant
k_{off}	receptor dissociation rate constant
MW	Molecular Weight
nM	nanomoles/litre
OFV	Objective Function Value
PKPD	pharmacokinetic and pharmacodynamic
PBPKPD	physiology-based pharmacokinetic and pharmacodynamic
Q	inter-compartmental clearance
SSE	stochastic simulation and estimation
RSE	Relative Standard Error
V_1	volume of the central compartment
V_2	volume of the peripheral compartment
V_{bv}	volume of brain-vascular compartment
V_{bev}	volume of brain-extravascular compartment

Appendix 1

Full Model :

$$d(A_1)/dt = (Q/V_2)*A_2 - (Q/V_1)*A_1 - (CL/V_1)*A_1$$
$$d(A_2)/dt = (Q/V_1)*A_1 - (Q/V_2)*A_2$$
$$d(A_3)/dt = (CL_{bv}/V_1)*A_1 - (CL_{bv}/V_3)*A_3 - (CL_{bev}/V_3)*fu_{plasma}*A_3 + (CL_{bev}/V_4)*fu_{brain}*A_4$$
$$d(A_4)/dt = (CL_{bev}/V_3)*fu_{plasma}*A_3 - (CL_{bev}/V_4)*fu_{brain}*A_4 - (CL_{st}/V_4)*fu_{brain}*A_4 + (CL_{st}/V_5)*fu_{brain}*A_5$$
$$d(A_5)/dt = (CL_{st}/V_4)*fu_{brain}*A_4 - (CL_{st}/V_5)*fu_{brain}*A_5 - k_{on}*fu_{brain}*A_5*(B_{max} - CB) + k_{off}*A_6$$
$$d(A_6)/dt = k_{on}*fu_{brain}*A_5*(B_{max} - CB) - k_{off}*A_6$$

Where,

Subscripts 1-6 represent Volumes (V) and Amount (A) of olanzapine at central, peripheral, brain-vascular, brain-extravascular, striatum-free and striatum-bound compartments, respectively;

CL, Q, CL_{bv}, CL_{bev}, CL_{st} represent clearance of olanzapine in the central, peripheral, brain-vascular, brain-extravascular, striatum-free compartments, respectively.

CB is concentration bound to receptor as $(A_6/V_6)/(MW/1000)$ in nM;

MW is Molecular Weight of olanzapine;

D_2RO is calculated as CB/B_{max}.

Note that the transport from the central compartment to the brain-vascular compartment is not included in the equation $d(A_1)/dt$. This allows the plasma concentration-time profile to be described by a conventional two-compartment model, independent of the brain distribution.

Reduced Model:

Equations for $d(A_1)/dt$, $d(A_2)/dt$, and $d(A_3)/dt$ are identical to the Full Model.

$d(A_4)/dt = (CL_{bev}/V_3)*fu_{plasma}*A_3 - (CL_{bev}/V_4)*fu_{brain}*A_4$

$d(A_5)/dt = k_{on}*fu_{brain}*CEV*(1-A_5) - k_{off}*A_5$

Where,

Subscripts 1-4 represent Volumes (V) and Amount (A) of olanzapine at central, peripheral, brain-vascular, brain-extravascular compartments, respectively;

A_5 is the fractional D2 receptor occupancy;

CL, Q, CL_{bv}, CL_{bev} represent clearance of olanzapine in the central, peripheral, brain-vascular, brain-extravascular compartments, respectively;

CEV is the concentration in extravascular brain compartment as $(A_4/V_4)/(MW/1000)$ in nM.

References

1. Jones D, Gartlon J, Perry W, Geyer M. Developing New Drugs for Schizophrenia: From Animals to the Clinic. In: McArthur RA, Borsini F, editors. Animal and Translational Models for CNS Drug Discovery. Elsevier; 2008. p. 199-262.
2. Murray RM, Lappin J, Di FM. Schizophrenia: from developmental deviance to dopamine dysregulation. Eur Neuropsychopharmacol 2008 Aug;18 Suppl 3:S129-S134.
3. Laruelle M, bi-Dargham A. Dopamine as the wind of the psychotic fire: new evidence from brain imaging studies. J Psychopharmacol 1999 Dec;13(4):358-71.
4. Natesan S, Reckless GE, Nobrega JN, Fletcher PJ, Kapur S. Dissociation between in vivo occupancy and functional antagonism of dopamine D2 receptors: comparing aripiprazole to other antipsychotics in animal models. Neuropsychopharmacology 2006 Sep;31(9):1854-63.
5. Nucci G, Gomeni R, Poggesi I. Model-based approaches to increase efficiency of drug development in schizophrenia: a can't miss opportunity (vol 4, pg 837, 2009). Expert Opinion on Drug Discovery 2010;5(9):907.
6. Pickar D, Su TP, Weinberger DR, Coppola R, Malhotra AK, Knable MB, et al. Individual variation in D2 dopamine receptor occupancy in clozapine-treated patients. Am J Psychiatry 1996 Dec;153(12):1571-8.
7. Biojone C, Casarotto PC, Resstel LB, Zangrossi H, Jr., Guimares FS, Moreira FA. Anti-aversive effects of the atypical antipsychotic, aripiprazole, in animal models of anxiety. J Psychopharmacol 2010 Aug 10;Epub ahead of print Aug 10.
8. Kapur S, Seeman P. Does fast dissociation from the dopamine d(2) receptor explain the action of atypical antipsychotics?: A new hypothesis. Am J Psychiatry 2001 Mar;158(3):360-9.
9. Zhu HJ, Wang JS, Markowitz JS, Donovan JL, Gibson BB, DeVane CL. Risperidone and paliperidone inhibit p-glycoprotein activity in vitro. Neuropsychopharmacology 2007 Apr;32(4):757-64.

10. Yassen A, Kan J, Olofsen E, Suidgeest E, Dahan A, Danhof M. Mechanism-based pharmacokinetic-pharmacodynamic modeling of the respiratory-depressant effect of buprenorphine and fentanyl in rats. J Pharmacol Exp Ther 2006 Nov;319(2):682-92.

11. Yassen A, Olofsen E, van DE, Sarton E, Teppema L, Danhof M, et al. Mechanism-based pharmacokinetic-pharmacodynamic modelling of the reversal of buprenorphine-in-duced respiratory depression by naloxone : a study in healthy volunteers. Clin Pharma-cokinet 2007;46(11):965-80.

12. Danhof M, de Lange EC, la Pasqua OE, Ploeger BA, Voskuyl RA. Mechanism-based pharmacokinetic-pharmacodynamic (PK-PD) modeling in translational drug research. Trends Pharmacol Sci 2008 Apr;29(4):186-91.

13. Callaghan JT, Bergstrom RF, Ptak LR, Beasley CM. Olanzapine. Pharmacokinetic and pharmacodynamic profile. Clin Pharmacokinet 1999 Sep;37(3):177-93.

14. Knauer CS, Campbell JE, Galvan B, Bowman C, Osgood S, Buist S, et al. Validation of a rat in vivo [(3)H]M100907 binding assay to determine a translatable measure of 5-HT(2A) receptor occupancy. Eur J Pharmacol 2008 Sep 4;591(1-3):136-41.

15. Beal S, Sheiner LB, Boeckmann A. NONMEM User's Guides (1989-2006). Icon Develop-ment Solutions, Ellicott City, Maryland, USA, 2006.

16. Wilkins JJ. NONMEMory: a run management tool for NONMEM. Comput Methods Programs Biomed 2005 Jun;78(3):259-67.

17. R Development Core Team. R: A language and environment for statistical computing. R Fundation for Statistical Computing, Vienna, Austria; 2009.

18. Liu X, Smith BJ, Chen C, Callegari E, Becker SL, Chen X, et al. Use of a physiologically based pharmacokinetic model to study the time to reach brain equilibrium: an experi-mental analysis of the role of blood-brain barrier permeability, plasma protein binding, and brain tissue binding. J Pharmacol Exp Ther 2005 Jun;313(3):1254-62.

19. Summerfield SG, Read K, Begley DJ, Obradovic T, Hidalgo IJ, Coggon S, et al. Central nervous system drug disposition: the relationship between in situ brain permeability and brain free fraction. J Pharmacol Exp Ther 2007 Jul;322(1):205-13.

20. Barth VN, Chernet E, Martin LJ, Need AB, Rash KS, Morin M, et al. Comparison of rat dopamine D2 receptor occupancy for a series of antipsychotic drugs measured using ra-diolabeled or nonlabeled raclopride tracer. Life Sci 2006 May 22;78(26):3007-12.

21. Lindbom L, Pihlgren P, Jonsson EN. PsN-Toolkit--a collection of computer intensive sta-tistical methods for non-linear mixed effect modeling using NONMEM. Comput Meth-ods Programs Biomed 2005 Sep;79(3):241-57.

22. Kassahun K, Mattiuz E, Nyhart E Jr, Obermeyer B, Gillespie T, Murphy A, et al. Disposi-tion and biotransformation of the antipsychotic agent olanzapine in humans. Drug Me-tab Dispos 1997 Jan;25(1):81-93.

23. Rengachary SS, Ellenbogen RG. Principles of Neurosurgery. Edinburgh: Elsevier Mosby; 2005.

24. Fagerholm U. The highly permeable blood-brain barrier: an evaluation of current opin-ions about brain uptake capacity. Drug Discov Today 2007 Dec;12(23-24):1076-82.

25. Catafau AM, Penengo MM, Nucci G, Bullich S, Corripio I, Parellada E, et al. Pharmaco-kinetics and time-course of D(2) receptor occupancy induced by atypical antipsychotics in stabilized schizophrenic patients. J Psychopharmacol 2008 Nov;22(8):882-94.

26. Catafau AM, Suarez M, Bullich S, Llop J, Nucci G, Gunn RN, et al. Within-subject comparison of striatal D2 receptor occupancy measurements using [123I]IBZM SPECT and [11C]Raclopride PET. Neuroimage 2009 Jun;46(2):447-58.

27. Abraham AK, Krzyzanski W, Mager DE. Partial derivative-based sensitivity analysis of models describing target-mediated drug disposition. AAPS J 2007 Jun 8;9(2):E181-E189.

28. Bostrom E, Simonsson US, Hammarlund-Udenaes M. In vivo blood-brain barrier transport of oxycodone in the rat: indications for active influx and implications for pharmacokinetics/pharmacodynamics. Drug Metab Dispos 2006 Sep;34(9):1624-31.

29. Tunblad K, Jonsson EN, Hammarlund-Udenaes M. Morphine blood-brain barrier transport is influenced by probenecid co-administration. Pharm Res 2003 Apr;20(4):618-23.

30. Wang Y, Welty DF. The simultaneous estimation of the influx and efflux blood-brain barrier permeabilities of gabapentin using a microdialysis-pharmacokinetic approach. Pharm Res 1996 Mar;13(3):398-403.

31. Wang JS, Taylor R, Ruan Y, Donovan JL, Markowitz JS, Lindsay D, V. Olanzapine penetration into brain is greater in transgenic Abcb1a P-glycoprotein-deficient mice than FVB1 (wild-type) animals. Neuropsychopharmacology 2004 Mar;29(3):551-7.

32. Boulton DW, DeVane CL, Liston HL, Markowitz JS. In vitro P-glycoprotein affinity for atypical and conventional antipsychotics. Life Sciences 2002;71(2):163-9.

33. Abou El Ela A, Hartter S, Schmitt U, Hiemke C, Spahn-Langguth H, Langguth P. Identification of P-glycoprotein substrates and inhibitors among psychoactive compounds – implications for pharmaccokinetics of selected substrates. Journal of Pharmacy and Pharmacology 2004;56(8):967-75.

34. Linnet K, Ejsing TB. A review on the impact of P-glycoprotein on the penetration of drugs into the brain. Focus on psychotropic drugs. European Neuropsychopharmacology 2008;18(3):157-69.

35. Kapur S, Seeman P. Antipsychotic agents differ in how fast they come off the dopamine D2 receptors. Implications for atypical antipsychotic action. J Psychiatry Neurosci 2000 Mar;25(2):161-6.

36. Zasadny K, Callahan M, Watson M, Li Z. Comparison of dopamine D2 receptor occupancy measurements by ex vivo binding assay versus in vivo microPET imaging for typical and atypical antipsychotics. J NUCL MED MEETING ABSTRACTS 2006;47(suppl_1):9P-a.

37. Schotte A, Janssen PF, Gommeren W, Luyten WH, Van GP, Lesage AS, et al. Risperidone compared with new and reference antipsychotic drugs: in vitro and in vivo receptor binding. Psychopharmacology (Berl) 1996 Mar;124(1-2):57-73.

38. Seeman P. Atypical antipsychotics: mechanism of action. Can J Psychiatry 2002 Feb;47(1):27-38.

39. Danhof M, de Jongh J, de Lange EC, Della PO, Ploeger BA, Voskuyl RA. Mechanism-based pharmacokinetic-pharmacodynamic modeling: biophase distribution, receptor theory, and dynamical systems analysis. Annu Rev Pharmacol Toxicol 2007;47:357-400.:357-400.

40. Chien JY, Friedrich S, Heathman MA, de Alwis DP, Sinha V. Pharmacokinetics/Pharmacodynamics and the stages of drug development: role of modeling and simulation. AAPS J 2005 Oct 7;7(3):E544-E559.

41. Zuideveld KP, Van der Graaf PH, Peletier LA, Danhof M. Allometric scaling of pharmacodynamic responses: application to 5-Ht1A receptor mediated responses from rat to man. Pharm Res 2007 Nov;24(11):2031-9.

42. Woo S, Jusko WJ. Interspecies comparisons of pharmacokinetics and pharmacodynamics of recombinant human erythropoietin. Drug Metab Dispos 2007 Sep;35(9):1672-8.

43. Agoram BM, Martin SW, Van der Graaf PH. The role of mechanism-based pharmacokinetic-pharmacodynamic (PK-PD) modelling in translational research of biologics. Drug Discov Today 2007 Dec;12(23-24):1018-24.

Pharmacokinetic-Pharmacodynamic Modeling of the D_2 and 5-HT$_{2A}$ Receptor Occupancy of Risperidone and Paliperidone in Rats

Magdalena Kozielska[1], Martin Johnson[1],
Venkatesh Pilla Reddy[1], An Vermeulen[2],
Cheryl Li[3], Sarah Grimwood[3], Rik de Greef[4],
Geny M.M. Groothuis[1], Meindert Danhof[5]
and Johannes H. Proost[1]

[1] *Dept. of Pharmacokinetics, Toxicology and Targeting, University of Groningen, The Netherlands*
[2] *Advanced PKPD Modeling and Simulation, Janssen Research and Development, a division of Janssen Pharmaceutica NV, Beerse, Belgium*
[3] *Worldwide Research & Development, Pfizer, Inc., Groton, CT, USA*
[4] *Clinical PK-PD, Pharmacokinetics, Pharmacodynamics & Drug Metabolism, Merck Sharp & Dohme, Oss, The Netherlands*
[5] *Division of Pharmacology, Leiden-Amsterdam Center for Drug Research, Leiden, The Netherlands*

Abstract

Purpose A pharmacokinetic-pharmacodynamic model was developed to describe the time course of brain concentration and dopamine D_2 and serotonin 5-HT_{2A} receptor occupancy (RO) of the atypical antipsychotic drugs risperidone and paliperidone in rats.

Methods A population approach was utilized to describe the pharmacokinetics and pharmacodynamics of risperidone and paliperidone using plasma and brain concentrations and D_2 and 5-HT_{2A} RO data. A previously published physiology- and mechanism-based (PBPKPD) model describing brain concentrations and D_2 receptor binding in the striatum was expanded by including metabolite kinetics, active efflux from the brain and binding to 5-HT_{2A} receptors in the frontal cortex.

Results A two-compartment model best fit to the plasma pharmacokinetic profile of both risperidone and paliperidone. The expanded PBPKPD model described brain concentrations and D_2 and 5-HT_{2A} RO well. Inclusion of binding to 5-HT_{2A} receptors was necessary to describe observed brain-to-plasma ratios accurately. Simulations showed that the receptor affinity strongly influences the brain-to-plasma ratio pattern.

Conclusion Binding to both D_2 and 5-HT_{2A} receptors influences brain distribution of risperidone and paliperidone. This may stem from their high affinity for D_2 and 5-HT_{2A} receptors. Receptor affinities and brain-to-plasma ratios may need to be considered before choosing the best PKPD model for centrally active drugs.

Introduction

Schizophrenia is a chronic psychiatric disorder which affects almost 1 % of the population worldwide (1). It is characterized by the presence of positive symptoms (e.g. hallucinations, delusions), negative symptoms (e.g. social withdrawal, reduced motivation) and cognitive impairments. The majority of drugs for schizophrenia target psychotic symptoms as their primary goal (1). It has been hypothesized that elevated dopamine levels in the striatum lead to psychosis. This is consistent with the fact that all currently available antipsychotic drugs act as dopamine D_2 receptor antagonists (with one exception of a partial agonist – aripiprazole) (1). Usually 65-80% D_2 receptor occupancy (RO) is believed to be necessary for a clinically relevant outcome, but occupancy above 80% leads to side effects, i.e. Extra Pyramidal Symptoms (EPS) (2).

In addition to blocking D_2 receptors, newer antipsychotics (so-called second generation or atypical antipsychotics) have a high affinity towards other receptors. Specifically, many of them show a higher affinity towards serotonin 5-HT_{2A} receptors than towards D_2 receptors. It has been hypothesized that this higher $5\text{-HT}_{2A}/D_2$ affinity ratio contributes to the lower incidence of side effects of atypical antipsychotic drugs: EPS and prolactin elevation (3). Binding to 5-HT_{2A} receptors could theoretically also lead to improved efficacy towards negative symptoms in schizophrenia (4). 5-HT_{2A} antagonism may confer atypicality on antipsychotic drugs with relatively weaker D_2 antagonism (or partial D_2 agonism) because of the ability of 5-HT_{2A} receptors to modulate the activity of dopaminergic neurons differentially in different regions of the brain (5).

Predicting human receptor occupancy in a quantitative manner based on animal studies is one of the challenges in the drug discovery and development process. Pharmacokinetic and pharmacodynamic (PKPD) modeling tools are extensively used to describe drug distribution and effect (6). Recently utilization of mechanistic factors in the PKPD modeling has been strongly advocated (7). Inclusion of mechanistic factors like biophase distribution and receptor association and dissociation kinetics allows for a better understanding of processes leading to the observed data (8), as well as distinguishing between system- and drug-specific parameters and extrapolation of drug effects from rat to human (7).

The aim of this study was to develop a population PKPD model describing D_2RO for the atypical antipsychotics risperidone and paliperidone in rats. As a starting point we used a hybrid physiologically-based PKPD model which has recently been published for the atypical antipsychotic drug olanzapine in rats (9). This model describes the plasma pharmacokinetics using conventional compartmental analysis techniques while processes in the brain are described in a more physiological manner, taking into account the distribution of a drug in the brain and association and dissociation kinetics at the D_2 receptors. Here, we apply this model to other antipsychotics:

risperidone and 9-hydroxy-risperidone (paliperidone). Both drugs are atypical antipsychotics with high affinity for D_2 and 5-HT_{2A} receptors. Risperidone is metabolized to paliperidone and both drugs show similar binding properties and clinical effect profiles. Therefore, to properly describe the RO of risperidone and eventually its clinical effects it is necessary to take into account the formation of paliperidone, its distribution to the brain and its binding to receptors. Therefore, we extended the previously published model to incorporate metabolite formation, its brain kinetics and its receptor binding parameters. Also, since both risperidone and paliperidone are known P-glycoprotein (P-gp) substrates (10) we included an active efflux process at the blood-brain- barrier. We also investigated whether binding to 5-HT_{2A} receptors influenced the PK and PD of both drugs.

Methods

Data

This work was performed within the framework of the Dutch Top Institute Pharma project: Mechanism-based population PKPD modeling (http://www.tipharma.com). This modeling platform involves leading global pharmaceutical companies and academic institutions from The Netherlands. Data used for the modeling were generated previously by the pharmaceutical companies: Janssen Research and Development (Belgium), Merck Sharp & Dohme Limited (The Netherlands) and Pfizer Global Research and Development (USA) and were anonimized before releasing to the modelers. Results from a number of studies were used including dose-response and time course studies. Male Sprague Dawley or Wistar rats were used for the experiments. Risperidone (RIS) was administrated intravenously (IV), intraperitoneally (IP) or subcutaneously (SC) in a wide range of single doses (0.01 to 40 mg/kg). In most experiments, RIS plasma and brain concentrations and its RO (either D_2 or 5-HT_{2A}) were measured in one animal at one time point (since animals have to be euthanized for brain concentration and RO measurements). In a few studies paliperidone (PALI) concentrations were measured after RIS or PALI administration. An overview of the studies utilized is given in Table 4.1. For RO studies either the striatum or the frontal cortex was removed for the measurement of D_2 or 5-HT_{2A} receptor occupancy, respectively. The rest of the brain was homogenized and drug concentration was measured. An *in vivo* or *ex vivo* method was used for both 5-HT_{2A} and D_2 RO measurements. [³H] raclopride was used as a radioligand for D_2 RO studies and [³H]M100907 for 5-HT_{2A} RO studies. The experimental procedures for the plasma sample collection, brain dissection, tissue homogenization and RO measurements were similar across the different study sites and these procedures were based on published reports (11, 12).

Table 4.1: Overview of available data used in the PKPD analysis.

Study #	# of rats	drug[1]	ROA[2]	dose [mg/kg]	time points [h]	observation type	RO method[3]
1	3	RIS	IV	2.5	0.12, 0.33, 1, 2, 4, 8	PC-R	NA
2	4	RIS	IV	2	0.12, 0.33, 1, 2, 4	PC-R	NA
3a	23	PALI	SC	5	0.25, 0.5, 1, 2, 4, 8	PC-P, StrC-P, CorC-P	NA
3b	23	RIS	SC	5	0.25, 0.5, 1, 2, 4, 8	PC-R, PC-P, StrC-R, StrC-P, CorC-R, CorC-P	NA
4	42	RIS	IP	0.3, 3	0.25, 0.5, 1, 1.5, 2, 4, 7	PC-R, PC-P, BC-R, BC-P	NA
5	20	RIS	IP	1	0.25, 0.5, 1, 1.5, 2	PC-R, BC-R, RO-D$_2$	in vivo
6	23	RIS	IP	0.01, 0.03, 0.1, 0.3, 1, 3	1	PC-R, BC-R, RO-D$_2$	in vivo
7	36	RIS	SC	0.16, 10	0.5, 1, 2, 4, 8, 24	PC-R, BC-R, RO-D$_2$	ex vivo
8a	12	PALI	SC	0.16, 0.63, 2.5, 10	1	RO-D$_2$	in vivo
8b	18	RIS	SC	0.04, 0.16, 0.63, 2.5, 10, 40	1	RO-D$_2$	in vivo
9	19	RIS	IP	0.01, 0.03, 0.01, 0.3, 1	1	PC-R, BC-R, RO-5HT$_{2A}$	in vivo
10	20	RIS	IP	0.1	0.25, 0.5, 1, 1.5, 2	PC-R, BC-R, RO-5HT$_{2A}$	in vivo
11	24	RIS	IP	0.01, 0.03, 0.01, 0.3, 1, 3	1	PC-R, RO-5HT$_{2A}$	ex vivo
12	15	RIS	IP	0.1, 0.3, 0.8, 1	1	PC-R, RO-5HT$_{2A}$	in vivo

[1] – drug administered
[2] – route of administration
[3] – method used for RO measurement

RIS – risperidone, PALI – paliperidone, IV – intravascular, IP – intraperitoneal, SC – subcutaneous, PC-R – RIS plasma concentration, PC-P – PALI plasma concentration, BC – brain concentration, StrC – striatum concentration, CorC – cortex concentration, RO – receptor occupancy, NA – not applicable.

Model development

We used a population approach to describe the pharmacokinetics and pharmaco-dynamics (receptor binding) of RIS and PALI and to obtain population parameter estimates together with the inter-individual variability. Modeling was done using the non-linear mixed effects modeling software NONMEM (version VII level 2) (13). ADVAN 13 subroutine was used to allow explicit writing of differential equations describing receptor dynamics (APPENDIX). Log-transformed plasma and brain drug concentrations were used for the data analysis, and concentrations below the limit of quantification were excluded from this analysis.

Inter-individual variability (IIV) on each parameter was modeled assuming a log-normal distribution. Additive, proportional and combined residual error models were tested.

A number of structurally different PK and PD models have been evaluated (see below). Model selection was based on the likelihood ratio test, parameter estimates and their relative standard errors, residual error values and goodness-of-fit plots. An additional structural parameter or inter-individual variability was included in the model, if the resulting change in objective function value (ΔOFV) was >6.64 (p<0.01 assuming χ^2 distribution). The following goodness-of-fit plots were inspected visually in order to assess the fit of the model to the data: observations versus population and individual predictions, individual weighted residuals versus individual predictions and conditional weighted residuals (CWRES) versus time.

During the analysis, Pirana software (14) was used for NONMEM run management and Xpose package in R (15, 16) for making diagnostic plots.

General model structure and modeling approach

We did a sequential analysis where we first described the plasma PK of RIS and PALI in a conventional compartmental way. We assumed that this analysis provides an adequate description of concentration in plasma, which in turn is the driving concentration for the brain distribution and receptor binding model. Therefore, it is appropriate to fix plasma parameters while simultaneously estimating brain distribution and receptor binding parameters from brain concentration and receptor occupancy data. This has been done in the second part of the analysis.

Plasma PK model

One- and two-compartment models for both RIS and PALI were tested. For SC and IP administration different absorption models were tested: zero-order and first-order absorption in combination with a lag time. For IP dosing of RIS we checked models with and without first pass metabolism by assuming that part of the administered RIS dose is converted to PALI before reaching the systemic circulation. Bioavailability for IP and
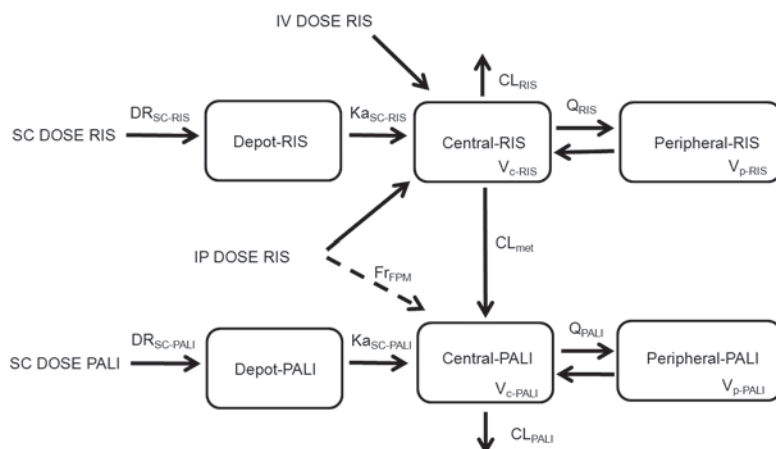
Figure 4.1: *A schematic representation of the plasma PK model. Plasma PK of both RIS and PALI follows a two-compartment model. IV and IP dosing goes directly to the central compartment. A fraction of the absorbed dose for IP RIS route of administration goes directly to the RIS central compartment and a fraction of the absorbed dose goes to the PALI central compartment (Fr_{FPM}) representing first pass metabolism. Absorption after SC dosing is described by consecutive zero- and first order processes for both RIS and PALI. DR_{SC} is the duration of the zero-order process after SC dosing. Total elimination clearance of RIS is divided into metabolic clearance (CL_{met}) and the clearance by other routes of elimination (CL_{RIS}).*

SC doses were estimated relative to IV dosing. Since there were no data after IV administration of PALI, we assumed that RIS and PALI have the same bioavailability for the SC route of administration. This allows estimating the volume of distribution and other absorption parameters of PALI. To account for metabolite formation we divided the elimination clearance for RIS into two clearances: metabolic clearance to PALI (CL_{met}) and clearance by other routes of elimination (CL_{RIS}). (Figure 4.1). First-order conditional estimation method (FOCE) was used to obtain PK parameter estimates.

PKPD modeling
After finding the appropriate plasma PK model, population parameters for plasma (mean and inter-individual variability) were fixed after which brain concentrations and RO were fitted simultaneously. Initially only D_2 RO was taken into account as D_2 binding is assumed to be crucial for the drug's antipsychotic action (2). We started with the previously published hybrid physiologically-based PKPD model (9), but

also checked simplifications of this model, i.e. binding not affecting brain kinetics (simplified model from (9)) and reduction in the number of brain compartments by merging intra- and extra-vascular compartments together or assuming only one compartment for drug not bound to receptors in the brain.
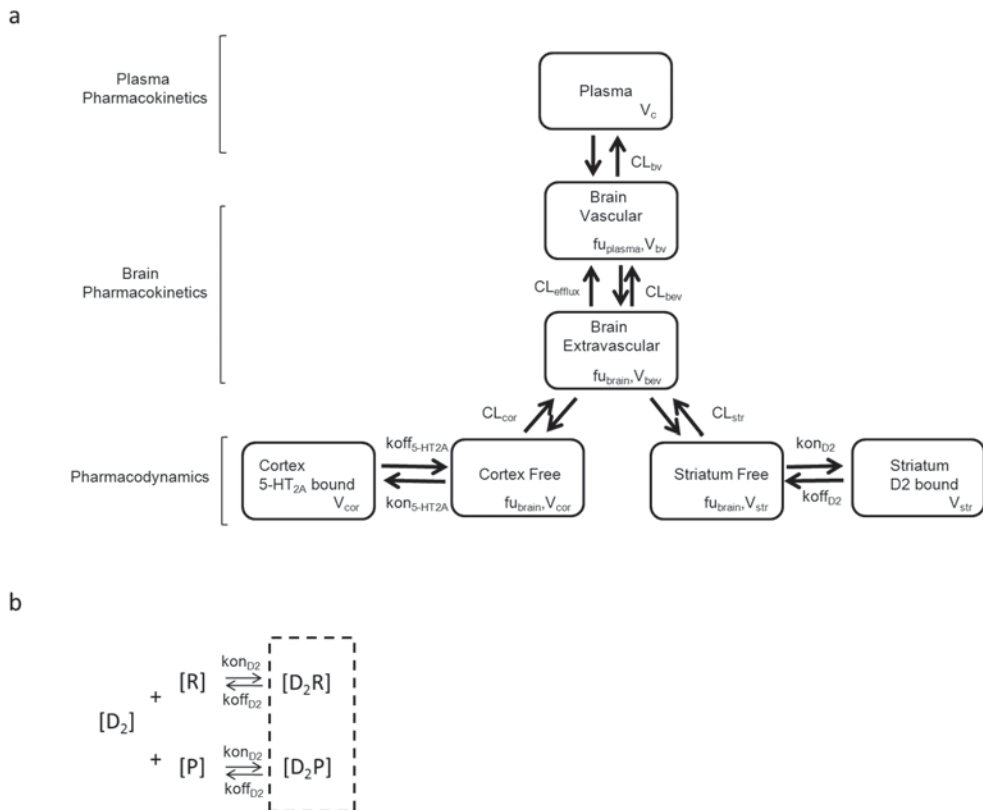
Figure 4.2: *(a) A schematic representation of the PKPD model. The plasma PK has been omitted (see Figure 1) and brain kinetics and receptor binding have been presented here for one drug only because of the complexity of the model. The same model structure applies for RIS and PALI. (b) Representation of the competitive binding to the same receptors by RIS and PALI. Measured RO is the sum of occupancies obtained by both drugs. Here only binding to D_2 receptors is shown. The same principle applies for 5-HT$_{2A}$ receptors. [D_2] – concentration of free D_2 receptors, [R] – unbound concentration of RIS, [D_2R] – concentration of D_2 receptor complex with RIS, [P] – unbound concentration of PALI, [D_2P] – concentration of D_2 receptor complex with PALI. D_2 receptor occupancy (RO) is the sum of RO exerted by both drugs.*

The hybrid physiology-based PKPD model consists of four compartments in brain: vascular, extra-vascular, striatum free and striatum bound compartment (Figure 4.2). Volumes of these compartments were fixed to physiological values: 0.00024, 0.00656, 0.0002 L/kg for vascular, total extra-vascular and striatum, respectively (17, 18). Clearance between plasma and vascular compartment (CL_{bv}) was assumed to be equal to cerebral blood flow in rats, which is 0.312 L/h/kg (17), for both RIS and PALI. In the model, transport of RIS and PALI between the vascular and extra-vascular compartment across the blood-brain barrier (BBB) was governed by two processes: passive diffusion and active efflux. Separate values of passive clearance (CL_{bev}) and active efflux clearance (CL_{efflux}) were estimated for RIS and PALI when possible. We checked whether linear or saturable efflux processes described the data best. Only unbound drug could cross the brain-blood barrier (BBB). Plasma protein binding is constant over wide range of concentrations in humans (19). We assumed that the same is true for rats and plasma and brain fraction unbound were fixed to literature values: $fu_{plasma-RIS}$=0.0798, $fu_{brain-RIS}$=0.0699, $fu_{plasma-PALI}$=0.129, $fu_{brain-PALI}$=0.0755 (20).

We assumed fast equilibration between the extra-vascular and striatum free compartments. This was achieved by fixing the corresponding clearance (CL_{str}) to a high value (500 L/h/kg). In striatum, RIS and PALI reversibly bind to D_2 receptors. Binding to receptors was described using k_{on} as the receptor association rate constant ($nM^{-1}h^{-1}$), K_{off} as the receptor dissociation rate constant (h^{-1}), and B_{max} as the maximum binding capacity of these drugs to the receptor. Including explicit binding kinetics is justified because of the hysteresis observed between D_2 (or $5-HT_{2A}$) receptor occupancy and brain concentration when excluding striatum or frontal cortex (from D_2 and $5-HT_{2A}$ occupancy studies, respectively; data not shown). RIS and PALI compete for the same receptors and hence the measured RO is the sum of occupancies obtained by both drugs.

Both RIS and PALI have a strong affinity towards $5-HT_{2A}$ receptors. Therefore, we decided to evaluate also an extended model in which we included binding to these receptors in the frontal cortex, where the density of $5-HT_{2A}$ receptors is the highest (21). To that end, we included two additional compartments: cortex free and cortex bound. We fixed the volume of frontal cortex to 0.0035 L/kg (22). As for striatum, we assumed fast equilibration between brain extra-vascular and cortex free compartments. Binding to $5-HT_{2A}$ receptors was described using k_{on}, K_{off} and B_{max} values specific for these receptors. Kd (dissociation rate constant) and K_{off} were estimated from the model and k_{on} was calculated as K_{off}/Kd. We checked whether we could estimate different binding constants for data obtained from *in vivo* and *ex vivo* binding experiments.

First-order conditional estimation method (FOCE) was used to fit the models.

Model evaluation

For the plasma PK model a bootstrap analysis was done to determine the precision of the parameter estimates. In the bootstrap technique, bootstrap replicates are generated by randomly sampling individuals from the original dataset with replacement. 1000 samples were used and they were stratified by study. Parameter estimates for each of the re-sampled datasets were obtained by fitting the final plasma PK model using NONMEM. Median, 5-th and 95-th percentiles were calculated for all the parameters and medians of bootstrap estimates were compared with parameter values obtained from the original dataset.

Additionally, since the original dataset is rather heterogeneous and bootstrapping may lead to biased results, we also did log-likelihood profiling (LLP). In this method each parameter is in turn fixed to lower or higher values than the one estimated by the model and the reduced model is fit to the data. Obtained OFV is compared with the OFV of the original model. The 90% confidence interval (CI) of a parameter is calculated by finding the value of the parameter at which the difference in OFV is 3.84 (p=0.05 assuming χ^2 distribution). Bootstrap analysis and log-likelihood profiling were done with the help of the software package Perl Speaks NONMEM (PsN) (23).

Due to the great heterogeneity of the dataset and very long run times we did not perform a bootstrap analysis for the PD model. However, we did the log-likelihood profiling to find 90% CIs of the parameter values.

In order to check the predictive performance of the model we simulated 1000 datasets from the final PKPD model. Then we graphically compared the observed plasma and brain concentrations and D_2 and 5-HT_{2A} RO with median and 90% prediction intervals calculated from the simulated data for each dose and route of administration separately.

Brain-to-plasma ratios

We simulated brain and plasma concentrations based on population parameter estimates (without inter-individual and residual variability) for doses and time points corresponding to the ones seen in the data set. For each simulated time point we calculated brain-to-plasma ratios and compared them graphically with the observed brain-to-plasma ratios, plotting only brain-to-plasma values if both plasma and brain concentrations were above the level of quantification. To check the influence of different parameters, we also simulated the brain-to-plasma ratio pattern in the absence of active efflux and with a 10 times higher value of brain clearances and of increases or decreases of the receptor association and dissociation constants k_{on} and K_{off}. To that end, we either fixed CL_{efflux} to zero or used CL_{bev} and CL_{efflux} 10 times higher than estimated from the model, or k_{on}/K_{off} values 10 times lower or higher than estimated by the model. All other parameter values were the same as estimated by the model. We used R software for the simulations.

Table 4.2: Parameter estimates of the plasma PK model from the original dataset and from 1,000 bootstrap replicates.

Parameter	Parameter estimate (% RSE)	Bootstrap median	5th-95th percentile from bootstrap	90% CI obtained from log-likelihood profiling
$F_{IP\text{-}RIS}$	0.412 (12)	0.413	0.314-0.540	0.321-0.530
F_{SC}	0.816 (9)	0.810	0.654-1.03	0.672-0.987
Fr_{FPM}	0.268 (12)	0.271	0.213-0.337	0.209-0.332
$Ka_{SC\text{-}RIS}$ (1/h)	2.84 (20)	2.90	2.25-4.07	2.13-4.16
$Ka_{SC\text{-}PALI}$ (1/h)	1.31 (22)	1.31	1.00-1.77	0.969-1.84
$DR_{SC\text{-}RIS}$ (h)	0.161 (55)	0.170	0.0157-0.313	0.0490-0.283
$DR_{SC\text{-}PALI}$ (h)	0.162 (54)	0.167	0.0848-0.261	0.0276-0.320
$V_{c\text{-}RIS}$ (L/kg)	1.29 (6)	1.28	1.07-1.56	1.11-1.49
CL_{RIS} (L/h/kg)	1.62 (9)	1.62	1.29-2.07	1.34-1.95
CL_{met} (L/h/kg)	0.775 (11)	0.757	0.591-0.974	0.623-0.961
$V_{p\text{-}RIS}$ (L/kg)	0.169 (16)	0.168	0.128-0.223	0.131-0.220
Q_{RIS} (L/h/kg)	0.0882 (25)	0.0891	0.0529-0.137	0.0601-0.132
$V_{c\text{-}PALI}$ (L/kg)	1.27 (15)	1.21	0.0647-1.64	0.0087-1.66
CL_{PALI} (L/h/kg)	1.06 (10)	1.04	0.768-1.36	0.847-1.32
$V_{p\text{-}PALI}$ (L/kg)	0.251 (54)	0.281	0.119-2.11	0.0767-75.5
Q_{PALI} (L/h/kg)	0.269 (128)	0.245	0.0428-23.4	0.0294-48.3
Inter-individual variability				
IIV-FIP (%CV)	80.6 (7.7)	80.4	70.8-89.7	70.0-92.9
IIV-$Ka_{SC\text{-}RIS}$ (%CV)	46.4 (52.3)	47.9	29.5-70.5	27.1-84.3
IIV-$Ka_{SC\text{-}PALI}$ (%CV)	34.4 (30.2)	33.0	11.12-50.6	17.0-58.7
IIV-$DR_{SC\text{-}RIS}$ (%CV)	91.2 (80.6)	84.2	0.912-287	17.3-211
IIV-CL_{RIS} (%CV)	30.5 (13.3)	29.7	16.3-38.2	23.2-39.0
IIV-CL_{PALI} (%CV)	16.2 (32.8)	16.0	10.4-22.6	10.9-24.5
Proportional residual error				
Risperidone	0.233 (16.5)	0.220	0.174-0.279	0.192-0.288
Paliperidone	0.186 (14.2)	0.171	0.131-0.214	0.147-0.238
% RSE – Relative Standard Error as calculated by NONMEM covariance step. Inter-individual variability is expressed as percent coefficient of variation.				

Results

Plasma PK

Plasma PK was best described by a two-compartment model for both RIS and PALI (Figure 4.1). For the SC route of administration consecutive zero- and first-order absorption described the data best. For the IP route absorption parameters could not be estimated and it was assumed that dosing was directly to the central compartment. However, including first pass metabolism where a fraction of the RIS dose goes directly to the PALI central compartment improved the fit of the model. Parameter estimates of the final model are given in Table 4.2. In the final model six inter-individual variability parameters (for F_{IP}, Ka_{SC-RIS}, $Ka_{SC-PALI}$, DR_{SC-RIS}, CL_{RIS}, CL_{PALI}) were retained.

Parameters for the rate of zero-order absorption and volume of distribution and inter-compartmental clearance for PALI could not be estimated precisely (Table 4.2). However, we decided to keep them in the model since removing them led to a significantly worse fit and it was important to describe the plasma PK as precisely as possible for the description of brain kinetics and receptor binding.

Goodness-of-fit plots did not show any systematic deviation between observations and population and individual predictions nor any trends in conditional weighted residuals versus time, which demonstrates that this model adequately describes the plasma PK of RIS and PALI (Figure 4.3).

PKPD

The previously published hybrid physiology-based PKPD model (9) fitted the data best after adjusting for binding to 5-HT$_{2A}$ receptors (Figure 4.2). A model with only D$_2$ receptor binding (9) led to high residual error (>60%) for brain concentration. Using a combined error model reduced the proportional error to some extent. However, this model did not explain the observed brain-to-plasma ratio adequately (Figure 4.6a-b). These problems were overcome when the model was extended to include 5-HT$_{2A}$ receptor binding in frontal cortex.

Our data did not allow us to estimate reliably all brain clearance parameters ($CL_{bev-RIS}$, $CL_{efflux-RIS}$, $CL_{bev-PALI}$, $CL_{efflux-PALI}$). Change in parameter values within relatively wide range did not lead to changes in model fit. Therefore, we assumed that CL_{bev} or CL_{efflux} is the same for RIS and PALI. Assuming a single CL_{efflux} parameter led to termination problems. However, the model with a single CL_{bev} value had an OFV only slightly lower (<0.5) than the model with four clearance parameters and RSE values obtained from the covariance step were acceptable. Therefore, in the final model CL_{bev} was assumed to be the same for RIS and PALI.
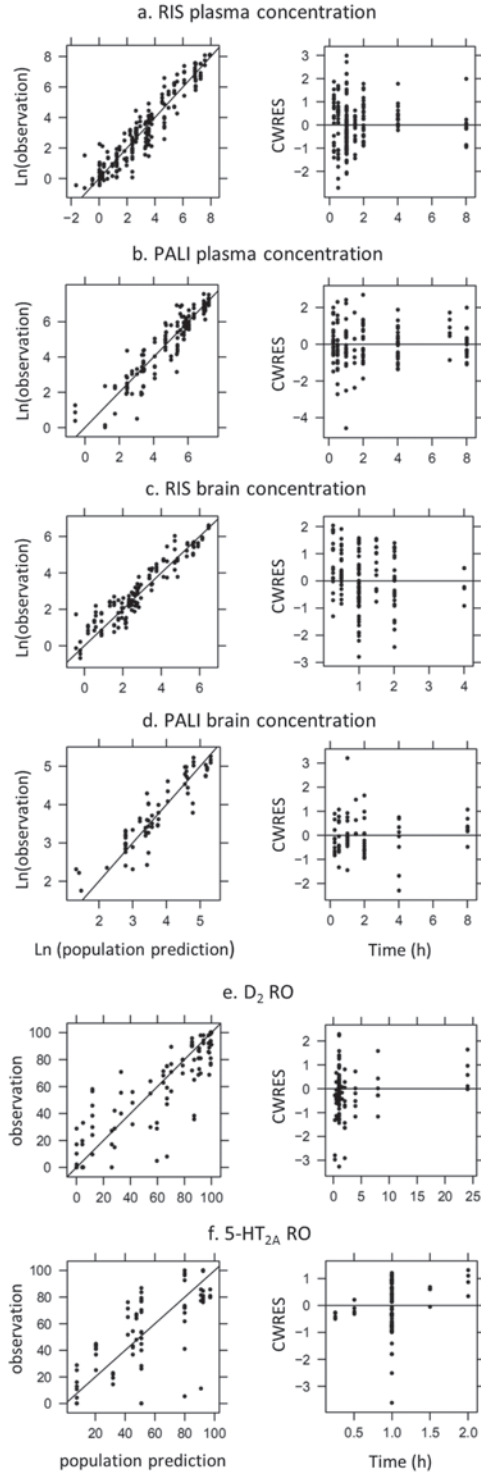
Figure 4.3: *Goodness-of-fit plots of the PKPD model. Presented are scatter plots of plasma and brain concentrations and D_2 and 5-HT_{2A} RO versus population predictions and conditional weighted residuals (CWRES) versus time.*

Different Kd and K_{off} values for D_2 and 5-HT$_{2A}$ were estimated by the model. However, we were not able to estimate different Kd and K_{off} values for RIS and PALI, therefore we assumed that Kd and K_{off} values are the same for RIS and PALI, which is consistent with literature *in vitro* values (24). Similarly, we also had to assume that the binding rate constants for both *in vivo* and *ex vivo* binding RO measurements were the same. Describing active efflux from brain as a saturable process did not improve the fit therefore in the final model the active efflux was assumed to be linear. Due to the complexity of the model we were not able to estimate IIV variability for the brain PKPD model parameters. Therefore, we fixed the IIV parameters to zero. Final parameter estimates of the model are given in Table 4.3.

4

Table 4.3: Parameter estimates of the PKPD model and their relative standard error.			
Parameter	Parameter estimate	% RSE	90% CI obtained from log-likelihood profiling
$CL_{bev\text{-}RIS}$ (L/h/kg)	2.13	29	0.333- >1000[c]
$CL_{bev\text{-}PALI}$ [a] (L/h/kg)	2.13	29	0.333- >1000[c]
$CL_{efflux\text{-}RIS}$ (L/h/kg)	9.97	28	1.49- >1000[c]
$CL_{efflux\text{-}PALI}$ (L/h/kg)	46.5	28	7.24- >1000[c]
Kd_{D2} (nM)	0.463	14	0.336-0.628
$K_{off\text{-}D2}$ (1/h)	0.671	19	0.427-1.03
$K_{on\text{-}D2}$ [b] (1/nM/h)	1.45	-	-
$B_{max\text{-}D2}$ (nM)	245	15	194-305
$Kd_{5\text{-}HT2A}$ (nM)	0.219	15	0.134-0.313
$K_{off\text{-}5\text{-}HT2A}$ (1/h)	0.525	25	0.257-0.970
$K_{on\text{-}5\text{-}HT2A}$ [b] (1/nM/h)	2.40	-	-
$B_{max\text{-}5\text{-}HT2A}$ (nM)	47.0	11	37.3-58.9
Residual error			
Proportional BC RIS	0.362	7	0.315-0.419
Proportional BC PALI	0.424	18	0.351-0.519
Additive % D_2 RO	17.7	8	15.1-20.7
Additive % 5-HT$_{2A}$ RO	18.2	7	1.49-22.4
% RSE – percent Relative Standard Error as calculated by NONMEM covariance step. BC – brain concentration [a] – assumed to be the same as $CL_{bev\text{-}RIS}$ [b] – calculated as $k_{on}=k_{off}/Kd$ [c] – OFV does not change with increasing parameter value			

Goodness-of-fit plots did not show any systematic deviation between observations and population and individual predictions nor trends in CWRES versus time, which demonstrates that this model adequately describes the brain concentrations of RIS and PALI and their D_2 RO (Figure 4.3). Some time-course pattern can be seen in the plot of CWRES versus time for 5-HT$_{2A}$ RO, but CWRES values are relatively low.

Model evaluation

Median bootstrap parameter estimates of the PK model were in good agreement with model estimated population values (Table 4.2). 90 % confidence intervals were large for some parameters, especially related to absorption and for the PALI peripheral compartment.

Results of log-likelihood profiling for brain parameters show that most parameters are estimated precisely with exception of the brain clearance parameters (Table 4.3). Further inspection of results showed that the values of clearance parameters (CL_{bev}, $CL_{efflux-RIS}$ and $CL_{efflux-PALI}$) did not influence model fit and other parameter estimates much. The upper limits of CI for these parameters could not be found, showing that the transport is fast and equilibration between brain and plasma is not much affected by the exact values of clearances. Moreover, close inspection of the results show that relative value of active efflux clearance to passive clearance seems to be very constant. For all the values of CL_{bev}, $CL_{efflux-RIS}$ and $CL_{efflux-PALI}$ inspected by LLP, the ratio of $CL_{efflux-RIS}$ to CL_{bev} was in range of 4.57-4.87 while ratio of $CL_{efflux-PALI}$ to CL_{bev} was in range of 21.1-22.2.

Some of the predictive check results are depicted in Figure 4.4. We present the result for the IP route of administration for doses of 0.1 and 1 mg/kg since for these doses there were time course data available for 5-HT$_{2A}$ and D_2 RO and they had more data points than other doses. Practically all observations fall within the range of the 5-th and 95-th percentile. Median time course of D_2 RO is predicted well. For 5-HT$_{2A}$, RO seemed to be underestimated for later time points. Prediction intervals are very wide since the residual error in our model is also relatively big. However, it should be noted that the variability of the data is also large (see for example 5-HT$_{2A}$ RO at 1h).

Inspection of the model-predicted plasma and brain concentrations for the cases where observations were reported to be below the level of quantification (LOQ), shows that exclusion of the observations below LOQ from the analysis did not lead to a significant bias. For the studies where LOQ was known, only around 15% of observations were above LOQ and in less than 5% of the cases of total predicted concentrations were outside the confidence intervals based on the residual standard error. For the studies where LOQ was not known the predicted concentrations were also low.
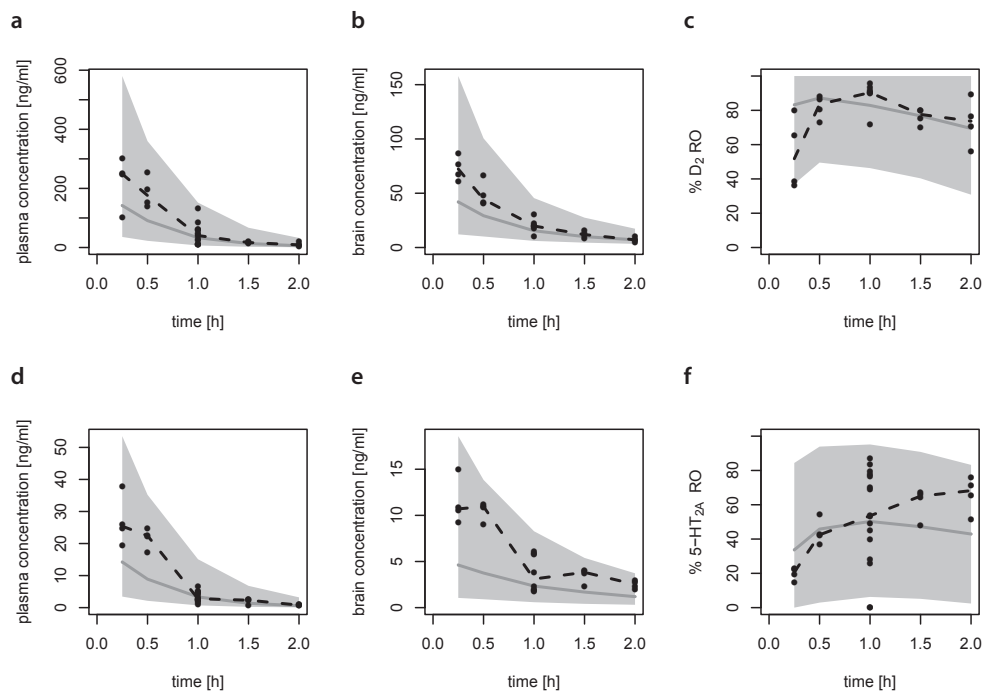
Figure 4.4: *Predictive check of the PKPD model.. Panels **a-c** represent respectively risperidone plasma concentration, risperidone brain concentration after removing striatum and D_2 RO after IP administration of a 1 mg/kg dose of risperidone. Panels **d-f** represent respectively risperidone plasma concentration, risperidone brain concentration after removing frontal cortex and 5-HT_{2A} RO after IP administration of a 0.1 mg/kg dose of risperidone. Dots represent the observed data; the dashed line represents the median of the observed data; the shaded area represents 90% prediction interval based on 1000 simulated datasets; the grey line represents the median of the simulated data.*

Brain-to-plasma ratios

The observed brain-to-plasma ratios were higher at lower plasma concentrations and even out as plasma (or brain) concentration increases, both for RIS and PALI (Figure 4.5). Even after multiplication of the brain-to-plasma ratio by $fu_{brain}/fu_{plasma}=0.876$ and obtaining "free brain-to-plasma ratio", the brain-to-plasma ratio at higher concentrations is lower than one due to active efflux from the brain. This brain-to-plasma ratio pattern was seen for both the total brain concentration and the concentration measured in brain excluding striatum (from the studies where D_2 RO was measured) or excluding frontal cortex (from studies where 5-HT_{2A} RO was measured). A model with only D_2 receptor binding in striatum did not predict higher brain-to-plasma

ratios for lower concentrations (Figure 4.6a-b). Including binding to 5-HT$_{2A}$ receptors in the model predicted brain-to-plasma ratios well (Figure 4.6a-c) over the entire concentration range.

Fixing CL$_{efflux}$ to zero led to an increase of brain-to-plasma ratios, but the general pattern stayed the same (Figure 4.6d). Increasing CL$_{bev}$ and CL$_{efflux}$ had virtually no effect on the brain-to-plasma ratios (not shown). If K$_{off}$ and k$_{on}$ values for both D$_2$ and 5-HT$_{2A}$ receptors were 10 times higher (implying no change in Kd) then brain-to-plasma ratios at lower concentrations were slightly lower and at higher concentrations they were the same as in the original model (Figure 4.6e). The same effect was
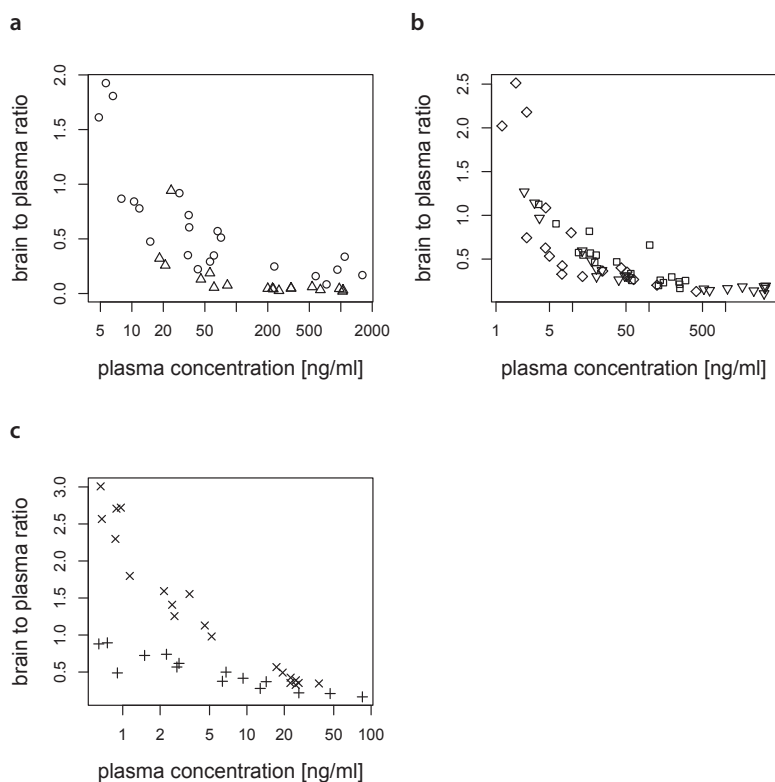

Figure 4.5: *Brain-to-plasma ratios against plasma concentrations. (**a**) Data from studies where total brain concentration was measured; circles – RIS, triangles – PALI. (**b**) Data from D$_2$ RO studies where brain concentration was measured after removing striatum. (**c**) Data from 5-HT$_{2A}$ RO studies where brain concentration was measured after removing frontal cortex. For b and c only RIS data was available and different symbols represent different studies.*
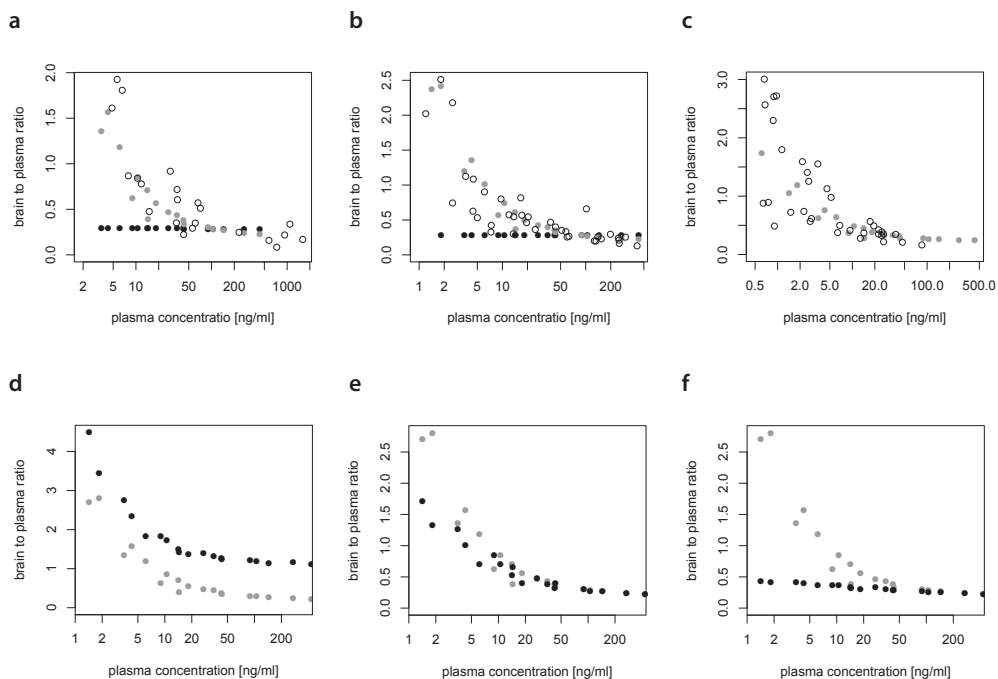
Figure 4.6: *Observed and simulated brain-to-plasma ratios. Open circles in panels a-c represent observed brain-to-plasma ratios for total brain (**a**), brain excluding striatum – from D_2 RO studies (**b**) and brain excluding frontal cortex – from 5-HT$_{2A}$ RO studies (**c**). In all the panels gray dots represent predictions of our final model. Black dots represent prediction of the model with only D_2 receptor binding (**a-b**), or prediction of final model but assuming no efflux (**d**), k_{on} and k_{off} values 10 times higher (**e**) or k_{off} values 10 times higher (**f**) than in the final model. Only total brain-to-plasma ratios are depicted in panels d-f. Qualitatively similar results were obtained for brain concentrations from D_2 and 5-HT$_{2A}$ studies.*

visible with and without efflux. Increasing Kd by increasing k_{off} leads to an almost constant brain-to-plasma ratio (Figure 4.6f). Increasing Kd by decreasing k_{on} had a similar effect, but less pronounced (data not shown). If we increased k_{off} for D_2 receptors only, then brain-to-plasma ratios became constant only for brain concentrations excluding cortex (brain concentration measured in 5-HT$_{2A}$ RO studies; data not shown). If we increased k_{off} only for 5-HT$_{2A}$ receptors then brain-to-plasma ratios became constant only for brain concentrations excluding striatum (brain concentration measured in D_2 RO studies; data not shown).

Discussion

In this paper we present an extension of the previously published PKPD model for olanzapine (9) to two other antipsychotic drugs: risperidone and paliperidone. This model describes the time course of D_2 receptor occupancy after administration of the antipsychotics and takes brain distribution into account. Here, we expand the model by taking into account metabolite formation and its receptor binding, active efflux from the brain and binding to 5-HT$_{2A}$ receptors.

Some antipsychotic drugs (such as risperidone and aripiprazole) have active metabolites. The active metabolite of risperidone, paliperidone, achieves high concentrations in plasma and brain (25, 26). It also shows potent binding to D_2 and 5-HT$_{2A}$ receptors and is by itself a potent antipsychotic drug (27, 28). Therefore, to describe receptor occupancy of a parent drug in a mechanistic way, it is necessary to take into account formation, brain kinetics and receptor binding of the metabolite.

It has been shown in *in vitro* studies and studies with knockout mice, that both risperidone and paliperidone are P-gp substrates (10). Inclusion of active efflux at the BBB in the model was indeed necessary to describe the data properly. Relative values of model predicted parameters for active efflux at the BBB for both drugs are in line with previous experimental studies. Most of the studies with mdr1a knockout mice (10, 29) show that the difference in brain-to-plasma ratios between the knockout and the wild-type mice is considerably larger for paliperidone in comparison to risperidone (with one exception where the ratio is slightly higher for risperidone (30)). Similar results have been found in *in vitro* experiments with MDCK cells in an transwell assay (31) and are in line with our results. It has been assumed in our model that the active efflux is a linear process. This seems to be a valid assumption for risperidone and paliperidone, since modeling the active transport as a saturable process did not improve the fit. This is in line with the finding that the highest brain concentrations of risperidone and paliperidone seen in our dataset were around 2 μM, while the Km values (concentration of substrate yielding half maximum activity) for P-gp transport from *in vitro* studies range between 5.6 to 26 μM (30, 32, 33). So clearly, the concentrations observed *in vivo* are far below the saturation levels for risperidone and paliperidone.

Paliperidone is less lipophilic than risperidone, therefore one would expect that it will diffuse slower through biological membranes. However, *in vitro* essays show that passive permeability of risperidone and paliperidone are quite similar (31). Therefore, assuming the same value for passive clearance through BBB can be justified. Probably more data, especially for paliperidone, would be needed to estimate separate parameters of both drugs. However, it should be noted that it might be difficult to estimate passive and active clearance parameters reliably. It seems that, at least in our dataset,

brain concentration is only informative about the ratio of active and passive processes. Extensive simulation study would be probably necessary to establish what data is needed in order to be able to estimate precisely brain clearance parameters.

Another extension of the previous model developed for olanzapine is the inclusion of binding to 5-HT$_{2A}$ receptors. We included binding to 5-HT$_{2A}$ receptors when we observed that the model with binding only to D$_2$ receptors in striatum did not provide a good fit to the data and also after inspecting observed and model predicted brain-to-plasma ratio plots (Figures 4.5, 4.6a-c). The brain-to-plasma ratio was not constant for risperidone, suggesting the influence of specific binding to receptors on the brain kinetics. Similar plots made for olanzapine show that the brain-to-plasma ratio is practically constant and that the brain concentrations of olanzapine are higher than those for risperidone (data not shown). This suggests that olanzapine shows a different pattern of brain kinetics than risperidone and paliperidone. Therefore, we explored the influence of the different parameters on the brain-to-plasma ratio. First, we simulated brain-to-plasma ratios assuming no active efflux, to see if higher brain concentrations would lead to more constant brain-to-plasma ratios. Our simulations show that even without efflux, the brain-to-plasma ratios were not constant (Figure 4.6d), suggesting that the higher brain-to-plasma ratio was not related to the active efflux process. Next we investigated whether the pattern could be explained by the disequilibrium between plasma and brain caused by slow transport between the two. However, increasing brain clearance had virtually no effect on brain-to-plasma ratios. We also looked at the influence of receptor binding parameters on the brain-to-plasma ratios. Therefore, we simulated the influence of increasing values for both k_{off} and k_{on} ten-fold, reflecting a more rapid equilibration of receptor binding, without changing the receptor affinity Kd. This resulted in slightly lower brain-to-plasma ratios at the lowest concentrations (Figure 4.6e). This suggests that the increased brain-to-plasma ratio may be only partly explained by disequilibrium between unbound and bound drug. Finally, an increase of the Kd values by increasing k_{off} or decreasing k_{on} ten-fold led to more constant brain-to-plasma ratios (Figure 4.6f). A higher Kd implies that receptor occupancy is lower at the same unbound brain concentration, and therefore the contribution of the bound drug to the total brain concentration is less pronounced, resulting in a lower brain-to-plasma ratio.

Olanzapine has lower binding affinity for D$_2$ and 5-HT$_{2A}$ receptors than risperidone and paliperidone (9, 34). According to our model, brain-to-plasma ratios are constant under these conditions. The lower D$_2$ binding affinity of olanzapine as compared with risperidone may explain why for olanzapine a simpler model with only binding to D$_2$ receptor and binding not affecting brain kinetics could explain the data well (9). Risperidone and paliperidone have relatively low values of the dissociation constant for 5-HT$_{2A}$ receptors compared to other antipsychotics (34, 35), so

one would expect that a simpler model (where binding to 5-HT$_{2A}$ receptors does not affect brain distribution) could be appropriate for these drugs. Even in cases where k$_{on}$ and k$_{off}$ values are unknown, plotting brain-to-plasma ratios against plasma concentrations would indicate whether a simpler model would be appropriate.

In the model for olanzapine, the receptor density (B$_{max}$) did not influence the model fit and could be removed from the model (9). For risperidone and paliperidone, receptor binding influenced brain kinetics, therefore receptor density was an important parameter. This was demonstrated by the precise estimate of B$_{max}$ for both D$_2$ and 5-HT$_{2A}$ receptors (Table 4.3). B$_{max}$ values estimated by the model were 245 nM and 47.0 nM for D$_2$ receptors in striatum and 5-HT$_{2A}$ receptors in frontal cortex, respectively. This 5-HT$_{2A}$ receptor density is in line with the values of 25-60 nM estimated from *in vitro* studies (36-39) (assuming 10% protein content (40)). Average D$_2$ receptor density from *in vitro* studies is 48 nM (40) with a highest estimated value of 75 nM (41). This is approximately 3 to 5 times lower than the value estimated by the model. However, some discrepancy is not surprising since in our model B$_{max}$ represents the theoretical receptor density, while in *in vitro* assays it represents the density of receptors available for the radioligand used. Fixing B$_{max}$ to values different than the ones estimated by the model worsened the model fit (results not shown). Simulations showed that changing B$_{max}$ values lead to considerable changes in brain concentration and receptor occupancy (data not shown).

To our knowledge, no values are published for *in vivo* or *in vitro* association and dissociation constants for D$_2$ or 5-HT$_{2A}$ receptors in rats for risperidone and paliperidone. *In vitro* binding constant (Ki) values (which can approximate Kd values) for D$_2$ binding found in literature are usually around 2 to 3 nM (34, 42-44), however a value of 0.44 for risperidone has also been reported (45). For 5-HT$_{2A}$ binding *in vitro* Ki values of 0.12-0.39 and 0.25 nM for risperidone and paliperidone, respectively, have been reported (34, 42, 43, 45). Therefore, the *in vivo* values obtained in our model are within the range of *in vitro* values in rat tissues for 5-HT$_{2A}$ binding and somehow on the lower end of the *in vitro* range for D$_2$ binding. Difference between values obtained *in vivo* and *in vitro* may be caused by different radioligands used in *in vitro* and *in vivo* studies. It is also conceivable that the receptor-binding properties of drugs in brain neuronal cells under *in vivo* conditions differ significantly from those in brain homogenates and membrane fractions (46).

We assumed the same binding affinities for risperidone and paliperidone, since our data sets did not allow estimation of separate k$_{on}$ and k$_{off}$ values for risperidone and paliperidone. More receptor occupancy data for paliperidone would be necessary to estimate paliperidone association and dissociation rate constants. However, since published *in vitro* Ki values in rat brain tissues are similar for risperidone and paliperidone (34), assuming the same rate constants for both drugs should not lead

to much bias, especially since the parameters were estimated quite precisely (RSE between 14 and 25%).

Assuming the same values for binding constants for risperidone and paliperidone may theoretically be one of the reasons why there are relatively big residual errors for brain concentrations and receptor occupancy estimated in our model (Table 4.3). This could also apply to RO measurements obtained from *in vivo* and *ex vivo* studies. Trying to estimate separate binding parameters for *in vivo* and *ex vivo* measurements or excluding the less common *ex vivo* RO data from the analysis resulted in problems with model convergence and in less precise parameter estimates. Use of different rat strains could also theoretically explain at least a part of the intra- and inter-individual variability. However, when we plotted individual post-hoc estimates for different parameters, we did not see any difference between the different rat strains or different RO measurement methods.

Considerable residual errors both in PK and PD may stem partly from differences in experimental procedures (especially brain dissection) on different occasions and at the different pharmaceutical companies that provided the data. Body weight variations could also potentially explain a part of the observed inter-individual variability, but we had no information of body weight of the rats allowing us to use it as a covariate in the model. Residual errors could probably be reduced if there was an inter-individual variability in brain PKPD parameters. However, we were not able to estimate these variabilities and decided to fix them to zero.

A predictive check of the PKPD model showed that it can predict D_2 RO reasonably well up to 8 hours (Fig 4.3e, 4.5). But the model seems to lead to underprediction at 24h (Fig 4.3e). Median 5-HT_{2A} RO also seems to be under-predicted for later time points (Figure 4.4). Only two studies had a time course of D_2 RO and one study a time course of 5-HT_{2A} RO while most of the studies had only observations at the 1h time point. On the one hand, this unbalanced dataset could lead to parameter estimates which explain all data well, but with some model misspecification for the later time points. On the other hand, with just a few observations for later time points it is difficult to judge if a deviation between observation and prediction is not just a random error. More D_2 and 5-HT_{2A} RO time course data are necessary in order to obtain better description of the full time course of receptor occupancy by the model.

Our dataset shows that binding to receptors influences brain concentrations and that D_2 binding alone could not explain the data well. In the model we included binding to D_2 and 5-HT_{2A} receptors (the only available data), but both risperidone and paliperidone also bind to other receptors. *In vitro* data with rat tissue or rat cloned cells show that risperidone and paliperidone have high affinity (Ki not more than 5 times higher than Ki for D_2 receptors) for α1 and α2 adrenoceptors and for serotonin 5-HT_7 receptors (34, 44, 45). However, densities of all of these receptors

in rat brain are relatively low (below 100 fmol/mg of protein) (47-50). Therefore, we would not expect the influence of binding to these receptors on brain kinetics to be significant. Risperidone and paliperidone bind also to histamine H_1 receptors and other subtypes of dopamine and serotonin receptors (34, 45). However, since Ki values for these receptors are more than 5 times higher than Ki values for D_2 and 5-HT_{2A} receptors, based on our simulations of brain-to-plasma ratio we would not expect this binding to affect the rat brain distribution. Similarly, based on *in vitro* binding to human cloned receptors and receptor densities in the human brain (34, 51) binding to other receptors should not strongly influence brain kinetics in human.

Our model can be utilized for the human prediction of D_2 and 5-HT_{2A} RO. Using the sequential approach, human plasma PK models can be developed separately in a conventional way and receptor occupancy can be predicted afterwards. Usage of a physiology-based approach in describing brain distribution and receptor binding allows utilization of human physiological values, *in vitro* information and rat-to-human scaling to predict human receptor occupancy. This translational approach can also be used for drugs which have an active metabolite or show active efflux at the brain-blood barrier. Since it is known that D_2 RO is linked with clinical outcome and side effects of antipsychotics (2), but that it is difficult and costly to measure, the ability to predict human D_2 RO based on plasma data can help with linking different doses of drugs with their clinical effect. This work is ongoing in our research group.

In conclusion, we have shown that the previously published hybrid physiologically-based model structure developed for olanzapine (9) can be utilized to describe the PKPD of risperidone and paliperidone in rats. However, some drug-specific adjustments were necessary. Addition of active metabolite formation and active efflux was straight-forward. Additionally, binding to 5-HT_{2A} receptors has been included in order to describe the brain distribution well. This may stem from the fact that risperidone and paliperidone have higher affinity to D_2 and 5-HT_{2A} receptors than olanzapine. Therefore, receptor affinities and brain-to-plasma ratios may need to be considered before choosing the best PKPD model for centrally active drugs.

Acknowledgements & disclosures

Abbreviations

BBB	blood-brain barrier
B_{max}	receptor density
CL	systemic clearance
CL_{bev}	passive brain-extravascular clearance
CL_{bv}	brain-vascular clearance
CL_{cor}	brain-cortex clearance
CL_{efflux}	active efflux clearance
CL_{met}	metabolic clearance of RIS to PALI
CL_{PALI}	systemic clearance of PALI
CL_{RIS}	systemic clearance of RIS by other routes than metabolism to PALI
CL_{str}	brain-striatum clearance
CWRES	conditional weighted residuals
FOCE	First Order Conditional Estimation method
fu_{plasma}	unbound fraction in plasma
fu_{brain}	unbound fraction in brain
GOF	Goodness Of Fit plots
F_{IP}	bioavailability for intraperitoneal route of administration
Fr_{FPM}	Fraction of the absorbed RIS IP dose going directly to PALI central compartment
F_{SC}	bioavailability for subcutaneous route of administration
IIV	inter-individual variability
IP	intraperitoneal
IV	intravenous/intravenously
Kd	receptor dissociation constant
k_{on}	receptor association rate constant
k_{off}	receptor dissociation rate constant
nM	nanomoles/litre
OFV	Objective Function Value
PALI	paliperidone
PKPD	pharmacokinetic and pharmacodynamic
P-gp	P-glycoprotein
Q	inter-compartmental flow between central and peripheral compartment
RIS	risperidone
RO	receptor occupancy
RSE	Relative Standard Error
SC	subcutaneous
V_c	volume of the central compartment
V_p	volume of the peripheral compartment
V_{bv}	volume of brain-vascular compartment
V_{bev}	volume of brain-extravascular compartment
V_{cor}	volume of frontal cortex compartment
V_{str}	volume of striatum compartment

Appendix

Differential equations used to describe plasma PK:

$$d(A_{depot-RIS})/dt = DOSE_{SC-RIS}/DR_{SC-RIS}(t<DR_{SC-RIS}) - ka_{SC-RIS}{}^*A_{depot-RIS}$$

$$d(A_{c-RIS})/dt = ka_{SC-RIS}{}^*A_{depot-RIS} + (Q_{RIS}/V_{p-RIS})^*A_{p-RIS} - (Q_{RIS}/V_{c-RIS})^*A_{c-RIS} - (CL_{RIS}/V_{c-RIS})^* \\ A_{c-RIS} - (CL_{met}/V_{c-RIS})^*A_{c-RIS}$$

$$d(A_{p-RIS})/dt = (Q_{RIS}/V_{c-RIS})^*A_{c-RIS} - (Q_{RIS}/V_{p-RIS})^*A_{p-RIS}$$

$$d(A_{depot-PALI})/dt = DOSE_{SC-PALI}/DR_{SC-PALI}(t<DR_{SC-PALI}) - ka_{SC-PALI}{}^*A_{depot-PALI}$$

$$d(A_{c-PALI})/dt = ka_{SC-PALI}{}^*A_{depot-PALI} + (Q_{PALI}/V_{p-PALI})^*A_{p-PALI} - (Q_{PALI}/V_{c-PALI})^*A_{c-PALI} - \\ (CL_{PALI}/V_{c-PALI})^*A_{c-PALI} + (CL_{met}/V_{c-RIS})^*A_{c-RIS}$$

$$d(A_{p-PALI})/dt = (Q_{PALI}/V_{c-PALI})^*A_{c-PALI} - (Q_{PALI}/V_{p-PALI})^*A_{p-PALI}$$

Differential equations used to describe brain kinetics and receptor binding:

$$d(A_{bv-RIS})/dt = (CL_{bv}/V_c)^*A_{c-RIS} - (CL_{bv}/V_{bv})^*A_{bv-RIS} - (CL_{bev-RIS}/V_{bv})^*fu_{plasma-RIS}{}^*A_{bv-RIS} + \\ (CL_{bev-RIS}/V_{bev})^*fu_{brain-RIS}{}^*A_{bev-RIS} + (CL_{efflux-RIS}/V_{bev})^*fu_{brain-RIS}{}^*A_{bev-RIS}$$

$$d(A_{bev-RIS})/dt = (CL_{bev-RIS}/V_{bv})^*fu_{plasma-RIS}{}^*A_{bv-RIS} - (CL_{bev-RIS}/V_{bev})^*fu_{brain-RIS}{}^*A_{bev-RIS} - \\ (CL_{efflux-RIS}/V_{bev})^*fu_{brain-RIS}{}^*A_{bev-RIS} - (CL_{str}/V_{bev})^*fu_{brain-RIS}{}^*A_{bev-RIS} + (CL_{str}/V_{str})^* \\ fu_{brain-RIS}{}^*A_{strF-RIS} - (CL_{cor}/V_{bev})^*fu_{brain-RIS}{}^*A_{bev-RIS} + (CL_{cor}/V_{cor})^*fu_{brain-RIS}{}^*A_{corF-RIS}$$

$$d(A_{strF-RIS})/dt = (CL_{str}/V_{bev})^*fu_{brain-RIS}{}^*A_{bev-RIS} - (CL_{str}/V_{str})^*fu_{brain-RIS}{}^*A_{strF-RIS} - k_{on-D2}{}^* \\ fu_{brain-RIS}{}^*A_{strF-RIS}{}^*(B_{max-D2} - CB_{D2-RIS} - CB_{D2-PALI}) + k_{off-D2}{}^*A_{strB-RIS}$$

$$d(A_{strB-RIS})/dt = k_{on-D2}{}^*fu_{brain-RIS}{}^*A_{strF-RIS}{}^*(B_{max-D2} - CB_{D2-RIS} - CB_{D2-PALI}) - k_{off-D2}{}^*A_{strB-RIS}$$

$$d(A_{corF-RIS})/dt = (CL_{cor}/V_{bev})^*fu_{brain-RIS}{}^*A_{bev-RIS} - (CL_{cor}/V_{cor})^*fu_{brain-RIS}{}^*A_{corF-RIS} - k_{on-5-HT2A}{}^* \\ fu_{brain-RIS}{}^*A_{corF-RIS}{}^*(B_{max-5-HT2A} - CB_{5-HT2A-RIS} - CB_{5-HT2A-PALI}) + k_{off-5-HT2A}{}^*A_{corB-RIS}$$

$$d(A_{corB-RIS})/dt = k_{on-5-HT2A}{}^*fu_{brain-RIS}{}^*A_{corF-RIS}{}^*(B_{max-5-HT2A} - CB_{5-HT2A-RIS} - CB_{5-HT2A-PALI}) - \\ k_{off-5-HT2A}{}^*A_{corB-RIS}$$

$$d(A_{bv-PALI})/dt = (CL_{bv}/V_{c-PALI})^*A_{c-PALI} - (CL_{bv}/V_{bv})^*A_{bv-PALI} - (CL_{bev-PALI}/V_{bv})^*fu_{plasma-PALI}{}^* \\ A_{bvv-PALI} + (CL_{bev\ PALI}/V_{bev})^*fu_{brain-PALI}{}^*A_{bev-PALI} + (CL_{efflux-PALI}/V_{bev})^*fu_{brain-PALI}{}^*A_{bev-PALI}$$

$$d(A_{bev-PALI})/dt = (CL_{bev-PALI}/V_{bv})^*fu_{plasma-PALI}{}^*A_{bv-PALI} - (CL_{bev-PALI}/V_{bev})^*fu_{brain-PALI}{}^*A_{bev-PALI} - \\ (CL_{efflux-PALI}/V_{bev})^*fu_{brain-PALI}{}^*A_{bev-PALI} - (CL_{str}/V_{bev})^*fu_{brain-PALI}{}^*A_{bev-PALI} + (CL_{str}/V_{str})^* \\ fu_{brain-PALI}{}^*A_{strF-PALI} - (CL_{cor}/V_{bev})^*fu_{brain-PALI}{}^*A_{bev-PALI} + (CL_{cor}/V_{cor})^*fu_{brain-PALI}{}^*A_{corF-PALI}$$

$$d(A_{strF-PALI})/dt = (CL_{str}/V_{bev})^*fu_{brain-PALI}{}^*A_{bev-PALI} - (CL_{str}/V_{str})^*fu_{brain-PALI}{}^*A_{strF-PALI} - k_{on-D2}{}^* \\ fu_{brain-PALI}{}^*A_{strF-PALI}{}^*(B_{max-D2} - CB_{D2-RIS} - CB_{D2-PALI}) + k_{off-D2}{}^*A_{strB-PALI}$$

$$d(A_{strB-PALI})/dt = k_{on-D2}{}^*fu_{brain-PALI}{}^*A_{strF-PALI}{}^*(B_{max-D2} - CB_{D2-RIS} - CB_{D2-PALI}) - k_{off-D2}{}^*A_{strB-PALI}$$

$$d(A_{corF-PALI})/dt = (CL_{cor}/V_{bev})^*fu_{brain-PALI}{}^*A_{bev-PALI} - (CL_{cor}/V_{cor})^*fu_{brain-PALI}{}^*A_{corF-PALI} - k_{on-5-HT2A}{}^* \\ fu_{brain-PALI}{}^*A_{corF-PALI}{}^*(B_{max-5-HT2A} - CB_{5-HT2A-RIS} - CB_{5-HT2A-PALI}) + k_{off-5-HT2A}{}^*A_{corB-PALI}$$

$$d(A_{corB-PALI})/dt = k_{on-5-HT2A}{}^*fu_{brain-PALI}{}^*A_{corF-PALI}{}^*(B_{max-5-HT2A} - CB_{5-HT2A-RIS} - CB_{5-HT2A-PALI}) - \\ k_{off-5-HT2A}{}^*A_{corB-PALI}$$

Where subscripts RIS and PALI denote parameters referring to risperidone and paliperidone, respectively. Subscripts depot, p, c, bv, bev, strF, strB, corF, corB represent volumes (V) and amounts (A) in depot (only for SC dosing), central, peripheral, brain vascular, brain extravascular, striatum free, striatum bound, frontal cortex free, frontal cortex bound compartments. DR_{SC} represents duration of zero-order absorption process for SC dosing. ka_{SC} is the absorption rate constant for SC dosing. CL, Q, CL_{bv}, CL_{str}, CL_{cor} represent clearance in the central, peripheral, brain vascular, striatum free, cortex free compartments, respectively. CL_{met} represent metabolic conversion of RIS to PALI. CL_{bev} and CL_{efflux} represent passive diffusion and active efflux through the BBB. B_{max} is the receptor density. CB are concentrations bound to receptor in nM. They are calculated as follows:

$CB_{D2-RIS} = 1000 * A_{strB-RIS} / V_{str} / MW_{RIS}$

$CB_{D2-PALI} = 1000 * A_{strB-PALI} / V_{str} / MW_{PALI}$

$CB_{5-HT2A-RIS} = 1000 * A_{corB-RIS} / V_{cor} / MW_{RIS}$

$CB_{5-HT2A-PALI} = 1000 * A_{corB-PALI} / V_{cor} / MW_{PALI}$

Where MW is a molecular weight.

RO is calculated as $(CB_{RIS} + CB_{PALI}) / B_{max}$.

References

1. Carpenter WT, Koenig JI. The evolution of drug development in schizophrenia: Past issues and future opportunities. Neuropsychopharmacology. 2008;33(9):2061-79.
2. Pani L, Pira L, Marchese G. Antipsychotic efficacy: Relationship to optimal D_2 receptor occupancy. Eur Psychiatry. 2007;22(5):267-75.
3. Meltzer HY, Matsubara S, Lee JC. Classification of typical and atypical antipsychotic drugs on the basis of Dopamine D-1, D-2 and Serotonin$_2$ Pk_i Values. J Pharmacol Exp Ther. 1989;251(1):238-46.
4. Kapur S, Remington G. Serotonin-dopamine interaction and its relevance to schizophrenia. Am J Psychiatry. 1996;153(4):466-76.
5. Meltzer HY, Li Z, Kaneda Y, Ichikawa J. Serotonin receptors: their key role in drugs to treat schizophrenia. Progress Neuro-Psychopharmacol Biol Psychiatry. 2003;27(7):1159-72.
6. Olsen CK, Brennum LT, Kreilgaard M. Using pharmacokinetic-pharmacodynamic modelling as a tool for prediction of therapeutic effective plasma levels of antipsychotics. Eur J pharmacol. 2008;584(2-3):318-27.
7. Danhof M, de Jongh J, De Lange ECM, Della Pasqua O, Ploeger BA, Voskuyl RA. Mechanism-based pharmacokinetic-pharmacodynamic modeling: Biophase distribution, receptor theory, and dynamical systems analysis. Ann Rev Pharmacol Toxicol. 2007;47:357-400.
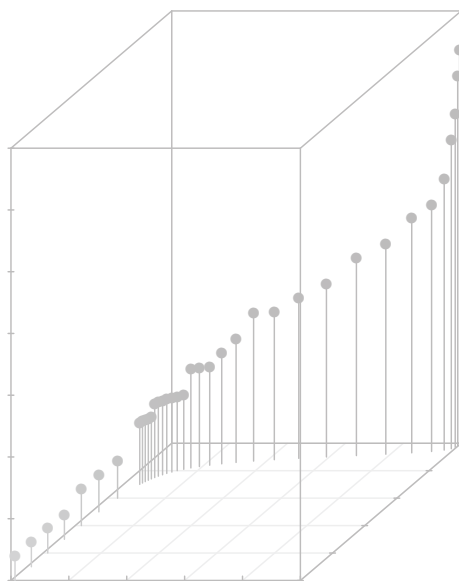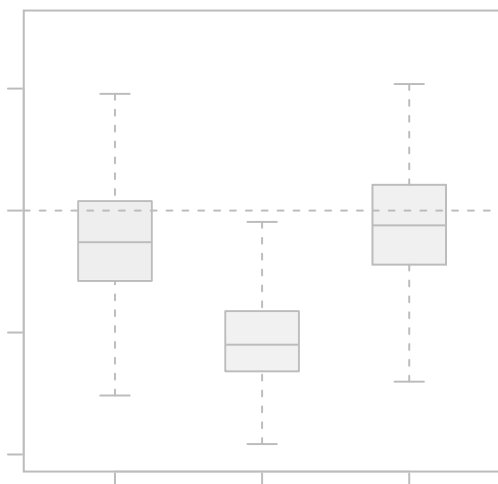
8. Yassen A, Olofsen E, Dahan A, Danhof M. Pharmacokinetic-pharmacodynamic modeling of the antinociceptive effect of buprenorphine and fentanyl in rats: Role of receptor equilibration kinetics. J Pharmacol Exp Ther. 2005;313(3):1136-49.

9. Johnson M, Kozielska M, Pilla Reddy V, Vermeulen A, Li C, Grimwood S, et al. Mechanism-based pharmacokinetic-pharmacodynamic modeling of the dopamine D_2 receptor occupancy of olanzapine in rats. Pharm Res. 2011;28(10):2490-504.

10. Wang JS, Ruan Y, Taylor RM, Donovan JL, Markowitz JS, De Vane CL. The brain entry of risperidone and 9-hydroxyrisperidone is greatly limited by P-glycoprotein. Int J Neuropsychopharmacol. 2004;7(4):415-9.

11. Knauer CS, Campbell JE, Galvan B, Bowman C, Osgood S, Buist S, et al. Validation of a rat *in vivo* [^{3}H] M100907 binding assay to determine a translatable measure of 5-HT$_{2A}$ receptor occupancy. Eur J pharmacol. 2008;591(1-3):136-41.

12. Natesan S, Reckless GE, Nobrega JN, Fletcher PJ, Kapur S. Dissociation between in vivo occupancy and functional antagonism of dopamine D_2 receptors: Comparing aripiprazole to other antipsychotics in animal models. Neuropsychopharmacology. 2006;31(9):1854-63.

13. Beal SS. NONMEM user's guides. Ellicott City, Maryland, USA: Icon Development Solutions; 2010.

14. Keizer RJ, van Benten M, Beijnen JH, Schellens JHM, Huitema ADR. Pirana and PCluster: A modeling environment and cluster infrastructure for NONMEM. Comput Methods Programs Biomed. 2011;101(1):72-9.

15. R Development Core Team. R: A language and environment for statistical computing. R Fundation for Statistical Computing, Vienna, Austria; 2011. http://www.R-project.org.

16. Jonsson EN, Karlsson MO. Xpose – an S-PLUS based population pharmacokinetic/pharmacodynamic model building aid for NONMEM. Comput Methods Programs Biomed. 1999;58(1):51-64.

17. Liu XR, Smith BJ, Chen CP, Callegari E, Becker SL, Chen X, et al. Use of a physiologically based pharmacokinetic model to study the time to reach brain equilibrium: An experimental analysis of the role of blood-brain barrier permeability, plasma protein binding, and brain tissue binding. J Pharmacol Exp Ther. 2005;313(3):1254-62.

18. Andersson C, Hamer RM, Lawler CP, Mailman RB, Lieberman JA. Striatal volume changes in the rat following long-term administration of typical and atypical antipsychotic drugs. Neuropsychopharmacology. 2002;27(2):143-51.

19. Mannens G, Meuldermans W, Snoeck E, Heykants J. Plasma-protein binding of risperidone and its distribution in blood. Psychopharmacology. 1994;114(4):566-72.

20. Liu XR, Van Natta K, Yeo H, Vilenski O, Weller PE, Worboys PD, et al. Unbound drug concentration in brain homogenate and cerebral spinal fluid at steady state as a surrogate for unbound concentration in brain interstitial fluid. Drug Metab Dispos. 2009;37(4):787-93.

21. Hoyer D, Pazos A, Probst A, Palacios JM. Serotonin receptors in the human brain. 2. Characterization and autoradiographic localization of 5-HT$_{1c}$ and 5-HT$_2$ recognition sites. Brain Res. 1986;376(1):97-107.

22. Mignini F, Vitaioli L, Sabbatini M, Tomassoni D, Amenta F. The cerebral cortex of spontaneously hypertensive rats: A quantitative microanatomical study. Clin Exp Hypertension. 2004;26(4):287-303.

23. Lindbom L, Pihlgren P, Jonsson N. PsN-Toolkit – A collection of computer intensive statistical methods for non-linear mixed effect modeling using NONMEM. Comput Methods Programs Biomed. 2005;79(3):241-57.

24. van Beijsterveldt LEC, Geerts RJF, Leysen JE, Megens A, Vandeneynde HMJ, Meuldermans WEG, et al. Regional brain distribution of risperidone and its active metabolite 9-hydroxy-risperidone in the rat. Psychopharmacology. 1994;114(1):53-62.

25. Meuldermans W, Hendrickx J, Mannens G, Lavrijsen K, Janssen C, Bracke J, et al. The metabolism and excretion of risperidone after oral administration in rats and dogs. Drug Metab Dispos. 1994;22(1):129-38.

26. Aravagiri M, Marder SR. Brain, plasma and tissue pharmacokinetics of risperidone and 9-hydroxyrisperidone after separate oral administration to rats. Psychopharmacology. 2002;159(4):424-31.

27. Arakawa R, Ito H, Takano A, Takahashi H, Morimoto T, Sassa T, et al. Dose-finding study of paliperidone ER based on striatal and extrastriatal dopamine D_2 receptor occupancy in patients with schizophrenia. Psychopharmacology. 2008;197(2):229-35.

28. Karlsson P, Dencker E, Nyberg S, Mannaert E, Boom S, Talluri K, et al. Pharmacokinetics and dopamine D_2 and serotonin 5-HT_{2A} receptor occupancy of paliperidone in healthy subjects: Two open-label, single-dose studies. Clin Pharmacol Ther. 2006;79(2):P74.

29. Doran A, Obach RS, Smith BJ, Hosea NA, Becker S, Callegari E, et al. The impact of P-glycoprotein on the disposition of drugs targeted for indications of the central nervous system: Evaluation using the MDR1A/1B knockout mouse model. Drug Metab Dispos. 2005;33(1):165-74.

30. Ejsing TB, Pedersen AD, Linnet K. P-glycoprotein interaction with risperidone and 9-OH-risperidone studied in vitro, in knock-out mice and in drug-drug interaction experiments. Hum Psychopharmacol Clin Exp. 2005;20(7):493-500.

31. Feng B, Mills JB, Davidson RE, Mireles RJ, Janiszewski JS, Troutman MD, et al. In vitro P-glycoprotein assays to predict the in vivo interactions of P-glycoprotein with drugs in the central nervous system. Drug Metab Dispos. 2008;36(2):268-75.

32. Boulton DW, DeVane CL, Liston HL, Markowitz JS. In vitro P-glycoprotein affinity for atypical and conventional antipsychotics. Life Sci. 2002;71(2):163-9.

33. Cousein E, Barthelemy C, Poullain S, Simon N, Lestavel S, Williame V, et al. P-glycoprotein and cytochrome P450 3A4 involvement in risperidone transport using an *in vitro* Caco-2/TC7 model and an *in vivo* model. Progress Neuro-Psychopharmacol Biol Psychiatry. 2007;31(4):878-86.

34. Schotte A, Janssen PFM, Gommeren W, Luyten W, VanGompel P, Lesage AS, et al. Risperidone compared with new and reference antipsychotic drugs: *In vitro* and *in vivo* receptor binding. Psychopharmacology. 1996;124(1-2):57-73.

35. Seeman P, Tallerico T. Antipsychotic drugs which elicit little or no Parkinsonism bind more loosely than dopamine to brain D_2 receptors, yet occupy high levels of these receptors. Mol Psychiatry. 1998;3(2):123-34.

36. Gauffre JC, Aguerre S, Mormede P, Chaouloff F. Cortical [³H] ketanserin binding and 5-HT_{2A} receptor-mediated inositol phosphate production in the spontaneously hypertensive rat and Lewis rat strains. Neurosci Lett. 1997;236(2):112-6.

37. Kulikov AV, Jeanningro R. The effects of hypothyroidism on 5-HT$_{1A}$ and 5-HT$_{2A}$ receptors and the serotonin transporter protein in the rat brain. Neurosci Behav Physiol. 2001;31(4):445-9.

38. Pazos A, Cortes R, Palacios JM. Quantitative autoradiographic mapping of serotoning receptors in the rat brain. 2. serotonin-2 receptors. Brain Res. 1985;346(2):231-49.

39. Vicentic A, Cabrera-Vera TM, Pinto W, Battaglia G. 5-HT$_{1A}$ and 5-HT$_{2A}$ serotonin receptor turnover in adult rat offspring prenatally exposed to cocaine. Brain Res. 2000;877:141-8.

40. Barth VN, Chernet E, Martin LJ, Need AB, Rash KS, Morin M, et al. Comparison of rat dopamine D$_2$ receptor occupancy for a series of antipsychotic drugs measured using radiolabeled or nonlabeled raclopride tracer. Life Sci. 2006;78(26):3007-12.

41. van der Werf JF, van het Schip F, Sebens JB, Korf J. Quantification of *in vivo* spiperone binding in the rat striatum after lesions produced by kainate or decortication. Eur J pharmacol. 1984;102:387-99.

42. Leysen JE, Gommeren W, Eens A, Decourcelles DD, Stoof JC, Janssen PAJ. Biochemical profile of risperidone, a new antipsychotic. J Pharmacol Exp Ther. 1988;247(2):661-70.

43. Leysen JE, Janssen PMF, Gommeren W, Wynants J, Pauwels PJ, Janssen PAJ. *In vitro* and *in vivo* receptor-binding and effects on monoamine turnover in rat-brain regions of the novel antipsychotics risperidone and ocaperidone. Mol Pharmacol. 1992;41(3):494-508.

44. Leysen JE, Janssen PMF, Schotte A, Luyten W, Megens A. Interaction of antipsychotic drugs with neurotransmitter receptor sites *in vitro* and *in vivo* in relation to pharmacological and clinical effects – role of 5HT$_2$ Receptors. Psychopharmacology. 1993;112(1):S40-S54.

45. Arnt J, Skarsfeldt T. Do novel antipsychotics have similar pharmacological characteristics? A review of the evidence. Neuropsychopharmacology. 1998;18(2):63-101.

46. Uchida S, Kato Y, Hirano K, Kagawa Y, Yamada S. Brain neurotransmitter receptor-binding characteristics in rats after oral administration of haloperidol, risperidone and olanzapine. Life Sci. 2007;80(17):1635-40.

47. Ramakrishna D, Subhash MN. Differential modulation of alpha-1 adrenoceptor subtypes by antidepressants in the rat brain. J Neural Transm. 2010;117(12):1423-30.

48. Olmos G, Miralles A, Barturen F, Garciasevilla JA. Decreased density and sensitivity of α$_2$-adrenoceptors in the brain of spontaneously hypersensitive rats. Eur J pharmacol. 1991;205(1):93-6.

49. Ribas C, Miralles A, Busquets X, Garcia-Sevilla JA. Brain α$_2$-adrenoceptors in monoamine-depleted rats: increased receptor density, G coupling proteins, receptor turnover and receptor mRNA. Brit J Pharmacol. 2001;132(7):1467-76.

50. Thomas DR, Atkinson PJ, Hastie PG, Roberts JC, Middlemiss DN, Price GW. [^{3}H] -SB-269970 radiolabels 5-HT$_7$ receptors in rodent, pig and primate brain tissues. Neuropharmacology. 2002;42(1):74-81.

51. Callado LF, Meana JJ, Grijalba B, Pazos A, Sastre M, Garcia-Sevilla JA. Selective increase of α$_{2A}$-adrenoceptor agonist binding sites in brains of depressed suicide victims. J Neurochem. 1998;70(3):1114-23.

Translational Modeling in Schizophrenia
Predicting Human Receptor Occupancy

Martin Johnson[1], Magdalena Kozielska[1],
Venkatesh Pilla Reddy[1], An Vermeulen[2],
Hugh A. Barton[3], Sarah Grimwood[3],
Rik de Greef[4], Geny M.M. Groothuis[1],
Meindert Danhof[5] and Johannes H. Proost[1]

[1] Dept. of Pharmacokinetics, Toxicology and Targeting, University of Groningen, The Netherlands
[2] Advanced PKPD Modeling and Simulation, Janssen Research and Development, a division of Janssen Pharmaceutica NV, Beerse, Belgium
[3] Worldwide Research & Development, Pfizer, Inc., Groton, CT, USA
[4] Clinical PK-PD, Pharmacokinetics, Pharmacodynamics & Drug Metabolism, Merck Sharp & Dohme, Oss, The Netherlands
[5] Division of Pharmacology, Leiden-Amsterdam Center for Drug Research, Leiden, The Netherlands

Abstract

Objectives To assess the ability of a previously developed hybrid physiology-based pharmacokinetic and pharmacodynamic (PBPKPD) model to predict the dopamine D_2 receptor occupancy (D_2RO) in human striatum following administration of antipsychotic drugs.

Methods A hybrid PBPKPD model, previously developed using information on plasma concentrations, brain exposure and D_2RO in rats, was used as the basis for the prediction of D_2RO in human. The rat pharmacokinetic and brain physiology parameters were substituted with human population pharmacokinetic parameters and human physiological information. To predict the passive transport across the human blood brain barrier, apparent permeability values were scaled based on rat and human brain endothelial surface area. Active efflux clearance in brain was scaled from rat to human using MDR1 expression. Binding constants at the D_2 receptor were corrected based on the differences between *in vitro* and *in vivo* systems of the same species. The predictive power of this physiology-based approach was determined by comparing the D_2RO predictions with the observed human D_2RO of six antipsychotics at clinically relevant doses.

Results Predicted human D_2RO was in good agreement with clinically observed D_2RO for five antipsychotics. Human D_2RO predictions improved when based on models integrating *in vitro* and *in vivo* information. However, D_2RO was under-predicted for haloperidol.

Conclusions The rat hybrid PBPKPD model structure, integrated with *in vitro* and preclinical *in vivo* model parameters and human pharmacokinetic and physiological information, constitutes a scientific basis to predict the time course of D_2RO in man.

Introduction

In schizophrenia drug therapy and research, dopamine D_2 receptor occupancy (D_2RO) is often used as a target biomarker to quantify the relationship between efficacy and side effects (1). Several studies suggest that blockade of 65% to 80% of D_2 receptors is the key to antipsychotic efficacy for both conventional neuroleptics and novel antipsychotics (2-4). D_2RO higher than 80% increases the risk of adverse effects such as extra pyramidal symptoms (5). Thus, D_2RO has a central role in schizophrenia drug discovery, drug development and therapy. Target occupancy is important both in early drug discovery, where accurate knowledge of the degree of occupancy could help to determine the suitability of a drug candidate for further development, and later in the drug development process, when target site occupancy measurements can guide dose selection (6). D_2RO is clinically measured using positron emission tomography (PET) or single-photon emission computed tomography (SPECT) methodology, which are both expensive and time-consuming. Tools to predict clinical D_2RO in preclinical drug discovery phases are therefore valuable. It is well known that current antipsychotics also activate or antagonize other targets in the central nervous system. For example, risperidone has a higher affinity for serotonin ($5\text{-}HT_{2A}$) receptors than for D_2 receptors (5). Extensions of this tool to other receptors would therefore increase the value of the current translation framework.

Recently, we have reported physiology-based pharmacokinetic and pharmacodynamic (PKPD) models to characterize the time course of D_2RO and $5\text{-}HT_{2A}$ receptor occupancy ($5\text{-}HT_{2A}RO$) in rats (7,8). The mechanistic and physiology basis of these models should potentially allow the prediction of human PKPD properties using physiological parameters and prior information from *in vitro* and *in vivo* preclinical studies (9). The present investigation is aimed to determine how these models can be used for translating receptor occupancy from rat to humans.

Development of a translation tool to predict human D_2RO (based on PKPD models) involves scaling information from rat to human. This involves accounting for drug distribution to the brain and the drug's ability to bind to striatal D_2 receptors. Drug distribution to the brain is not only characterized by passive diffusion process but also by active efflux transporters present at the luminal surface of the blood-brain-barrier (BBB). Similarities in the *in vitro permeability* values determined by various types of experiments provide a basis to integrate and scale information on passive drug transport to the brain from *in vitro* to *in vivo* or from one species to the other (10). However, differential expression and heterogeneity in the homology of drug transporters involved in the active drug transport across the BBB leads to challenges when scaling active transport related information from one species to another (11). Notwithstanding divergent reports on the species independence of

drug-specific parameters, integration of *in vitro* parameters with a physiologically based PKPD modeling would increase the potential of successfully translating effects from preclinical species to humans (12).

Hence, the objective of this work was to explore different approaches to predict human striatal D_2RO using a generic translational PBPKPD model structure, which allows integration and scaling of information from preclinical *in vitro* or *in vivo* data to the human situation. Different approaches were compared to determine the minimal amount of information required for this translational work. A previously developed extended model structure was also used to predict human $5\text{-}HT_{2A}RO$ based on these approaches.

5

Methods

Data

This work was performed within the framework of the Dutch Top Institute Pharma project: Mechanism-based PKPD modeling (http://www.tipharma.com). This mechanism-based PKPD modeling platform involves leading pharmaceutical companies worldwide, and academic institutes from The Netherlands. Three pharmaceutical companies who are the members of this mechanism-based PKPD modeling platform, namely, Janssen Research and Development – Belgium, *Merck* Sharp and Dohme – The Netherlands and Pfizer Worldwide Research and Development – USA, provided human plasma concentration data for haloperidol (HAL) and paliperidone (PAL) and helped with collection of human D_2 and $5\text{-}HT_{2a}$ receptor occupancy data. Clozapine (CLZ), HAL, olanzapine (OLZ), PAL and quetiapine (QTP) were used in this study as model antipsychotic drugs. The observed human D_2RO for these antipsychotics were taken from the literature (2, 13-25). For risperidone (RIS), human D_2RO was provided from the pharmaceutical companies who are involved in this project.

Population pharmacokinetic (PK) parameters for CLZ, OLZ, QTP and RIS were obtained from literature (1,26,27). However, no population PK models have been reported in literature for HAL and PAL. So, for these compounds in-house population PK models were developed. The population PK model for haloperidol was developed on the basis of data from 7 studies, comprised of 122 individuals [healthy volunteers (n=20) and schizophrenic patients (n=102)] and 515 plasma concentrations obtained across a wide dose range of 1 to 60 mg/day administered either as single or multiple doses. The population PK model for paliperidone-extended release was developed on the basis of data from 3 studies, comprised of 870 individuals and 4169 plasma concentrations obtained across a wide dose range of 3 to 15 mg/day administered as an OROS® once daily formulation.

Physiology-Based PKPD Model Structure

A physiology-based PKPD (PBPKPD) model was previously developed and evaluated for its usefulness in describing the time course of brain concentration and D_2RO in rats (7). This model contains expressions to describe the kinetics in brain-vascular, brain-extravascular, striatum-free and striatum-bound compartments (Figure 5.1). Following administration, drug is transported from the plasma compartment to the
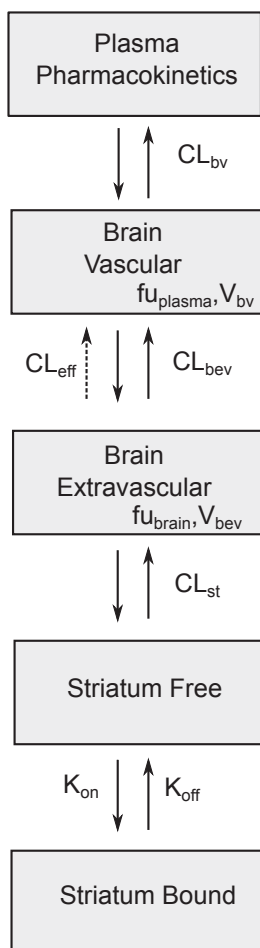

Figure 5.1: *A schematic representation of the PBPKPD model. The model incorporates different processes to explain the time course of D_2RO. The brain pharmacokinetics describes the processes involved in the transport of drug from plasma to brain, and the striatum compartment explains the drug binding to receptors through the binding constants.*

brain-vascular compartment; this process is assumed to be determined only by the cerebral blood flow. Only the unbound drug in this vascular compartment crosses the BBB and is transported into the brain-extravascular compartment, which is governed by the brain-extravascular clearance (CL_{bev}). Furthermore, drug is transported from the brain-extravascular compartment to the striatal-free compartment. The brain-extravascular and striatum-free compartments were assumed to be equilibrating rapidly. In striatum-bound compartment, drug can reversibly bind to the dopamine receptor complex (Figure 5.1). The receptor association and dissociation processes were described using k_{on} as the second-order receptor association rate constant (nM^{-1}h^{-1}), and k_{off} as the first-order receptor dissociation rate constant (h^{-1}). Dopamine D$_2$ receptor density in striatum was parameterized as B_{max}.

In addition to the previously developed rat PBPKPD model structure, an active efflux clearance (CL_{eff}) component between brain-extravascular and brain-vascular compartments was included in this predictive model to explain the active drug transport from brain, when appropriate (i.e. for RIS and PAL). Additionally, this rat PBPKPD model structure was extended to account for binding of RIS and PAL to the 5-HT$_{2A}$ receptor (8). This extended model included two additional compartments (cortex-free and cortex-bound). Binding to 5-HT$_{2A}$ receptors was described using association and dissociation constants and receptor density values specific for 5-HT$_{2A}$ receptors. This extended model structure was used to predict both D$_2$ and 5-HT$_{2A}$ receptor occupancy in humans in this simulation study.

Human D$_2$RO predictions

The rat PBPKPD model structure (Figure 5.1) was used to predict the D$_2$RO versus time profile of antipsychotics in humans by substituting all parameters of the rat model by their human analogues, according to the following methods:

(1) Human population PK parameters estimated using total plasma concentrations were obtained either from models developed in-house or from published literature (Table 5.1).

(2) Physiological parameters, such as blood flow to the brain and the brain volumes were obtained from literature (Table 5.2).

(3) Passive permeability transport across the BBB was scaled from *in vitro* or *in vivo* rat to *in vivo* human based on the assumption that permeability for passive diffusion per cm^2 of brain endothelial surface is identical between different systems.

(4) Active efflux transport for PAL and RIS was scaled using pertinent information on P-gp protein expression in different systems as a scaling factor.

(5) Receptor binding was either derived from *in vitro* Ki values or *in vivo* Kd values corrected for differences between in *vitro* and *in vivo* system of the same species.

Table 5.1: Parameter Estimates Used in the Population Pharmacokinetic Models					
	Clozapine	Haloperidol	Olanzapine	Paliperidone	Quetiapine
Population mean values (IIV as %CV)					
Vc (L)	719(62)	401 (37)	1150 (75)	395.4 (47)	380 (10)
CL (L/h)	37.9 (28)	53 (44)	19.5 (58)	14.15 (45)	96.0 (59)
Vp (L)	-	1500	-	-	-
Q (L/h)	-	140	-	-	-
F (%)	-[#]	60	-[#]	-[#]	-[#]
Ka (h^{-1})	1.37 (24)	0.230	0.600 (32)	2.49	2.50 (80)
DUR (h)				22.87	

Clozapine, Olanzapine and Quetiapine : Reference (26); Haloperidol and Paliperidone: Parameters obtained from in-house developed model
Population PK parameters for Risperidone was obtained reference from (27). Reader is requested to refer there for more details
Vc – central volume of distribution, CL – clearance, Vp – peripheral volume of distribution, Q – inter-compartmental clearance, F – absolute bioavailability, Ka – absorption rate constant, DUR – duration of zero-order absorption, IIV-Inter-individual variability, %CV coefficient of variation
[#]Not estimated and CL and V are corrected for F

Table 5.2: Physiological values used in human D$_2$RO predictive model		
Parameter	Value	Reference
Human cerebral blood flow (L/h)	36.0	(30)
Human brain extravascular volume (L)	1.40	(44)
Human brain vascular volume (L)	0.150	(44)
Human striatal volume (L)	0.00700	(45)
Human cortex volume (L)	1.08	(44)
Dopamine D$_2$ receptor density in human striatum (nM)	28.0	(46)
5-HT$_{2A}$ receptor density in human frontal cortex (nM)	195	(47)

(6) Experimentally determined values of the fraction unbound in human plasma and in rat brain were obtained from the literature. Unbound fraction in human brain is assumed to be equal to the unbound fraction in rat brain.

Different approaches were used to obtain human parameters and they were detailed as Approaches A-C in this section.

Approach A was based only on human *in vitro* information (*in vitro* apparent permeability, efflux ratio (ER), *in vitro* Ki and k_{off}).

Approach B was based on the *in vivo* parameters (rCL_{bev}, rCL_{eff}, Kd_{rat}, $k_{off-rat}$) obtained from the rat PBPKPD model.

Approach C was aimed at using minimal information to get the best predictions of human D_2RO by integrating the approaches A and B.

All the parameters values used for these simulations are presented in Table 5.3.

Approach A: Human D_2RO predictions based on *in vitro* information

Passive drug transport to the brain

Experimentally determined *in vitro* apparent permeability (P_{app}) values were used to predict passive distribution of antipsychotics across the BBB. Specifically, values of the *in vitro* permeability across multidrug resistance Madin-Darby canine kidney (MDR1-MDCK) type II cell monolayers were obtained from Summerfield *et al* (28). Permeability determined while attenuating transporters denotes the ability of the molecule to traverse membranes by passive means (29). These P_{app} values were translated to a meaningful parameter of human brain extra-vascular clearance (hCL_{bev}) across the BBB by taking the product of P_{app} and human brain endothelial surface area of 20 m² (30).

Active drug transport from the brain

For antipsychotics, PAL and RIS which are known to have both active and passive transport across the BBB, the active transport component was derived from *in vitro* efflux ratio determinations. ER is commonly used as an indicator of active drug transport in CNS drug discovery. ER is calculated as the ratio of effective permeability for a drug from the basal side to the apical side [Passive + Active] to that in the opposite direction [Passive – Active] (31). ER was used to calculate the human active efflux clearance (hCL_{eff}) of RIS and PAL.

Derivation of *in vitro* CL_{eff} from ER is shown below.

$$ER = \frac{\text{Drug Transport (Passive + Active)}}{\text{Drug Transport (Passive – Active)}} \qquad – Eq\ (1)$$

After rearrangement this gives,

$$\textit{In vitro } CL_{eff}\ (L/h) = CL_{bev} * \frac{ER - 1}{ER + 1} \qquad – Eq\ (2)$$

where, CL_{bev} represents the passive permeability across the BBB (L/h).

Table 5.3: *In vitro*, *in vivo* and *ex vivo* values estimates used in human D_2RO predictive model

Parameter	Clozapine	Haloperidol	Olanzapine	Paliperidone	Quetiapine	Risperidone
fraction unbound in brain	0.011 [a]	0.023 [b]	0.034 [a]	0.0755 [c]	0.025 [a]	0.0699 [c]
fraction unbound in plasma	0.0300 [d]	0.0800 [e]	0.0700 [f]	0.226	0.170 [f]	0.100
Approach A: Human D2RO predictions based on *in vitro* information						
$Papp \times 10^{-6}$ (cm/s)	28.3 [a]	28.6 [a]	15.7 [a]	16.8 [g]	33.0 [a]	19.8 [g]
CL_{bev} (L/h) derived from P_{app} values	2.04	2.06	1.13	1.21	2.36	1.43
Efflux Ratio	-	-	-	2.10 [g]	-	1.20 [g]
CL_{eff}(L/h) based on ER	-	-	-	6.82	-	2.07
In vitro Ki (nM)	82.0 [h]	0.700 [h]	5.10 [i]	2.07 [e]	155 [h]	2.17 [e]
K_{off} (h^{-1})	83.16 [h]	1.02 [h]	2.34 [h]	1.56 [#]	180.78 [h]	1.56 [j]
Approach B: Human D2RO predictions based on *in vivo* information						
$Papp_{calc} \times 10^{-6}$ (cm/s)	-	-	100	493 [#]	-	493
CL_{bev} (L/h) based on $Papp_{calc}$	-	-	72.2	355 [#]	-	355
CL_{eff} (L/h) scaled from rat	-	-	NA	11594	-	2486
K_{off} (h^{-1})	-	-	3.04 [k]	0.671 [l#]	-	0.671 [l]
Approach C: Human D2RO predictions integrating *in vitro* and *in vivo* information						
Corrected *In vivo* Kd (nM)	-	-	4.38	0.352	-	0.395

[a] Reference (28); [b] Reference (48); [c] Reference (49) ; [d] Reference (50); [e] In-house values ; [f] Reference (51); [g] Reference (52); [h] Reference (53); [i] Reference (54); [j] Reference (55); [k] Reference (7); [l] Reference (8)
[#] Assumed to be equal to risperidone
NA – Not applicable

In vitro CL_{eff} was scaled to the *in vivo* human system based on MDR1 expression. MDR1 expression in MDR1-MDCKII cells *in vitro* was reported as 359.6 μg/cm^2 (32). This expression was normalized for the surface area of the cell monolayer (0.0625 cm^2) as 22.4 μg of MDR1 protein. MDR1 expression in human brain was calculated as 357.6 μg/1400 g of brain based on the documented expression levels of 6.06 fmol/μg of protein (11).

Therefore,

$$\text{hCL}_{eff} \text{ (L/h)} = \textit{In vitro } \text{CL}_{eff} \text{ (L/h)} * \frac{\text{mdr1 expression (human brain)}}{\text{mdr1 expression (\textit{in vitro} system)}} \qquad - \text{Eq (3)}$$

5

Receptor binding parameters

In vitro Ki_{human} values were used as the parameter Kd (equilibrium constant). If available, i*n vitro* or *ex vivo* experimentally determined k_{off} values were used in these simulations (Table 5.3). If experimental k_{off} values were not available, then calculated k_{off} values based on Ki and k_{off} correlation of different antipsychotics were used, as reported previously (5).

Approach B: Human D$_2$RO predictions based on *in vivo* information

Appropriateness of available rat hybrid PBPKPD model determined *in vivo* parameters for human D$_2$RO predictions was assessed. Binding constants, rCL_{bev} and $rCL_{eff,}$ were obtained using PBPKPD models developed by us previously (7, 8). This *in vivo* model based information was only available for OLZ, PAL and RIS.

Passive drug transport to the brain

Calculated Papp ($Papp_{calc}$) values were derived as the ratio between PBPKPD model-estimated *in vivo* rCL_{bev} and rat brain endothelial surface area (150 cm^2/g) and then normalized for an average rat brain weight of 2 g/250 g of rat (28). The product of $Papp_{calc}$ and the human brain endothelial surface area (20 m^2) was used as the hCL_{bev} – the passive transport clearance across the human BBB.

Active drug transport from the brain

Human active efflux clearance was predicted based on the PBPKPD model-estimated rCL_{eff} and mdr1a protein expression in micro vessels in rat. Mdr1a expression values for rats were not available, hence, mdr1a expression in rat brain was assumed to be equal to that of mouse. Mouse mdr1a expression was documented as 14.1 fmol/μg of protein (11). The following equation (4) describes the assumed relationship which was used to derive the hCL_{eff}.

$$hCL_{eff} \ (L/h) \ in \ human = rCL_{eff} \ (L/h) \ * \ \frac{MDR1 \ expression \ in \ human \ brain}{Mdr1a \ expression \ in \ rat \ brain}$$

– Eq (4)

Receptor binding parameters

In vivo human k_{on} and k_{off} were assumed to be equal to the model estimated *in vivo* $k_{on\text{-}rat}$ and $k_{off\text{-}rat}$ values as they are often believed to be drug-specific parameters (33). For OLZ, model estimated *in vivo* Kd_{rat} and $k_{off\text{-}rat}$ values were taken from our previous publication (31). For RIS and PAL, *in vivo* binding constants were obtained from the extended model structure where the time courses for D_2 and $5\text{-}HT_{2A}$ receptor binding were modeled together. These parameters are shown in Table 5.4.

Table 5.4: Brain PKPD model parameter estimates obtained from Rat PBPKPD model and used in the predictive model			
	Olanzapine[a]	Paliperidone[b]	Risperidone[b]
Parameters (RSE)			
CL_{bev} (L/h/kg)	0.433 (16)	2.13[#]	2.13 (29)
Kd (nM) – D_2 binding	14.6 (7)	0.463[#]	0.463 (14)
K_{off} (h^{-1}) – D_2 binding	3.04 (24)	0.671[#]	0.671 (19)
CL_{eff} (L/h/kg)	NA	46.5 (28)	9.97 (28)
Kd (nM) – $5\text{-}HT_{2A}$ binding	NA	0.156[#]	0.219 (15)
K_{off} (h^{-1}) – $5\text{-}HT_{2A}$ binding	NA	0.310[#]	0.525 (25)
[#]Assumed to be equal to risperidone [a]Reference (7); [b]Reference (8) NA – Not applicable RSE – Relative standard Error RSE is not available for CL_{eff} as it is derived parameter			

Approach C: Human D_2RO predictions integrating *in vitro* and *in vivo* information

Passive and active drug transport to the brain

Scaling and calculation used in Approach A were also applied in the integrated Approach C.

Receptor binding parameters

In vivo Kd_{human} parameters were corrected for the differences between *in vitro* and *in vivo* scenarios by normalizing model estimated *in vivo* Kd_{rat} and *in vitro* Ki values for rat and human, as shown in equation (5).

$$Kd_{human} \ (nM) = \textit{In vitro } Ki_{human} * \frac{\textit{In vivo } Kd_{rat}}{\textit{In vitro } Ki_{rat}} \qquad - Eq \ (5)$$

In vivo $k_{off-human}$ values were assumed to be equal to *in vitro* or *ex vivo* experimentally determined k_{off} values.

Human 5-HT$_{2A}$RO predictions

The objective of this exercise was to check the utility of the extended model structure to predict human D$_2$RO and 5-HT$_{2A}$RO. *In vitro* Ki_{human} and Ki_{rat} for PAL were 0.250 nM (34). *In vitro* Ki_{human} and Ki_{rat} for RIS were 0.160 and 0.210 nM, respectively (34, 35). Since the k_{off} value for 5-HT$_{2A}$ binding was not available from any *in vitro* source, the *in vivo* based Approach B and the integrated Approach C were applied for these predictions.

Human D$_2$ receptor occupancy simulations

For each approach (approach A-C), 1000 human D$_2$RO- time course curves were simulated at clinically relevant doses, administered orally. Differential equations (Appendix 1) explaining the pharmacokinetics and pharmacodynamics of antipsychotics were used in these simulations as implemented in R (Version 2.10.1) using the deSolve package (36). Inter-individual variability (IIV) in the population pharmacokinetic parameters was accounted for in these simulations. The predictive power of this translational approach was determined by comparing these simulations with observed human D$_2$RO. Hence, the conditions or the scenario for the simulations were based on the nature of the human D$_2$RO information. For most antipsychotics time course of D$_2$RO was simulated and results at steady state (achieved within 2 or 3 weeks of repeated drug dosing) were compared with the observed steady state RO.

For all the drugs, prediction of time course was plotted and compared graphically with observed D$_2$RO. Additionally, for OLA, RIS and PAL box plots of prediction errors were made to compare the applicability of the different approaches and their predictive power. For this purpose, D$_2$RO or both D$_2$RO and 5-HT$_{2a}$RO predictions were made for a drug treatment of 3 weeks, at a single time point (12 h after the last dose of OLZ, RIS and 2 h after the last dose of PAL). These predictions were then
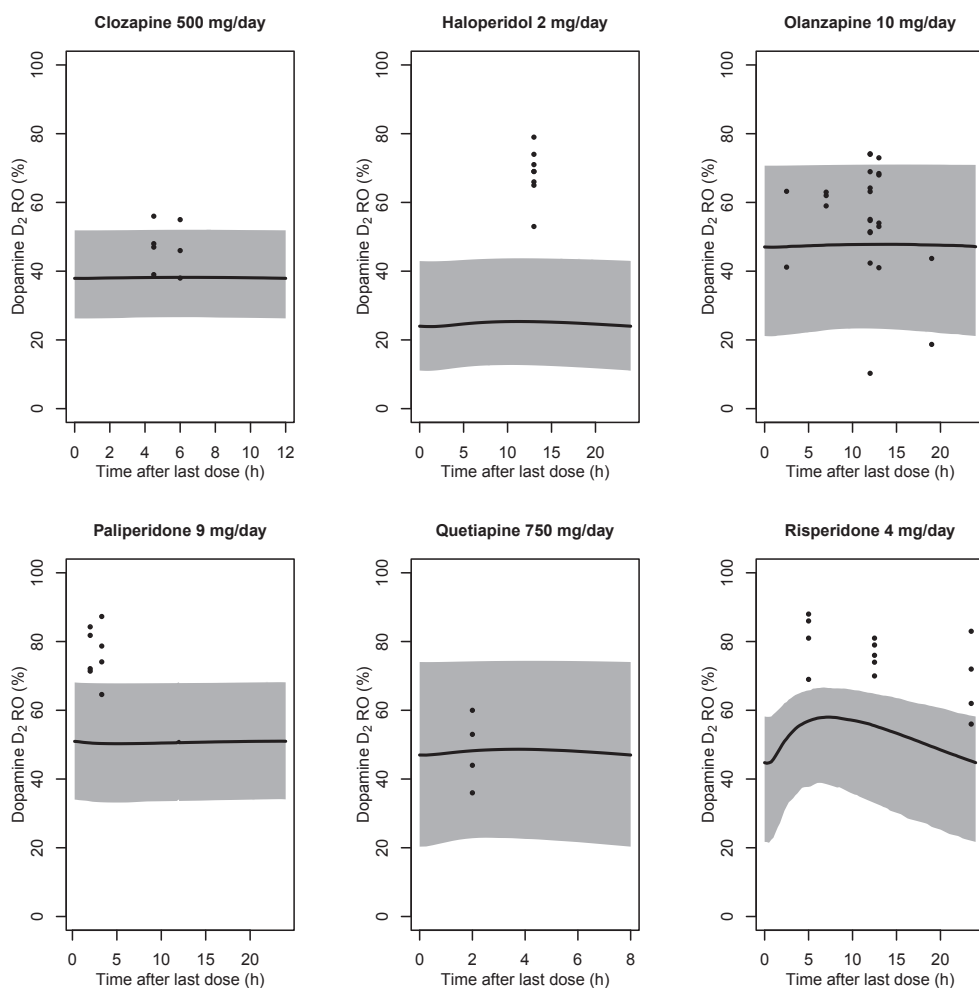
Figure 5.2: *Observed and predicted steady-state D$_2$ receptor occupancy in humans after oral administration of antipsychotics at clinically relevant doses. Simulations were performed using the rat PBPKPD model structure integrated with in vitro apparent permeability, efflux ratio and in vitro binding information (Approach A). Depicted are the observed D$_2$RO (dots) and the shaded area represent the 95% prediction limits of the simulated D$_2$RO. The medians of the simulated D$_2$RO are represented as a solid line.*

compared with the median of the actual observations. The selection of dose and time points was based on the availability of data.

% Prediction Error (PE) was calculated as follows,

$$\% \text{ PE} = 100 * \frac{\text{Median Predicted RO} - \text{Median Observed RO}}{\text{Median Observed RO}} \quad - \text{Eq (6)}$$

The median D_2RO observed experimentally for OLZ, PAL and RIS were 54.9 %, 77.4%, 75.8%, respectively. The 5-HT_{2A}RO observed for RIS was 100% (37).

5

Results

Human D_2RO predictions

Approach A
This approach predicted the time course of human D_2RO very well for four of the antipsychotics, but not for HAL, RIS and PAL. The result of these simulations is depicted in Figure 5.2. The percentage prediction bias of these predictions is depicted for OLZ, PAL and RIS in Table 5.5 and Figure 5.3.

Table 5.5: Percentage Prediction bias across different approaches used for predicting human D_2RO			
Information used in predictions	Olanzapine	Paliperidone	Risperidone
Approach A	-13	-35	-28
Approach B	-53	-39	-33
Approach C	-7	10	15
Human D_2RO using extended model structure			
Approach B	NA	NA	-23
Approach C	NA	NA	15
Human 5-HT_{2A}RO using extended model structure			
Approach B	NA	NA	-26
Approach C	NA	NA	-9
NA – Not applicable			

Approach B

The predictive model based on *in vivo* model estimated parameters under-predicted the human D_2RO for OLZ, RIS and PAL (Table 5.5, Figure 5.3).

Approach C

The predictive model using the "corrected" *in vivo* Kd_{human} estimates predicted human D_2RO for OLZ, RIS and PAL the best when compared to the other approaches. For OLZ, the predictions based on either combined approach or *in vitro* information alone were similar (Figure 5.3). For PAL and RIS, the D_2RO was slightly over-predicted and the prediction bias was small in comparison to the other approaches (Figure 5.3-5.4) and Table 5.5.
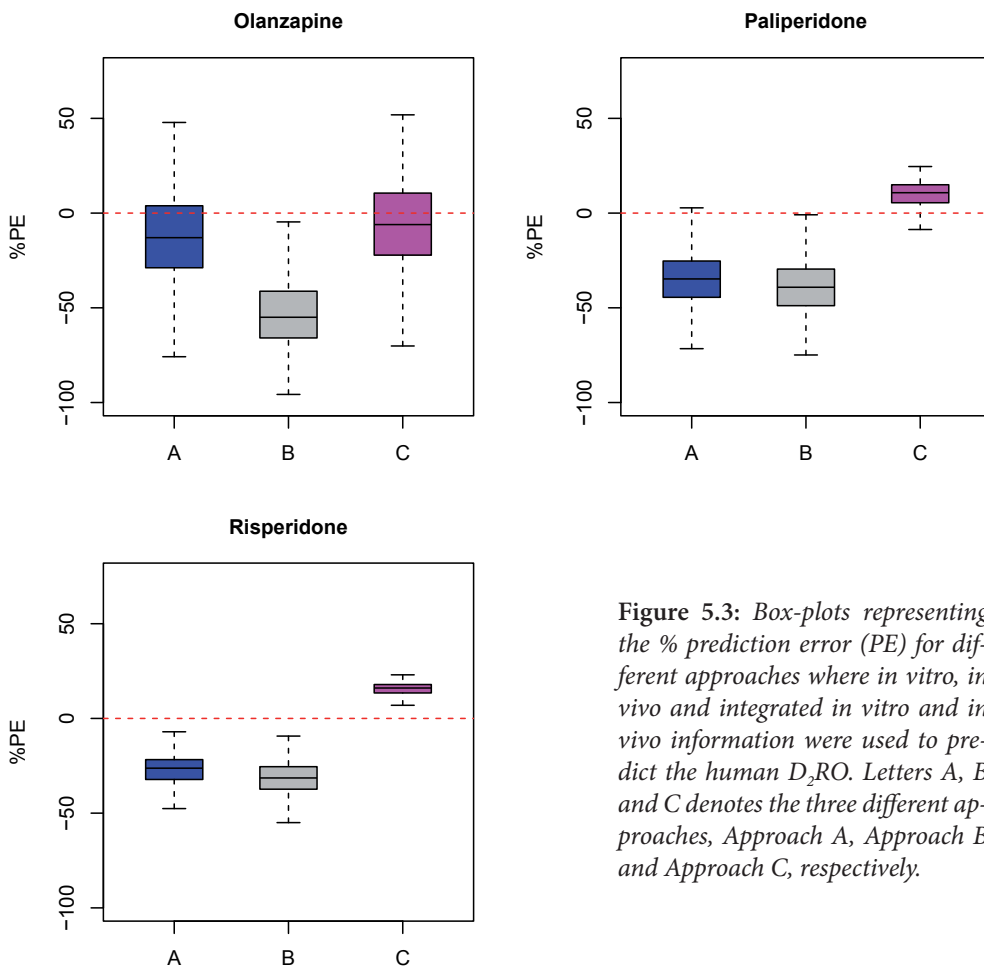
Figure 5.3: *Box-plots representing the % prediction error (PE) for different approaches where in vitro, in vivo and integrated in vitro and in vivo information were used to predict the human D_2RO. Letters A, B and C denotes the three different approaches, Approach A, Approach B and Approach C, respectively.*
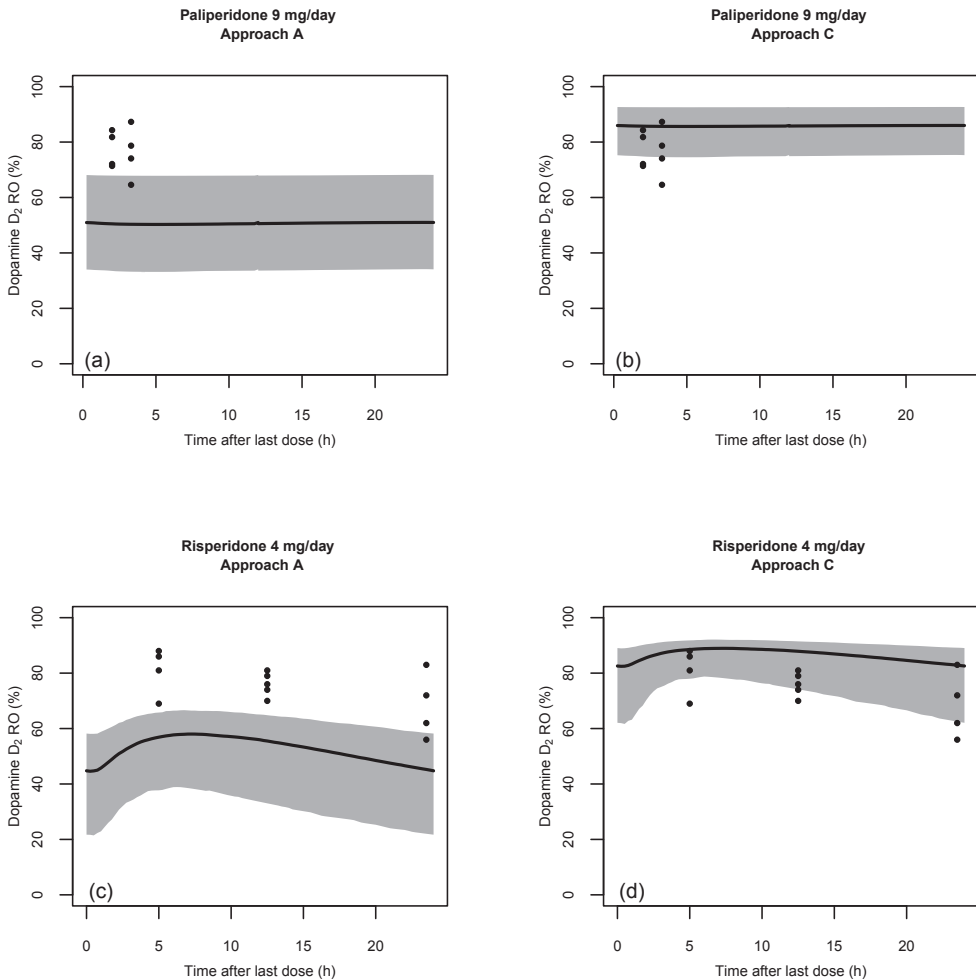
Figure 5.4: *Observed and predicted steady-state D₂ receptor occupancy (D₂RO) in humans after oral administration of risperidone or paliperidone at clinically relevant doses. Depicted are the observed D₂RO (dots) and the shaded area represent the 95% prediction limits of the simulated D₂RO. The medians of the simulated D₂RO are represented as a solid line. Panel (a) and Panel (b) represent the human D₂RO predictions for paliperidone achieved by approaches A and C, respectively. Panel (c) and Panel (d) represent the human D₂RO predictions for risperidone based on approaches A and C, respectively.*

Human 5-HT$_{2A}$RO predictions

The extended predictive model using the "corrected" *in vivo* Kd$_{human}$ estimates predicted the human 5-HT$_{2A}$RO for risperidone better than approach B. Human D$_2$RO predictions were similar to that of the model which only accounts for the D$_2$ receptor binding (Table 5.5, Figure 5.5).
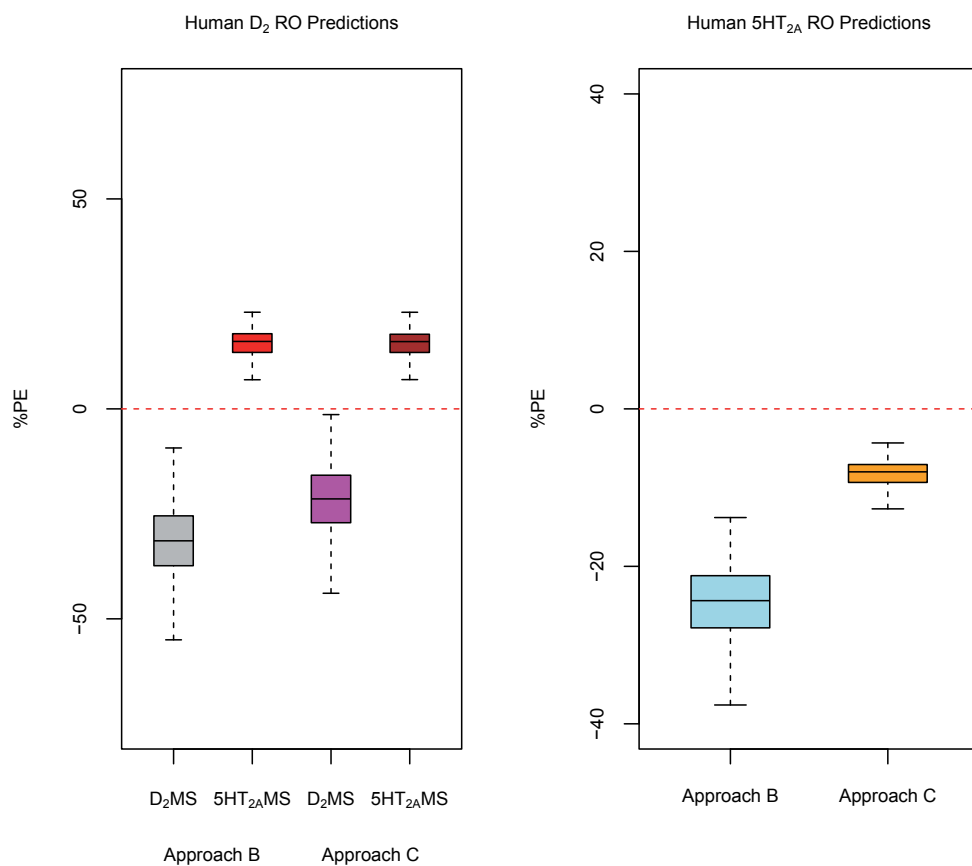

Figure 5.5: *Box-plots represent the % prediction error (PE) for human D$_2$RO and 5-HT$_{2A}$ RO predictions of risperidone at 4 mg/day dose. % PE for human D$_2$RO predictions obtained by both D2 model structure (D$_2$MS) and an extended model structure (5-HT$_{2A}$MS) are compared in the left hand panel. Right hand panel represents the human 5-HT$_{2A}$RO predictions of risperidone obtained from the extended model structure using approach B and C.*

Discussion

This study aimed to utilize the recently proposed rat PBPKPD model structure (7, 8) in a translational framework to scale pharmacokinetic and pharmacodynamic information from rats to human. The objective of this work was also to determine the minimal information required to be included in this translational framework to predict the D_2RO during the early drug discovery phase, while taking into account distribution to the brain and receptor binding.

It is well known that drug distribution to the brain is not only limited by tight junctions but also by active efflux transporters present at the luminal surface of the BBB. Hence, hCL_{bev} and hCL_{eff} were included in this model structure to explain passive permeability and active efflux processes in a mechanistic manner.

Passive permeability of drugs across the BBB was calculated based on the product of human brain endothelial surface area and P_{app} values obtained from *in vitro* MDR1-MDCK. *In vitro* effective permeability of compounds with various characteristics across human primary brain endothelial cells was comparable to those obtained with bovine and rat capillary endothelial cells (10). Nevertheless, it is likely that in *in vivo* condition that there would be differences in efficiency in permeability between species, given the difference in surface area of brain. Hence, it is also reasonable to evaluate the utility of PKPD model-estimated *in vivo* parameters in this translational approach. This may help to fill the gaps in the predictions based on *in vitro* values and hence, Approach B was developed, where *in vivo* PBPKPD model estimated parameters were used in the simulations.

The hCL_{bev} calculated based on *in vitro* P_{app} or $Papp_{calc}$ (calculated based on rCL_{bev}) values were different (Table 5.3). This could direct towards an explanation for the different efficiency of drug transport in *in vitro* and *in vivo* systems. However, it should be noted that $Papp_{calc}$ was derived using reported rat brain endothelial surface area, which ranges from 100 to 240 cm^2 per g brain tissue (38,39). Notwithstanding to this uncertainty in rat brain endothelial surface area, deriving a relationship between model-estimated rCL_{bev} (and thereby $Papp_{calc}$) and *in vitro* P_{app} based on more compounds might help to improve the translation approach. However, the limited number of compounds used in our PKPD analysis did not allow us to elicit such a relationship. So, in the absence of such a relationship, it seems to be more appropriate to base the scaling of *in vitro* P_{app} values to hCL_{bev} on human brain endothelial surface area only. Hence, while integrating *in vitro* and *in vivo* information (i.e. Approach C), calculated hCL_{bev} was based only on *in vitro* P_{app} value and human brain endothelial surface area.

Predicting or calculating active efflux clearance at the human BBB using *in vitro* information was a challenging and complicated task. In this simulation study, ER was used to account for the active drug transport out of the brain. Subsequently, active

efflux transport was also scaled to human based on the estimates obtained from the rat PBPKPD model and expression of mdr1(a) protein in both species (i.e. Approach B). Due to non-availability of the appropriate mdr1a expression data in rats, it was assumed that it is equal to that of mouse, which may lead to some bias in the predictions. Nevertheless, this work provides a framework to account for the active drug transport in humans. It is noteworthy that both these approaches (Approach A and B) are plausible because of their mechanistic basis. Additionally, the active transport was included as a linear process rather than non-linear as usually described for *in vitro* systems, since the free concentrations of drug at the BBB (in rats) were much lower than the concentrations used *in vitro*, and remain most likely below the Km (concentration require for the half -maximal transport) for the transporter, which makes this assumption acceptable.

There is a lack of human brain drug exposure information to evaluate these approaches. Extension of this method to other types of drugs (such as P-glycoprotein substrates) needs to be tested, which will also serve as an evaluation tool for both these approaches.

This predictive model structure was obtained from a preclinical system where the drug binding to D_2 receptors was explained by accounting for the association and dissociation rates of antipsychotics. Hence, it is appropriate to include *in vitro* or *in vivo* binding constants in this model structure to predict human D_2RO. Danhof *et al* (40) proposed that the values of drug-specific parameters such as target affinity are likely to be identical between species and individuals. This would imply that the binding rate constants estimated in rats can be used to extrapolate the pharmacodynamics from rat to human. The model estimated *in vivo* Kd_{rat} values for OLZ were close to *in vitro* Ki_{rat} values (rat cloned D_{2L} system – 17 nM), but *in vitro* Ki_{human} values (human cloned D_{2L} system – 5.1 nM) were different from both these values of the rat system. Additionally, PAL and RIS *in vitro* Ki_{rat} values (most commonly reported as 2 nM) are different from the model estimated *in vivo* Kd_{rat} values (0.364 nM). The human D_2RO predictions for OLZ, RIS and PAL were not consistent with the observed human D_2RO data when model estimated *in vivo* Kd_{rat} was used as the *in vivo* Kd_{human} parameter in the predictive model. This challenges the general belief that drug-specific parameters like Kd can be used across species without any scaling. However, this difference in drug-specific parameters between species needs to be examined with more drugs before being generalized. This difference between the *in vivo* and *in vitro* scenario for the same species could arise from the assumptions used in both *in vitro* calculations and model estimations. Additionally, radio-ligand selection and disturbances in assumed equilibrium conditions in *in vitro* and *in vivo* systems could lead to biased or inappropriate Ki calculations (41). The model estimates of *in vivo* Kd_{rat} for RIS are influenced by the brain distribution kinetics and it was elucidated that

the brain-to-plasma ratio (in rats) is not constant for RIS, suggesting an influence of specific binding to receptors on the brain-kinetics (8). It has already been shown that the binding to both D_2 and 5-HT2$_A$ receptors (extended model) was essential to explain the relationship between drug exposure and receptor occupancy in the preclinical system with good precision (8). Hence, this extended model structure was used to predict both D_2 and 5-HT$_{2A}$ receptor occupancy in humans. The extended structure predicted 5-HT$_{2A}$RO well. Surprisingly, the D_2RO predictions achieved by using these two different model structures remained closer to each other; and this extension, which was essential for model fitting in a preclinical system, did not significantly improve the human D_2RO predictions. Nevertheless, this extended model structure underscores the ability of this model framework to be flexible and extendable to other receptor types.

Our objective was also to study the minimal information required to predict human D_2RO. In general, human D_2RO was predicted well for CLZ, OLZ and QTP, when only *in vitro* information (Approach A) was used in the simulations. This demonstrates the ability of this model structure to predict human D_2RO with minimal *in vitro* information. However, for PAL and RIS human D_2RO, it seems more appropriate to correct human *in vitro* information with rat *in vitro* and *in vivo* values. Hence, a correction was applied as explained in equation-5. This correction might help with the normalization of the scaling from an *in vitro* to an *in vivo* system for different species.

In this simulation study, the time course of plasma concentrations was obtained from available population pharmacokinetic parameters. It is also possible to predict these pharmacokinetic parameters based on *in silico* and *in vitro* information using commercially available tools, like Simcyp (Simcyp Ltd., Sheffield, UK). So, the requirement of population pharmacokinetic parameters is not essential.

For HAL, D_2RO predictions were lower than the observations. This may be related to the high ratio of unbound concentrations of HAL in brain and plasma, which is close to 4 in rats (42). This high brain to plasma ratio may indicate a unique active influx transport to the brain. In addition, it has been documented that the metabolism of HAL involves a conversion of HAL to reduced haloperidol, and back-conversion of reduced haloperidol to HAL (43) in the brain of guinea pigs. Accounting for this metabolism and/or active influx transport may help to improve predictions. Extending this predictive model structure to include such complexity is practically possible, if sufficient information about any related process is provided beforehand.

Applications of this predictive tool are not limited to only predicting D_2RO in early drug discovery but also in selecting appropriate first in human doses based on pharmacodynamics. It is not anticipated that predictive tools will completely replace the need for experiments, though it is plausible that this tool can help to design more informative and more efficient clinical studies.

Conclusion

A general translational framework was developed which is based on a mechanism-based approach and accounts for the different processes involved in the transport of drug to the brain. *In vitro* information (P_{app} and Ki) were good enough to predict the human D_2RO for those drugs distributed to the brain by passive permeability processes. An integrated approach where *in vitro* and *in vivo* information were combined, predicted the human D_2RO better than other approaches for drugs with active efflux transport from brain. This model structure with an appropriate extension also predicted the human $5\text{-HT}_{2A}RO$ well.

Acknowledgements

Appendix 1

PBPKPD Model used to predict human D_2RO

Plasma pharmacokinetics varies depends on the antipsychotic drug used (Table 5.1)

$$d(A_{bv})/dt = (CL_{bv}/V_{plasma})*A_{plasma} - (CL_{bv}/V_{bv})*A_{bv} - (CL_{bev}/V_{bv})*fu_{plasma}*A_{bv} + (CL_{bev}/V_{bev})*fu_{brain}*A_{bev} + (CL_{eff}/V_{bev})*fu_{brain}*A_{bev}$$

$$d(A_{bev})/dt = (CL_{bev}/V_{bv})*fu_{plasma}*A_{bv} - (CL_{bev}/V_{bev})*fu_{brain}*A_{bev} - (CL_{eff}/V_{bev})*fu_{brain}*A_{bev} - (CL_{st}/V_{bev})*fu_{brain}*A_{bev} + (CL_{st}/V_{stf})*fu_{brain}*A_{stf}$$

$$d(A_{stf})/dt = (CL_{st}/V_{bev})*fu_{brain}*A_{bev} - (CL_{st}/V_{stf})*fu_{brain}*A_{stf} - k_{on}*fu_{brain}*A_{stf}*(B_{max} - CB) + k_{off}*A_{stb}$$

$$d(A_{stb})/dt = k_{on}*fu_{brain}*A_{stf}*(B_{max} - CB) - k_{off}*A_{stb}$$

Where,

Subscripts plasma, bv, bev, stf, sb represent Volumes (V) and Amount (A) of drug at plasma, brain-vascular, brain-extravascular, striatum-free and striatum-bound compartments, respectively;

CL_{bv}, CL_{bev}, CL_{st} represent transport of drug to brain-vascular, brain-extravascular, striatum-free compartments, respectively.

CL_{eff} represents the active efflux transport of drug from brain-extravascular compartment.

CB is concentration bound to receptor as $(A_{stb}/V_{stb})/(MW/1000)$ in nM;

MW is Molecular Weight of the drug used;

D_2RO is calculated as $CB/B_{max}*100\%$

References

1. de Greef R, Maloney A, Olsson-Gisleskog P, Schoemaker J, Panagides J. Dopamine D(2) Occupancy as a Biomarker for Antipsychotics: Quantifying the Relationship with Efficacy and Extrapyramidal Symptoms. Aaps Journal 2011 Mar;13(1):121-30.

2. Farde L, Nordstrom AL, Wiesel FA, Pauli S, Halldin C, Sedvall G. Positron Emission Tomographic Analysis of Central D1-Dopamine and D2-Dopamine Receptor Occupancy in Patients Treated with Classical Neuroleptics and Clozapine – Relation to Extrapyramidal Side-Effects. Arch Gen Psychiatry 1992 Jul;49(7):538-44.

3. Nordstrom AL, Farde L, Wiesel FA, Forslund K, Pauli S, Halldin C, et al. Central D2-Dopamine Receptor Occupancy in Relation to Antipsychotic Drug Effects – A Double-Blind Pet Study of Schizophrenic-Patients. Biological Psychiatry 1993 Feb 15;33(4):227-35.

4. Kapur S, Remington G, Jones C, Wilson A, DaSilva J, Houle S, et al. High levels of dopamine D-2 receptor occupancy with low-dose haloperidol treatment: A PET study. American Journal of Psychiatry 1996 Jul;153(7):948-50.

5. Horacek J, Bubenikova-Valesova V, Kopecek M, Palenicek T, Dockery C, Mohr P, et al. Mechanism of action of atypical antipsychotic drugs and the neurobiology of schizophrenia. CNS Drugs 2006;20(5):389-409.

6. Grimwood S, Hartig PR. Target site occupancy: emerging generalizations from clinical and preclinical studies. Pharmacol Ther 2009;122(3):281-301.

7. Johnson M, Kozielska M, Reddy VP, Vermeulen A, Li C, Grimwood S, et al. Mechanism-Based Pharmacokinetic-Pharmacodynamic Modeling of the Dopamine D(2) Receptor Occupancy of Olanzapine in Rats. Pharm Res 2011 Oct;28(10):2490-504.

8. Kozielska M, Johnson M, Reddy VP, Vermeulen A, Li C, Grimwood S, et al. Pharmacokinetic-Pharmacodynamic Modeling of the D2 and 5-HT2A Receptor Occupancy of Risperidone and Paliperidone in Rats. Pharm Res 2011;Accepted.

9. Danhof M, De Lange ECM, la Pasqua OE, Ploeger BA, Voskuyl RA. Mechanism-based pharmacokinetic-pharmacodynamic (PK-PD) modeling in translational drug research. Trends in Pharmacological Sciences 2008;29(4):186-91.

10. Garberg P, Ball M, Borg N, Cecchelli R, Fenart L, Hurst RD, et al. In vitro models for the blood-brain barrier. Toxicology in Vitro 2005 Apr;19(3):299-334.

11. Uchida Y, Ohtsuki S, Katsukura Y, Ikeda C, Suzuki T, Kamiie J, et al. Quantitative targeted absolute proteomics of human blood-brain barrier transporters and receptors. J Neurochem 2011 Apr;117(2):333-45.

12. Mager DE, Jusko WJ. Development of translational pharmacokinetic-pharmacodynamic models. Clinical Pharmacology & Therapeutics 2008 Jun;83(6):909-12.

13. Attarbaschi T, Geiss-Granadia T, Sacher J, Klein N, Mossaheb N, Wiesegger G, et al. Striatal D2 receptor occupancy in bipolar patients treated with olanzapine. Biol Psychiatry 2005 Apr 15;57(8):169S.

14. Dresel S, Mager T, Rossmuller B, Meisenzahl E, Hahn K, Moller HJ, et al. In vivo effects of olanzapine on striatal dopamine D-2/D-3 receptor binding in schizophrenic patients: an iodine-123 iodobenzamide single-photon emission tomography study. European Journal of Nuclear Medicine 1999 Aug;26(8):862-8.
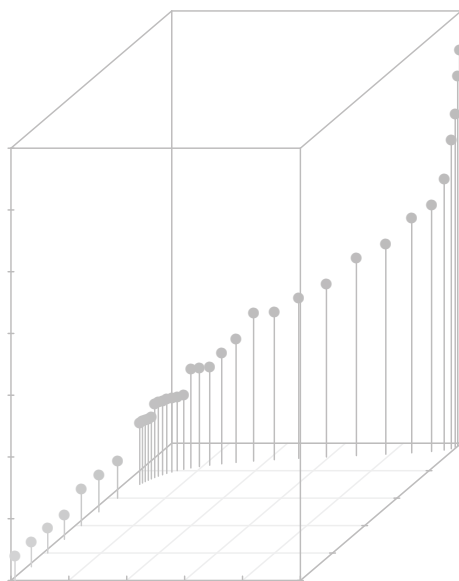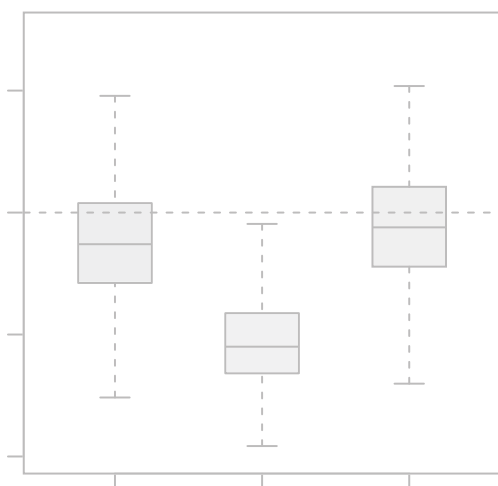
15. Nordstrom AL, Farde L, Nyberg S, Karlsson P, Halldin C, Sedvall G. D-2 Receptor Occupancy in Relation to Clozapine Serum Concentration – A Pet Study in Schizophrenic-Patients. Psychopharmacology (Berl) 1995 Mar;118(2):B8.

16. Kapur S, Remington G, Jones C, Wilson A, DaSilva J, Houle S, et al. High levels of dopamine D-2 receptor occupancy with low-dose haloperidol treatment: A PET study. American Journal of Psychiatry 1996 Jul;153(7):948-50.

17. Nordstrom AL, Farde L, Halldin C. Time Course of D2-Dopamine Receptor Occupancy Examined by Pet After Single Oral Doses of Haloperidol. Psychopharmacology (Berl) 1992 Apr;106(4):433-8.

18. Lavalaye J, Linszen DH, Booij J, Reneman L, Gersons BPR, van Royen EA. Dopamine D-2 receptor occupancy by olanzapine or risperidone in young patients with schizophrenia. Psychiatry Research-Neuroimaging 1999 Nov 8;92(1):33-44.

19. Nordstrom AL, Nyberg S, Olsson H, Farde L, Seeman P. Positron Emission Tomography Finding of a High Striatal D2Receptor Occupancy in Olanzapine-Treated Patients. Arch Gen Psychiatry 1998 Mar 1;55(3):283-4.

20. Nyberg S, Farde L, Halldin C. A PET study of 5-HT2 and D-2 dopamine receptor occupancy induced by olanzapine in healthy subjects. Neuropsychopharmacology 1997 Jan;16(1):1-7.

21. Pilowsky LS, OConnell P, Davies N, Busatto GF, Costa DC, Murray RM, et al. In vivo effects on striatal dopamine D-2 receptor binding by the novel atypical antipsychotic drug sertindole – A I-123 IBZM single photon emission tomography (SPET) study. Psychopharmacology (Berl) 1997 Mar;130(2):152-8.

22. Tauscher J, Kufferle B, Asenbaum S, Fischer P, Pezawas L, Barnas C, et al. In vivo I-123 IBZM SPECT imaging of striatal dopamine-2 receptor occupancy in schizophrenic patients treated with olanzapine in comparison to clozapine and haloperidol. Psychopharmacology (Berl) 1999 Jan;141(2):175-81.

23. Xiberas X, Martinot JL, Mallet L, Artiges E, Loc'h C, Maziere B, et al. Extrastriatal and striatal D-2 dopamine receptor blockade with haloperidol or new antipsychotic drugs in patients with schizophrenia. British Journal of Psychiatry 2001 Dec;179:503-8.

24. Hagberg G, Gefvert O, Bergstrom M, Wieselgren IM, Lindstrom L, Wiesel FA, et al. N-[C-11]methylspiperone PET, in contrast to [C-11]raclopride, fails to detect D-2 receptor occupancy by an atypical neuroleptic. 1998;82(3):147-60.

25. Arakawa R, Ito H, Takano A, Takahashi H, Morimoto T, Sassa T, et al. Dose-finding study of paliperidone ER based on striatal and extrastriatal dopamine D2 receptor occupancy in patients with schizophrenia. 2008;197(2):229-35.

26. Catafau AM, Penengo MM, Nucci G, Bullich S, Corripio I, Parellada E, et al. Pharmacokinetics and time-course of D(2) receptor occupancy induced by atypical antipsychotics in stabilized schizophrenic patients. Journal of Psychopharmacology 2008 Nov;22(8):882-94.

27. Vermeulen A, Piotrovsky V, Ludwig EA. Population pharmacokinetics of risperidone and 9-hydroxyrisperidone in patients with acute episodes associated with bipolar I disorder. J Pharmacokinet Pharmacodyn 2007 Apr;34(2):183-206.

28. Summerfield SG, Read K, Begley DJ, Obradovic T, Hidalgo IJ, Coggon S, et al. Central nervous system drug disposition: The relationship between in situ brain permeability and brain free fraction. Journal of Pharmacology and Experimental Therapeutics 2007;322(1):205-13.

29. Sun HD, Pang KS. Permeability, transport, and metabolism of solutes in caco-2 cell monolayers: A theoretical study. Drug Metab Disposition 2008 Jan;36(1):102-23.

30. Fagerholm U. The highly permeable blood-brain barrier: an evaluation of current opinions about brain uptake capacity. Drug Discovery Today 2007 Dec;12(23-24):1076-82.

31. Feng B, Mills JB, Davidson RE, Mireles RJ, Janiszewski JS, Troutman MD, et al. In vitro P-glycoprotein assays to predict the in vivo interactions of P-glycoprotein with drugs in the central nervous system. Drug Metab Dispos 2008;36(2):268-75.

32. Shirasaka Y, Sakane T, Yamashita S. Effect of P-glycoprotein expression levels on the concentration-dependent permeability of drugs to the cell membrane. J Pharm Sci 2008 Jan;97(1):553-65.

33. Danhof M, De Lange ECM, la Pasqua OE, Ploeger BA, Voskuyl RA. Mechanism-based pharmacokinetic-pharmacodynamic (PK-PD) modeling in translational drug research. Trends in Pharmacological Sciences 2008;29(4):186-91.

34. Schotte A, Janssen PF, Gommeren W, Luyten WH, Van GP, Lesage AS, et al. Risperidone compared with new and reference antipsychotic drugs: in vitro and in vivo receptor binding. Psychopharmacology (Berl) 1996 Mar;124(1-2):57-73.

35. Seeman P, Tallerico T. Antipsychotic drugs which elicit little or no Parkinsonism bind more loosely than dopamine to brain D2 receptors, yet occupy high levels of these receptors. Mol Psychiatry 1998 Mar;3(2):123-34.

36. R Development Core Team. R: A language and environment for statistical computing. R Fundation for Statistical Computing, Vienna, Austria; 2009.

37. Kapur S, Zipursky RB, Remington G. Clinical and theoretical implications of 5-HT(2) and D(2) receptor occupancy of clozapine, risperidone, and olanzapine in schizophrenia. American Journal of Psychiatry 1999 Feb;156(2):286-93.

38. Hammarlund-Udenaes M, Friden M, Syvanen S, Gupta A. On the rate and extent of drug delivery to the brain. Pharm Res 2008 Aug;25(8):1737-50.

39. Avdeef A. How well can in vitro brain microcapillary endothelial cell models predict rodent in vivo blood-brain barrier permeability? European Journal of Pharmaceutical Sciences 2011 Jun 14;43(3):109-24.

40. Danhof M, de Jongh J, De Lange ECM, la Pasqua O, Ploeger BA, Voskuyl RA. Mechanism-based pharmacokinetic-pharmacodynamic modeling: Biophase distribution, receptor theory, and dynamical systems analysis. Annual Review of Pharmacology and Toxicology 2007;47:357-400.

41. Hulme EC, Trevethick MA. Ligand binding assays at equilibrium: validation and interpretation. Br J Pharmacol 2010 Nov;161(6):1219-37.

42. Zhang G, Terry AV, Bartlett MG. Sensitive liquid chromatography/tandem mass spectrometry method for the simultaneous determination of olanzapine, risperidone, 9-hydroxyrisperidone,, clozapine, haloperidol and ziprasidone in rat brain tissue. Journal of

Chromatography B-Analytical Technologies in the Biomedical and Life Sciences 2007 Oct 15;858(1-2):276-81.

43. Chang WH, Lin SK, Jann MW. Interconversions Between Haloperidol and Reduced Haloperidol in Schizophrenic-Patients and Guinea-Pigs – A Steady-State Study. J Clin Psychopharmacol 1991 Apr;11(2):99-105.

44. Rengachary SS, Ellenbogen RG. Principles of Neurosurgery. Edinburgh: Elsevier Mosby; 2005.

45. Yin DL, Valles FE, Fiandaca MS, Forsayeth J, Larson P, Starr P, et al. Striatal volume differences between non-human and human primates. Journal of Neuroscience Methods 2009 Jan 30;176(2):200-5.

46. Farde L, Hall H, Pauli S, Halldin C. Variability in D-2-Dopamine Receptor Density and Affinity – A Pet Study with [C-11] Raclopride in Man. Synapse 1995 Jul;20(3):200-8.

47. Pazos A, Probst A, Palacios JM. Serotonin Receptors in the Human-Brain .4. Autoradiographic Mapping of Serotonin-2 Receptors. Neuroscience 1987 Apr;21(1):123-39.

48. Summerfield SG, Lucas AJ, Porter RA, Jeffrey P, Gunn RN, Read KR, et al. Toward an improved prediction of human in vivo brain penetration. Xenobiotica 2008;38(12):1518-35.

49. Liu XR, Van Natta K, Yeo H, Vilenski O, Weller PE, Worboys PD, et al. Unbound Drug Concentration in Brain Homogenate and Cerebral Spinal Fluid at Steady State as a Surrogate for Unbound Concentration in Brain Interstitial Fluid. Drug Metab Disposition 2009 Apr;37(4):787-93.

50. Keck PE, McElroy SL. Clinical pharmacodynamics and pharmacokinetics of antimanic and mood-stabilizing medications. Journal of Clinical Psychiatry 2002;63:3-11.

51. Mannens G, Meuldermans W, Snoeck E, Heykants J. Plasma-protein binding of risperidone and its distribution in blood. 1994;114(4):566-72.

52. Feng B, Mills JB, Davidson RE, Mireles RJ, Janiszewski JS, Troutman MD, et al. In vitro P-glycoprotein assays to predict the in vivo interactions of P-glycoprotein with drugs in the central nervous system. Drug Metab Dispos 2008;36(2):268-75.

53. Kapur S, Seeman P. Antipsychotic agents differ in how fast they come off the dopamine D2 receptors. Implications for atypical antipsychotic action. J Psychiatry Neurosci 2000 Mar;25(2):161-6.

54. Seeman P. Atypical antipsychotics: mechanism of action. Can J Psychiatry 2002 Feb;47(1):27-38.

55. Horacek J, Bubenikova-Valesova V, Kopecek M, Palenicek T, Dockery C, Mohr P, et al. Mechanism of action of atypical antipsychotic drugs and the neurobiology of schizophrenia. CNS Drugs 2006;20(5):389-409.

Pharmacokinetic-Pharmacodynamic Modeling of Catalepsy in Rats

Predicting Extra-pyramidal Side Effects in Humans

Martin Johnson[1], Magdalena Kozielska[1],
Venkatesh Pilla Reddy[1], An Vermeulen[2],
Hugh A. Barton[3], Sarah Grimwood[3],
Rik de Greef[4], Geny M.M. Groothuis[1],
Meindert Danhof[5] and Johannes H. Proost[1]

[1] Dept. of Pharmacokinetics, Toxicology and Targeting, University of Groningen, The Netherlands
[2] Advanced PKPD Modeling and Simulation, Janssen Research and Development, a division of Janssen Pharmaceutica NV, Beerse, Belgium
[3] Worldwide Research & Development, Pfizer, Inc., Groton, CT, USA
[4] Clinical PK-PD, Pharmacokinetics, Pharmacodynamics & Drug Metabolism, Merck Sharp & Dohme, Oss, The Netherlands
[5] Division of Pharmacology, Leiden-Amsterdam Center for Drug Research, Leiden, The Netherlands

Abstract

Objectives Dopamine D_2 receptor occupancy (D_2RO) is the major determinant of efficacy and safety in schizophrenia drug therapy. Excessive D_2RO (>80 %) is known to cause catalepsy (CAT) in rats and extrapyramidal side effects (EPS) in human. The relationship between CAT scores in rats and EPS events in human is not yet clear. The objective of this study was to use pharmacokinetic and pharmacodynamic modeling tools to relate CAT with D_2RO in rats and compare that with the relationship between D_2RO and EPS in human. Additionally, we aimed to develop a model that can predict the CAT score for other antipsychotics.

Methods Severity of CAT was assessed in rats at hourly intervals over a period of 8 hours after antipsychotic drug treatment. These CAT scores were ordered categorical in nature and each score may be correlated with the adjacent observation. In addition, we observed a time-delay between D_2RO and effects. Hence, we used an indirect response model with and without Markov elements to explain the relationship of D_2RO and CAT.

Results Both models explained the CAT data well for olanzapine, paliperidone and risperidone. However, only the model with the Markov elements predicted the CAT severity well for clozapine and haloperidol. The relationship between CAT scores in rat and EPS scores in humans was elucidated in a quantitative manner. The probability of having EPS for 0% D_2RO is approximately 5%, which shows the effect placebo on EPS. The risk of EPS does not exceed 10% over placebo correlates with less than 86% D_2RO and less than 30% probability of CAT events in rats. This tool may be useful to predict the severity of human EPS from D_2RO and CAT scores in rats.

Conclusion The relationship between D_2RO and CAT scores was elucidated using the indirect response model with Markov elements. A quantitative relationship between CAT as observed in rats and EPS as observed in humans was elucidated and may be used in drug discovery to predict the risk of EPS in humans from D_2RO and CAT scores in rats.

Introduction

In schizophrenia drug therapy and research, dopamine D_2 receptor occupancy (D_2RO) is used as a biomarker for both efficacy and incidence of side effects (1). Several studies suggest that blockade of 65% to 80% of D_2 receptors is the basis for to the antipsychotic efficacy of both the conventional neuroleptics and the novel antipsychotics (2-4). D_2RO higher than 80% increases the risk of adverse effects such as extrapyramidal symptoms (EPS) (5). In preclinical research, catalepsy (CAT) is used as a rodent model for evaluating EPS liability (6). CAT is a condition characterized by wax-like muscular rigidity, in which an abnormal body posture is maintained over an extended period of time. This effect is generally considered to be an animal model for the antipsychotic-induced EPS in human. In general, the procedure to assess CAT measures the time that an animal maintains an unusual position. It has been suggested that mechanisms involved in the mediation of CAT in rats and EPS in humans might indeed be similar (7). However, a translation of dose-response relationships for CAT and EPS thus far has not been established.

Recently, pharmacokinetic and pharmacodynamic (PKPD) models are increasingly being used to characterize and predict the time course of pharmacodynamic responses for both preclinical and clinical scenarios. These models use the principles of capacity limitation and turnover processes to describe the time course of pharmacological effects in a mechanistic manner (8). The key feature of these mechanistic models is their ability to differentiate between the system- and drug-specific parameters, which have been proven to be useful in the prediction and extrapolation of treatment effects (9-11). These PKPD models were applied in the present study, in order to elucidate the D_2RO-CAT relationship in rats and to predict any side effects in humans. Modeling is not only useful to summarize and characterize data, but also for predicting answers to questions without performing the new experiments (12). This "applied" modeling concept can be used to simulate and extrapolate treatment effects to different scenarios. This characteristic of PKPD modeling tools may be used to predict the relationship between D_2RO and side effects during early drug discovery phases.

Hence, the objective of this modeling study was to characterize a relationship between D_2RO and CAT in rats using PKPD modeling tools. We related the different scales of side effects in rats and human, in a quantitative manner. Furthermore, we aimed at a model structure that can predict CAT severity for other antipsychotics. These tools and approaches might be useful to predict side effects and thereby accelerate the drug development process.

Methods

Data

This work was performed within the framework of the Dutch Top Institute Pharma project: Mechanism-based PKPD modeling (http://www.tipharma.com). This mechanism-based PKPD modeling platform involves leading pharmaceutical companies worldwide, and academic institutes from The Netherlands. The pharmaceutical companies who are the members of this mechanism-based PKPD modeling platform, namely, Janssen Research and Development – Belgium, *Merck* Sharp & Dohme – The Netherlands and Pfizer Worldwide Research and Development – USA, provided data on D_2RO and CAT scores after treatment with clozapine (CLZ), haloperidol (HAL), olanzapine (OLZ), paliperidone (PAL) and risperidone (RIS).

Catalepsy experiments

CAT studies were performed using Wistar rats at different dose levels for each drug (modified after Janssen et al., 1965) (13). CAT was assessed in rats at hourly intervals over a period of 8 hours after the administration of test compound or vehicle. A control group (vehicle treatment) was included in all these experiments and the historical data from vehicle treatment was available and used for the following categorization. Each rat was scored based on the severity of the CAT as pronounced (score=3), moderate (score=2), slight (score=1), and absent (score=0). Evaluations of CAT were based on the sum of the scores from two independent observers, resulting in a score that ranged from 0 to 6. However, the criteria for drug-induced CAT were determined as absent for the scores ≤ 2, as mild for the scores between 3 and 5 (occurrence 0.1% of control animals) and severe for scores of 6 (not observed in controls). During this model development, CAT scores of absent, mild and severe were coded as 0, 1 and 2, respectively. Details of these animal studies are presented in Table 6.1.

Table 6.1: Details of animal studies used in this analysis			
Name of the antipsychotics	Dose Range (mg/kg)	Number of Rats used	Number of observations
Clozapine	0.63-320	85	765
Haloperidol	0.16-10	70	630
Olanzapine	0.16-40	99	891
Paliperidone	0.08-40	46	414
Risperidone	0.04-10	80	720

Dopamine D2 Receptor Occupancy Simulations

The animal study protocol for CAT experiments was aimed to measure the time course of CAT severity. Hence, it was not possible to measure D_2RO in the same animals and plasma drug concentrations were not available for these rats. Hence, we used previously developed PKPD models to simulate D_2RO for each dose level.

Previously, we developed hybrid physiology-based pharmacokinetic and pharmacodynamic (PBPKPD) models to describe the relationship between drug exposure in plasma and brain with D_2RO in rats for OLZ, PAL and RIS. These models have been described elsewhere (14, 15). Briefly, classical pharmacokinetic models based on a population approach were used to describe the plasma concentration time profiles.
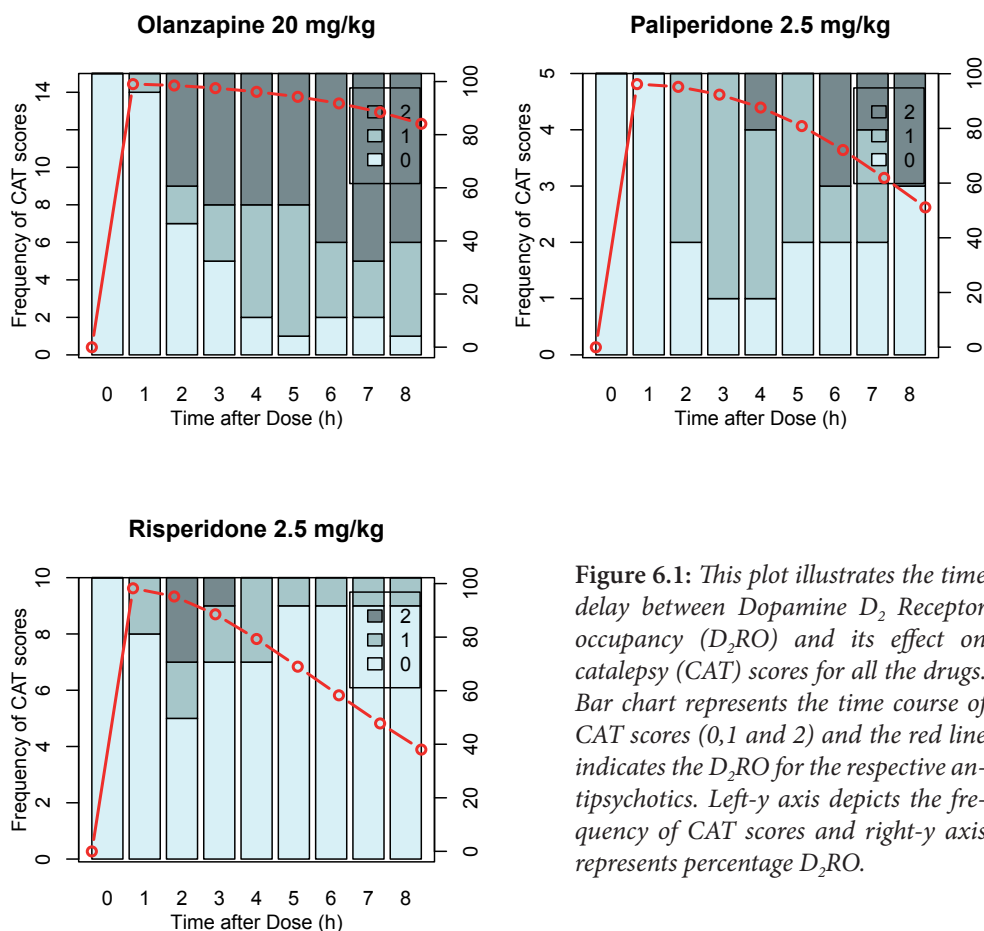
Figure 6.1: *This plot illustrates the time delay between Dopamine D_2 Receptor occupancy (D_2RO) and its effect on catalepsy (CAT) scores for all the drugs. Bar chart represents the time course of CAT scores (0,1 and 2) and the red line indicates the D_2RO for the respective antipsychotics. Left-y axis depicts the frequency of CAT scores and right-y axis represents percentage D_2RO.*

Distribution of drug to the brain was described based on passive and if applicable, active drug transport mechanisms. Subsequent binding to D_2 receptors in striatum was characterized using association and dissociation constants of these drugs to D_2 receptors. So, we used this previously developed PBPKPD model to simulate D_2RO for OLZ, PAL and RIS and used the simulated D_2RO to develop a model to explain the time course of CAT severity in rats.

In addition, we also had CAT severity information for CLZ and HAL in rats. However, there was not enough information available on plasma and brain drug concentrations and D_2RO to develop a PBPKPD model. We therefore simulated the time course of D_2RO based on a published empirical PKPD model. We referred to the original publications for more details on PKPD modeling (14-17). For HAL, the pharmacokinetic parameters were obtained from a PK model developed by us. We intended to use the D_2RO of CLZ and HAL to predict the D_2RO-CAT relationship obtained using the PKPD model that was developed using the CAT scores from OLZ, PAL and RIS.

Pharmacodynamic Model
Modeling ordered categorical nature of CAT score consisted of an indirect response (IDR) model combined with a logistic regression model to describe the relationship between D_2RO and the CAT scores. Further, we explored the requirement of Markov element to properly account for the correlation between frequently observed CAT scores.

Indirect response model
During exploratory data analysis, a time delay between D_2RO and severity of CAT scores (Figure. 6.1) was evident. Model building was therefore initiated by accounting for this time delay using biophase, transduction and IDR models. It was found that IDR model gave better results than other models on the basis of objective function and model fit.

The IDR (18) model as implemented in this analysis, utilizes K_{in} as zero-order rate constant for the production of response and K_{out} as first-order rate constant for the loss of response.

$$d(R)/dt = K_{in}*(Q/(Q_{50}+Q)) - K_{out}*R$$

Q is the transformed form of D_2RO which was derived as RO / (100- RO), where RO refers to the D_2 receptor occupancy. This transformation allows Q to have a value from 0 to infinity for D_2RO from 0 to 100%. A similar transformation was applied to estimate RO_{50}, as $Q_{50} = (RO_{50}/ (100-RO_{50}))$. This model assumed that there was

no CAT severity in the absence of D_2RO. The response variable, R, is an observed response which is a function of D_2RO. RO_{50} is the receptor occupancy at which the production of CAT response is 50% of the maximal K_{in}. RO_{50} was estimated by fitting this model to the D_2RO and CAT score data.

Severity of CAT is an ordered categorical variable that can take a value of 0 (absence of catalepsy), 1 (a mild catalepsy) or 2 (severe catalepsy). Hence, the probability of each severity was modeled with a logistic regression model (19,20). This model is intended to describe the relationship between D_2RO and severity of CAT in rats. Simulated D_2RO were used to sequentially fit this model to CAT score data. The mixed effects logistic regression model was implemented as explained in the following equation:

$$\text{logit}[P(CAT_{ij} \geq m|CAT_i, \eta_i)] = \sum_{k=1}^{m} \beta_k + R + \eta_i$$

where CAT_{ij} denotes the CAT severity score for the ith individual at time j; $\text{logit}[P(CAT_{ij} \geq m|CAT_i, \eta_i)]$ denotes the logit function of the cumulative probability that the CAT severity score is $\geq$ m (m = 1 or 2) for rat i at time t_j given the rat has a CAT event at some time point during the study; β_k specifies the baseline set of logit probabilities of the various degrees of CAT severity; For example, β_1 specifies the baseline set of probabilities for the CAT score to be $\geq$ 1. R is an observed response which is a function of D_2RO; and η_i is a random individual effect determining the individual sensitivity assumed to be 0. The time course of CAT was investigated for the drug effect.

Indirect response – Markov model
The CAT severity scores were observed every hour during the animal experiments. Therefore, there may be a correlation between neighboring observations within a rat. This model estimates the cumulative probabilities of having a certain CAT score given the previous observation:

$$\text{logit}[P(CAT_{ij} \geq m|CAT_i, CAT_{ij-1} = h, \eta_i)] = \sum_{k=1}^{m} \beta_{kh} + R + \eta_i$$

where CAT_{ij} denotes the CAT severity score for the ith individual at tj, and CAT_{ij-1} is the CAT severity for that rat at t_{j-1} (the previous CAT score), the β_{kh} specifies the baseline set of logit probabilities of the various degrees of CAT severity, given the previous state of CAT (h). For example, β_{10} specifies the baseline set of probabilities for the CAT score to be $\geq$ 1, given the previous observation is 0. R is the outcome of IDR model, which describes the effect of D_2RO on CAT response; and η_i is a random individual effect determining the individual sensitivity assumed to be 0.

Model building

Model fitting was performed using a population analysis approach as implemented in NONMEM (version VII level 2.0) (21). Diagnostic graphics, post processing of NONMEM output and data simulations were performed using R (version 2.10) (22).

During the model building, the goodness-of fit of different models to the data was evaluated using change in objective function relative to the change in the number of parameters, assuming a chi-square distribution.

Model Evaluation

Standard visual predictive check (VPC) was performed to check the adequacy of the models. If the model provides an adequate description of the data, then the simulated data should mimic the important features of the real data. To evaluate the integrity of the model, 95% confidence intervals (CIs) were calculated by a log-likelihood profiling (LLP) method. VPC and LLP were done as implemented in PsN (version 3.2.4) (23).

The performance of the IDR and IDR-Markov model for explaining the different transition was evaluated by a predictive check based on the simulations obtained from these models. Transition refers to the change of CAT severity from one state to other state. One hundred datasets with identical design to the original dataset were used to simulate the distribution of the number of the transitions using the parameters obtained from both the IDR and the IDR-Markov models and compared with the original number of transitions.

Extrapolation to other drugs

The performance of the IDR and IDR-Markov models were evaluated by simulating CAT severity scores for two other antipsychotics, CLZ and HAL. This simulation was done as described below. Initially, D_2RO for CLZ and HAL was predicted using an empirical PKPD model (16, 17). The IDR and IDR-Markov model parameters were used in this simulation study to simulate CAT severity over time for CLZ and HAL. One hundred datasets with identical design to the original design were simulated using both models and the simulations were graphically compared with observations.

EPS and Catalepsy

The secondary objective of this study was to relate the rat CAT scores with the human EPS scores at steady-state conditions. To simulate the CAT scores at steady-state conditions, the IDR-Markov model estimated parameters were used. Since the Markov model accounts for the correlation with previous observations, the probability of severity at the given time-point is conditioned on the previous observation, hence,

$P_0 = P'_0 * (P_{00}) + P'_1 * (P_{10}) + P'_2 * (P_{20})$, where P_{00}, P_{10}, P_{20} are the probabilities of being at 0, when their previous observation was 0, 1 and 2 respectively. At steady state conditions, P'_0 is assumed to be equal to P_0. Similar equations can be written for P_1 and P_2. The probability of each severity was plotted against D_2RO.

Pilla Reddy *et al* (24) described the relationship between human D_2RO obtained from different antipsychotics and EPS using PKPD modeling with a Markov approach. This model was used to simulate the probability of EPS as absent, mild and moderate in steady-state conditions after 6 weeks of drug treatment. The relationship between D_2RO and probability of CAT in rats was related to the D_2RO-EPS relationship in human using a polynomial equation.

Results

Pharmacodynamic model

Indirect response models with and without Markov elements were used to describe the drug effect on the severity of CAT in rats. The IDR with proportional odds model for ordered categorical data provided a good fit of the model to the olanzapine,

Table 6.2: Parameter estimates for IDR model			
Parameters	Description	Population Mean (SE)	95% CI (Lower … Upper)
β_1	Baseline probability (logit) for CAT ≥ 1	-5.17 (0.275)	-5.74 … -4.66
β_2	Baseline probability (logit) for CAT ≥ 2	-1.74 (0.118)	-1.98 … -1.52
K_{in} (h^{-1})	zero-order rate constant for the production of response	4.70 (0.251)	4.22 … 5.20
K_{out} (h^{-1})	first-order rate constant for the loss of response	0.249 (0.0229)	0.206 … 0.297
RO_{50} (%)	Receptor occupancy at which the production of CAT response is 50% of the maximal production K_{in}	95.7 (0.007)	94.0 … 96.9
SE – standard error as obtained from the COVARIANCE option of NONMEM CI – confidence interval estimated using likelihood profiling			

Table 6.3: Parameter estimates for IDR-Markov model			
Parameters	Description	Population Mean (SE)	95% CI (Lower … Upper)
β_{10}	Baseline probability (logit) for CAT ≥ 1, when the previous CAT was 0	-5.14 (0.378)	-6.00 … -4.49
β_{20}	Baseline probability (logit) for CAT ≥ 2, when the previous CAT was 0	-1.46 (0.188)	-1.86 … -1.12
β_{11}	Baseline probability (logit) for CAT ≥ 1, when the previous CAT was 1	-0.926 (0.382)	-1.74 … -0.213
β_{21}	Baseline probability (logit) for CAT ≥ 2, when the previous CAT was 1	-3.43 (0.297)	-4.03 … -2.87
β_{12}	Baseline probability (logit) for CAT ≥ 1, when the previous CAT was 2	-0.019 (0.552)	-1.11 … 1.09
β_{22}	Baseline probability (logit) for CAT ≥ 2, when the previous CAT was 2	-2.50 (0.386)	-3.36 … -1.83
K_{in} (h^{-1})	zero-order rate constant for the production of response	6.41 (0.987)	4.94 … 8.85
K_{out} (h^{-1})	first-order rate constant for the loss of response	0.818 (0.213)	0.493 … 1.28
RO_{50} (%)	Receptor occupancy at which the production of CAT response is 50% of the maximal production K_{in}	94.5 (0.021)	89.1 … 97.4
SE – standard error as obtained from the COVARIANCE option of NONMEM CI – confidence interval estimated using likelihood profiling			

6

paliperidone and risperidone data; K_{in}, K_{out}, RO_{50} and baseline probabilities were estimated with good precision (Table 6.2). Model parameter estimates obtained from the IDR-Markov model are presented in Table 6.3. Both these models estimated baseline probabilities for the severity of CAT. K_{in}, K_{out} and RO_{50} were estimated with good precision. We also estimated separate RO_{50} for each drug, which turned

Table 6.4: Objective function values and different RO_{50} estimates of IDR-Markov Model		
Model Description	Objective function value	Estimated RO_{50} (%)
Common RO_{50} for OLZ, PAL and RIS	1037	94.5
Separate RO_{50} for OLZ, PAL and RIS	1030	OLZ – 95.9 PAL – 94.2 RIS – 96.2
OLZ – Olanzapine PAL – Paliperidone RIS – Risperidone RO_{50} is the receptor occupancy at which the production of CAT response is 50% of the maximal production K_{in}		

out to be similar between OLZ, PAL and RIS and the objective function was not significantly (P<0.01) decreased when compared to the model with common RO_{50} for all these drugs (Table 6.4). Inter-rat variability was assumed to be equal to zero in both models.

Model Evaluation
For both IDR and IDR-Markov models, 95% CI obtained using LLP were within acceptable limits for all the parameters, except for the baseline probability estimate β_{12} (Table 6.2 & 6.3). VPC plots demonstrated that the model fits obtained by both IDR and IDR-Markov models were similar (Figure 6.2). The time-dependent transition from one state of catalepsy to other state of catalepsy is depicted in Figure 6.3. Both IDR and IDR-Markov models predicted the transition states equally well.

Extrapolation to other drugs
For CLZ and HAL, IDR-Markov model performed slightly better than IDR model in predicting CAT severity score (Figure 6.4).

CAT and EPS relationship
The relationship between D_2RO and side effect scores in rat and human is depicted in Figure 6.5. Excessive D_2RO (>80%) changed the probability towards mild and severe CAT in rats, whereas in human a similar type of change was not observed. The relationship between CAT and EPS scores is shown in Figure 6.6. A polynomial function was used to quantitatively relate the CAT and EPS scores.

(a) IDR Model
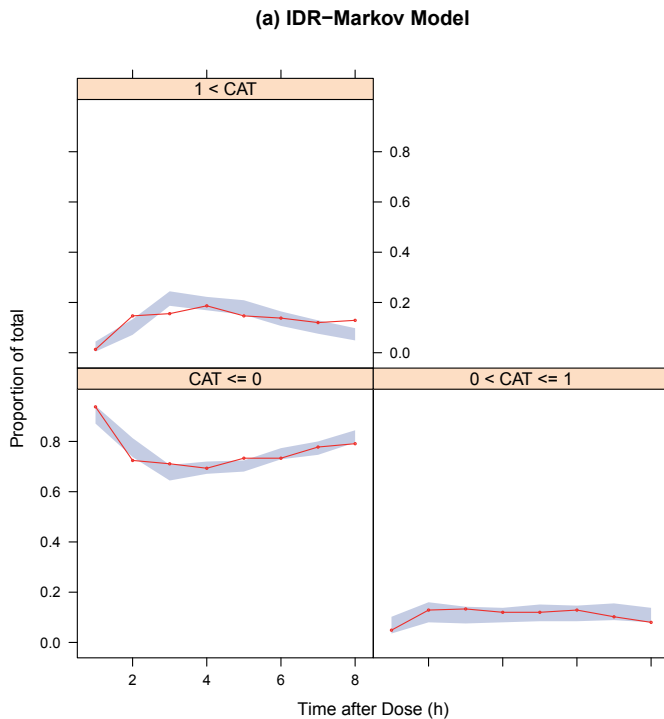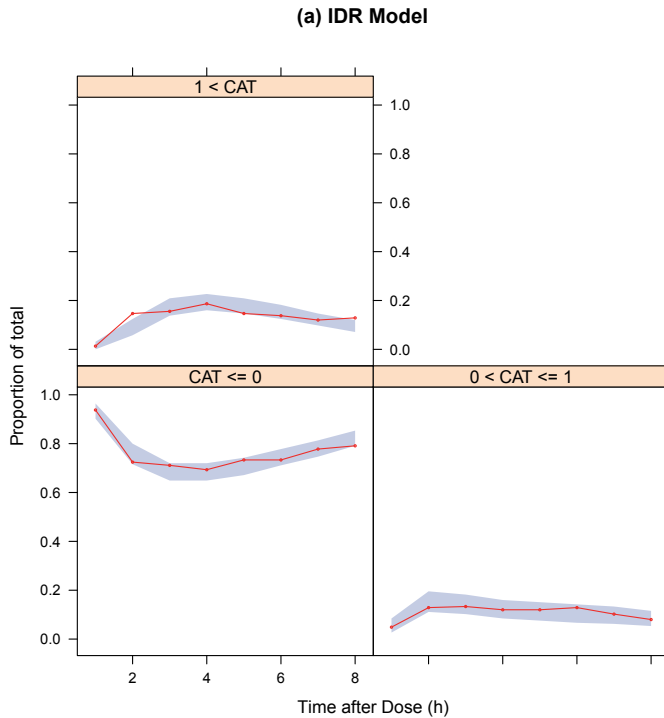
(a) IDR-Markov Model

Figure 6.2: *Plot represents the visual predictive checks for the adequacy of indirect response (IDR) and indirect response with Markov (IDR-Markov) model. Shaded area depicts the 90% prediction interval for the simulated probabilities and the red solid line represents the median probability from the original data.*
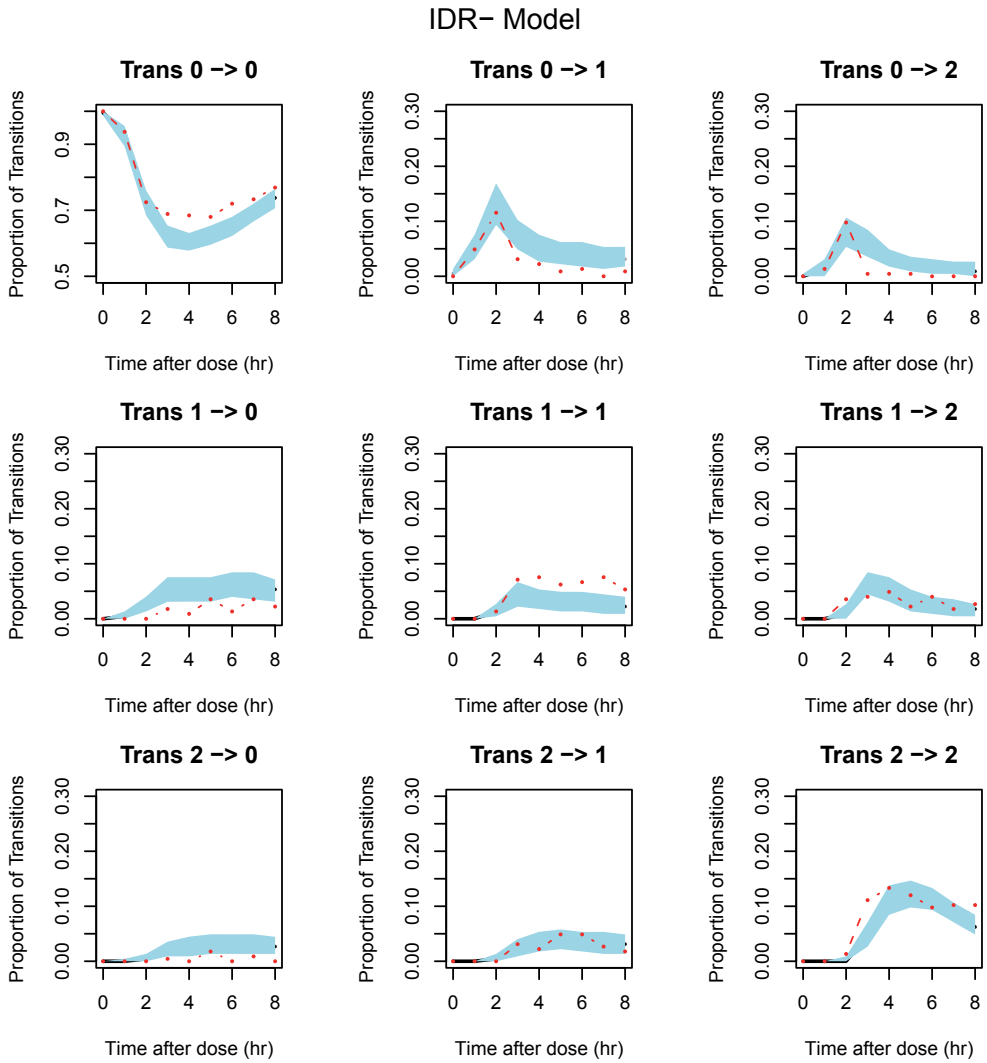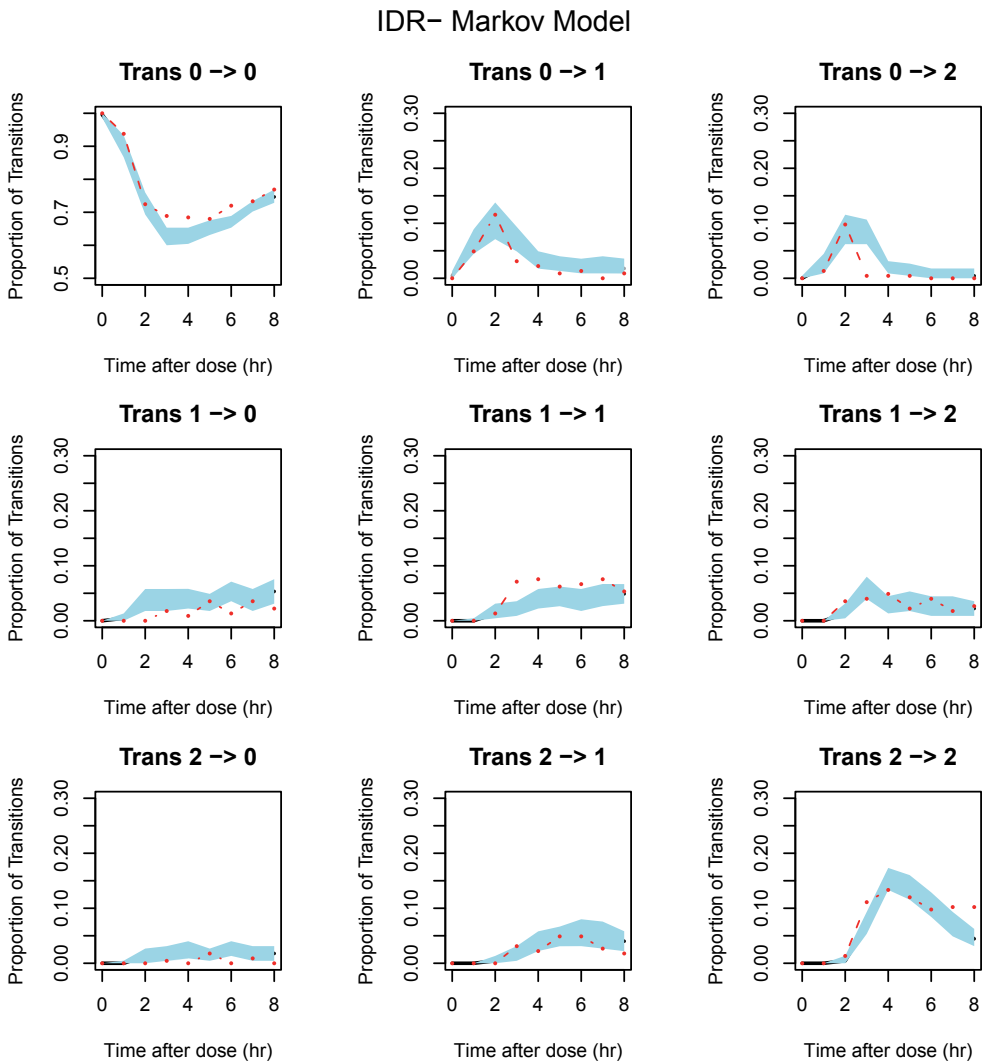
Figure 6.3: *Predictive check results for the distribution of transitions in catalepsy severity. Red dotted lines represent the observed median for the proportion of transitions and shaded areas*

IDR− Markov Model

the 90% prediction interval from the indirect response (IDR) and indirect response with Markov (IDR-Markov) model simulations.

(a) IDR Model − Clozapine
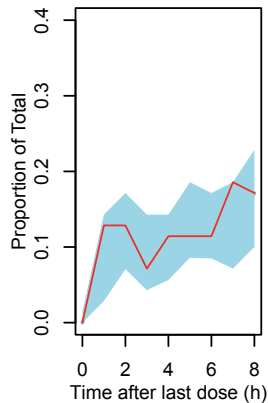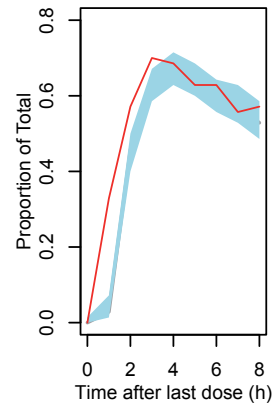
(b) IDR−Markov Model − Clozapine
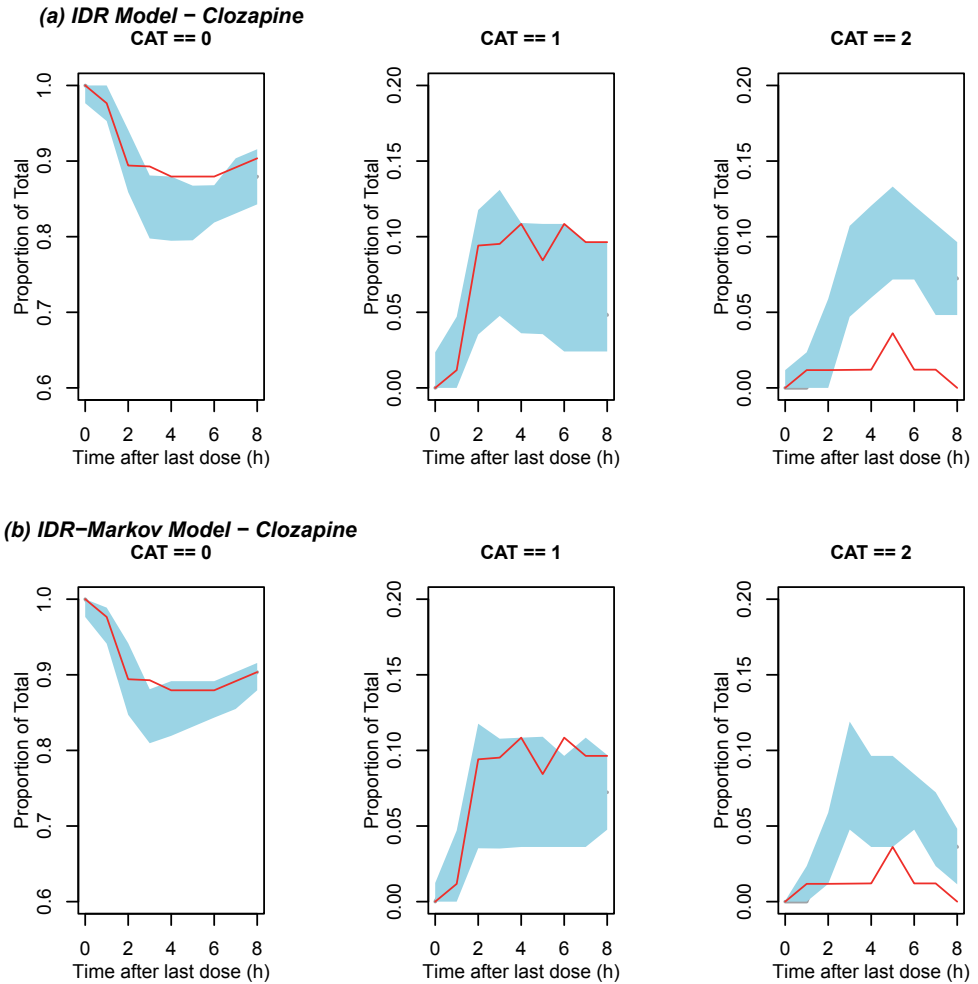
Figure 6.4: *Plot represents the simulated probabilities of catalepsy for clozapine and haloperidol. Red dotted lines represent the observed median probability and shaded areas the 90% prediction interval from the indirect response (IDR) and indirect response with Markov (IDR-Markov)*

(c) IDR Model − Haloperidol
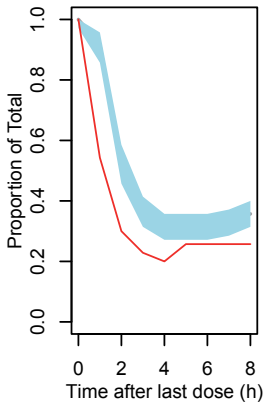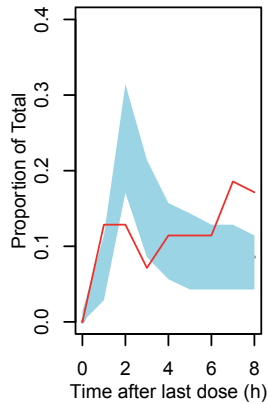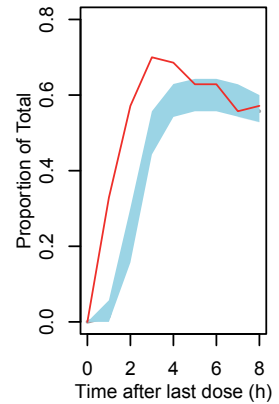
(d) IDR−Markov Model − Haloperidol
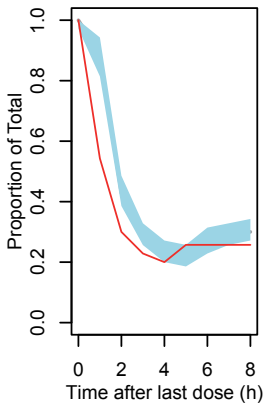
model simulations. (a) and (b) show the prediction probabilities of catalepsy for clozapine using IDR and IDR-Markov models, respectively. (c) and (d) show the probabilities of catalepsy for haloperidol using IDR and IDR-Markov models, respectively.

6
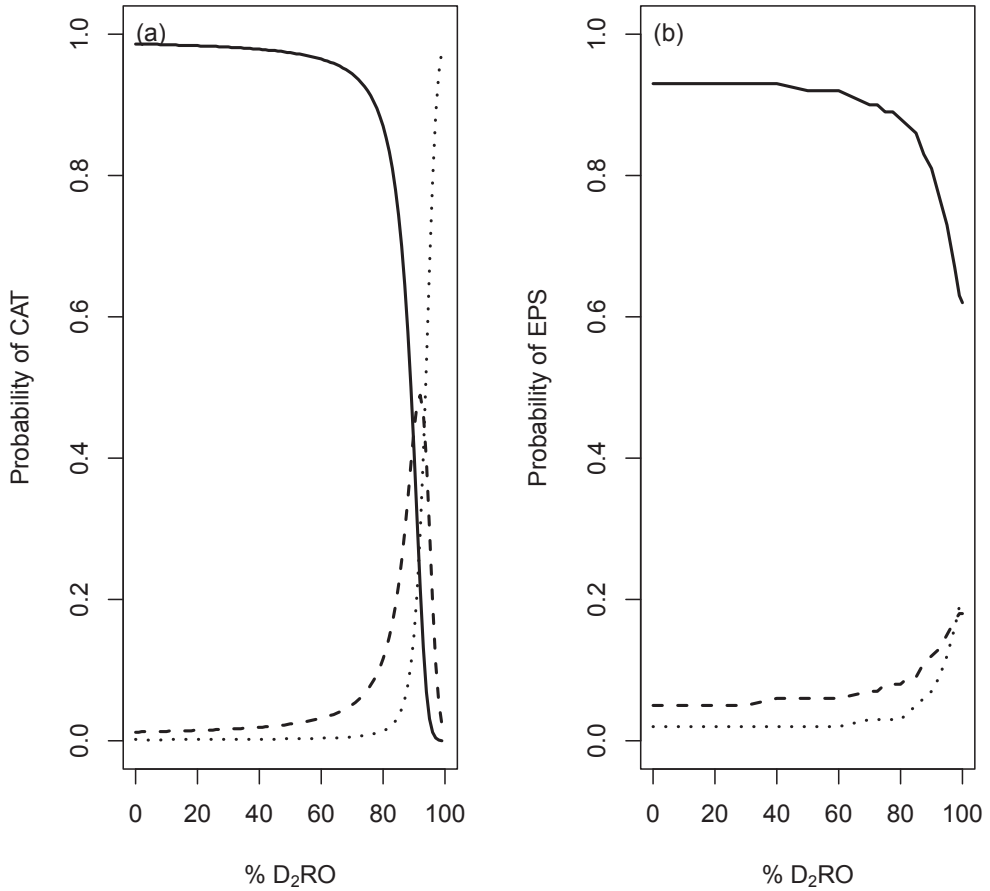
Figure 6.5: *Plot represents the relationship between D_2 receptor occupancy and side-effects. Panel (a) represents the probability of catalepsy (CAT) scores in rats at steady state conditions. Solid, dashed and dotted lines depict the probabiliti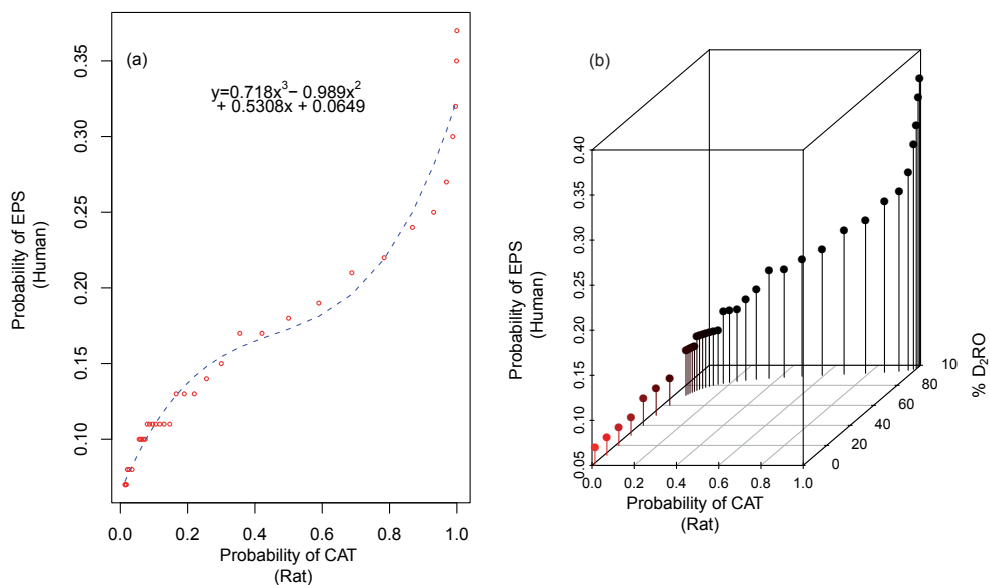es of CAT severity as absent, mild and severe, respectively. Panel (b) represents the probability of extrapyramidal symptom (EPS) scores in humans at steady state conditions. Solid, dashed and dotted lines depict the probabilities of CAT severity as absent, mild and moderate to severe, respectively.*

Figure 6.6: *Panel (a) represents the relationship of side-effects between rat and humans. The blue dotted line is obtained by fitting a polynomial model to the probability of side effects in rats (CAT) and humans (EPS). In panel (b), the dots with dropped lines depict the relationship between catalepsy in rats and the probability of extrapyramidal symptoms in humans for respective D_2 receptor occupancies.*

Discussion

The objective of our PKPD analysis was to utilize the information on CAT in rats to describe the relationship between D_2RO and CAT and to extrapolate this relationship to other drugs to predict CAT scores. We also linked the CAT in rat to EPS in human using PKPD modeling and simulation approaches.

Several studies seem to indicate that the dopaminergic pathway involved in the mediation of CAT in rats and EPS in humans could be similar (7). Moreover, it was reported that CAT in rats is a reliable indicator of gradual dissociation of the antipsychotic agent from D_2 receptors (6). Hence, our approach to relate D_2RO and CAT severity is substantiated. Moreover, using D_2RO-CAT relation rather than drug exposure-CAT relation gives the way to introduce a compound independent variable, which may be used to extrapolate the D_2RO-CAT relationship to other drugs and also to scale this relationship between different species. In general, proportional

odds models, introduced in the field of PKPD modeling by Sheiner *et al* (20) have been proven to describe the ordered categorical data well. In our data analysis, the proportional odds model was used to explain the probability of the degree of CAT.

It is evident that D_2RO and CAT severity scores are not directly related with time (Figure 6.1). So, it is appropriate to use an IDR model to explain the relationship between D_2RO and CAT scores rather than a direct response model (e.g., Emax model). The semi-mechanistic nature of IDR models allows for distinguishing the drug-specific parameters (RO_{50}) and system-specific parameters (K_{in} and K_{out}). It is acceptable to assume that these system-specific parameters could be the same for different antipsychotic drugs. This characteristic of the IDR model is used as a base to extrapolate the D_2RO-CAT relationship to other drugs (discussed later). In our analysis we assumed a common RO_{50} to determine the receptor occupancy to produce a half-maximal effect. This assumption allows for considering RO_{50} as a "system" parameter, which can be used for extrapolating the D_2RO-CAT relationship to other drugs.

It was expected that for frequently measured categorical type data, there might be correlation between neighboring observations. The standard proportional odds model with IDR model may not be able to account for these correlations. These series of probable transitions between states can be described with Markov modeling (19, 25). Zingmark *et al* (25) modeled spontaneously reported side-effects using a Markov approach which is a hybrid between the proportional odds model and the transition model. We adapted this approach in our modeling work in combination with the IDR model.

Markov models have been reported to describe frequently observed and correlated scores better than the models without Markov elements (19, 25). However, we did not observe any significant difference in the predictions of the probability of CAT obtained from the IDR and IDR-Markov models. The VPC plots representing the probability at the three states of CAT were also similar between these two models. It was also reported that Markov models predict the number of transitions much better than non-Markov models (19, 25). In our modeling, both these models predicted the transition states adequately. Precision of the predictions was limited by the fact that the D_2RO was not observed for individual rats, but predicted based on previously developed models. For this same reason, inter-rat variability was assumed to be zero in these models. One of the baseline probabilities (β_{12}) was estimated with lower precision and wide confidence intervals were seen in likelihood profiling. It is common that Markov models are over-parameterized to handle the correlation between adjacent observations (25).

Dopamine D_2 receptor occupancy was simulated using previously developed PBPKPD models. These models are available only for OLZ, PAL and RIS. So, we used the CAT scores from OLZ, PAL and RIS to develop the IDR and IDR-Markov

models. However, we intended to extend the D_2RO-CAT relationship to CLZ and HAL. Since we do not have PBPKPD models for CLZ and HAL, we utilized empirical PKPD models to simulate D_2RO for CLZ and HAL and to predict CAT severity in rats. Using both IDR and IDR-Markov model structure and parameter estimates, CAT scores were predicted for CLZ and HAL. IDR-Markov models performed slightly better than the IDR models in predicting CAT scores for CLZ and HAL. Moreover, the unique feature of the Markov model to account for the correlation between adjacent observations may be responsible for its good predictions. However, it should be noted that this approach had not been tested on antipsychotics, which have a different mechanisms of action than D_2 antagonism (e.g. Aripiprazole).

The relationship between CAT scores in rat and EPS scores in humans was elucidated in a quantitative manner. Severity and occurrence of side effects and their relation with D_2RO are not same between these species. The probability for having any EPS event is less than 40% in clinical studies, even for very high D_2RO, whereas the probability of any CAT event is close to 1 for very high D_2RO in rats. Interestingly in humans, the probability of having EPS for 0% D_2RO is approximately 5%, which shows the effect of placebo on EPS. This tool may be used in drug discovery to predict the risk of EPS in humans from D_2RO and CAT scores in rats using the fitted polynomial function. For example, a risk of EPS does not exceed 10% over placebo may be predicted from 86% D_2RO and less than 30% probability of CAT events in rats (Figure 6.5 and Figure 6.6).

We have developed and evaluated an indirect relationship between D_2RO and CAT scores using PKPD modeling tools. However, this IDR-Markov modeling approach did not take into account for the involvement of endogenous dopamine and serotonin ($5HT_{2A}$) receptor occupancy on CAT severity. Furthermore, we previously developed a physiology-based PKPD model structure to predict the D_2RO in human, which is also applicable in preclinical scenarios (14, 15). This combination tool will be useful to design optimal studies with adequate doses using fewer animals. Moreover, these results imply that EPS events in human can be predicted from CAT events and D_2RO data in rats.

Conclusion

The relationship between D_2RO and CAT scores was elucidated using IDR and IDR-Markov models. The IDR-Markov model predicted the severity of CAT for CLZ and HAL better than the IDR model. The outcome of our simulations directed towards a link between CAT as observed in rats and EPS as observed in humans in a quantitative manner.

## Acknowledgements

References

1. de Greef R, Maloney A, Olsson-Gisleskog P, Schoemaker J, Panagides J. Dopamine D(2) Occupancy as a Biomarker for Antipsychotics: Quantifying the Relationship with Efficacy and Extrapyramidal Symptoms. Aaps Journal 2011 Mar;13(1):121-30.
2. Kapur S, Remington G, Jones C, Wilson A, DaSilva J, Houle S, et al. High levels of dopamine D-2 receptor occupancy with low-dose haloperidol treatment: A PET study. American Journal of Psychiatry 1996 Jul;153(7):948-50.
3. Farde L, Nordstrom AL, Wiesel FA, Pauli S, Halldin C, Sedvall G. Positron Emission Tomographic Analysis of Central D1-Dopamine and D2-Dopamine Receptor Occupancy in Patients Treated with Classical Neuroleptics and Clozapine – Relation to Extrapyramidal Side-Effects. Arch Gen Psychiatry 1992 Jul;49(7):538-44.
4. Nordstrom AL, Farde L, Wiesel FA, Forslund K, Pauli S, Halldin C, et al. Central D2-Dopamine Receptor Occupancy in Relation to Antipsychotic Drug Effects – A Double-Blind Pet Study of Schizophrenic-Patients. Biol Psychiatry 1993 Feb 15;33(4):227-35.
5. Horacek J, Bubenikova-Valesova V, Kopecek M, Palenicek T, Dockery C, Mohr P, et al. Mechanism of action of atypical antipsychotic drugs and the neurobiology of schizophrenia. CNS Drugs 2006;20(5):389-409.
6. Hoffman DC, Donovan H. Catalepsy As A Rodent Model for Detecting Antipsychotic-Drugs with Extrapyramidal Side-Effect Liability. Psychopharmacology (Berl) 1995 Jul;120(2):128-33.
7. Wadenberg MLG, Kapur S, Soliman A, Jones C, Vaccarino F. Dopamine D-2 receptor occupancy predicts catalepsy and the suppression of conditioned avoidance response behavior in rats. Psychopharmacology (Berl) 2000 Jul;150(4):422-9.
8. Mager DE, Jusko WJ. Development of translational pharmacokinetic-pharmacodynamic models. Clinical Pharmacology & Therapeutics 2008 Jun;83(6):909-12.
9. Yassen A, Olofsen E, Kan J, Dahan A, Danhof M. Animal-to-human extrapolation of the pharmacokinetic and pharmacodynamic properties of buprenorphine. Clin Pharmacokinet 2007;46(5):433-47.
10. Danhof M, De Lange ECM, la Pasqua OE, Ploeger BA, Voskuyl RA. Mechanism-based pharmacokinetic-pharmacodynamic (PK-PD) modeling in translational drug research. Trends Pharmacol Sci 2008;29(4):186-91.

11. Zuideveld KP, Van der Graaf PH, Peletier LA, Danhof M. Allometric scaling of pharmacodynamic responses: application to 5-Ht1A receptor mediated responses from rat to man. Pharm Res 2007 Nov;24(11):2031-9.

12. Bonate PL. Principles of Simulation. Pharmacokinetic-Pharmacodynamic Modeling and Simulation. Springer; 2011. p. 489.

13. Janssen PAJ, Niemegeers CJE, Schellekens KH. Is it possible to predict the clinical effects of neuroleptic drugs (major tranquilizers) from animal data? Part I. Neuroleptic activity spectra for rats. Arzneimittel Forschung 1965;15:104-17.

14. Johnson M, Kozielska M, Reddy VP, Vermeulen A, Li C, Grimwood S, et al. Mechanism-Based Pharmacokinetic-Pharmacodynamic Modeling of the Dopamine D(2) Receptor Occupancy of Olanzapine in Rats. Pharm Res 2011 Oct;28(10):2490-504.

15. Kozielska M, Johnson M, Reddy VP, Vermeulen A, Li C, Grimwood S, et al. Pharmacokinetic-Pharmacodynamic Modeling of the D2 and 5-HT2A Receptor Occupancy of Risperidone and Paliperidone in Rats. Pharm Res 2011;Accepted.

16. Parker TJ, la Pasqua OE, Loizillon E, Chezaubernard C, Jochemsen R, Danhof M. Pharmacokinetic-pharmacodynamic modelling in the early development phase of anti-psychotics: A comparison of the effects of clozapine, S 16924 and S 18327 in the EEG model in rats. Br J Pharmacol 2001;132(1):151-8.

17. Olsen CK, Brennum LT, Kreilgaard M. Using pharmacokinetic-pharmacodynamic modelling as a tool for prediction of therapeutic effective plasma levels of antipsychotics. Eur J Pharmacol 2008 Apr 28;584(2-3):318-27.

18. Dayneka NL, Garg V, Jusko WJ. Comparison of 4 Basic Models of Indirect Pharmacodynamic Responses. Journal of Pharmacokinetics and Biopharmaceutics 1993 Aug;21(4):457-78.

19. Ito K, Hutmacher MM, Liu J, Qiu R, Frame B, Miller R. Exposure-response analysis for spontaneously reported dizziness in pregabalin-treated patient with generalized anxiety disorder. Clinical Pharmacology & Therapeutics 2008 Jul;84(1):127-35.

20. Sheiner LB, Beal SL, Dunne A. Analysis of nonrandomly censored ordered categorical longitudinal data from analgesic trials. Journal of the American Statistical Association 1997 Dec;92(440):1235-44.

21. Beal S, Sheiner LB, Boeckmann A, Bauer RJ. NONMEM User's Guides (1989-2009). Icon Development Solutions, Ellicott City, Maryland, USA, 2009.

22. R Development Core Team. R: A language and environment for statistical computing. R Fundation for Statistical Computing, Vienna, Austria; 2009.

23. Lindbom L, Pihlgren P, Jonsson EN. PsN-Toolkit--a collection of computer intensive statistical methods for non-linear mixed effect modeling using NONMEM. Comput Methods Programs Biomed 2005 Sep;79(3):241-57.

24. Reddy VP, Petersson K.J., Suleiman AA, Vermeulen A, Proost JH, Friberg LE. Pharmacokinetic-Pharmacodynamic Modeling of Severity Levels of Extrapyramidal Side Effects with Markov Property. Manuscript in Preparation 2012.

25. Zingmark PH, Kagedal M, Karlsson MO. Modelling a spontaneously reported side effect by use of a Markov mixed-effects model. J Pharmacokinet Pharmacodyn 2005 Apr;32(2):261-81.

6

Concepts and Challenges in Translation of Receptor Occupancy

General Discussion
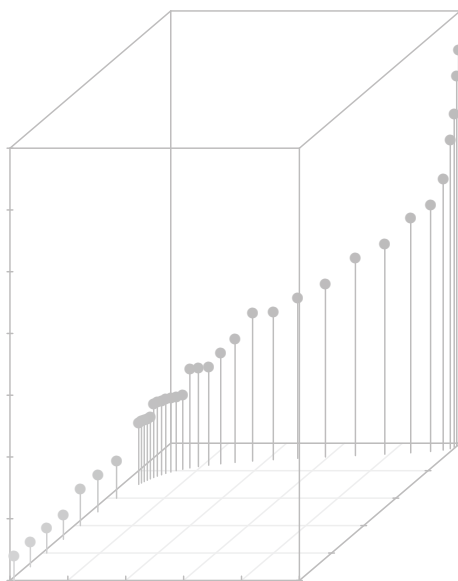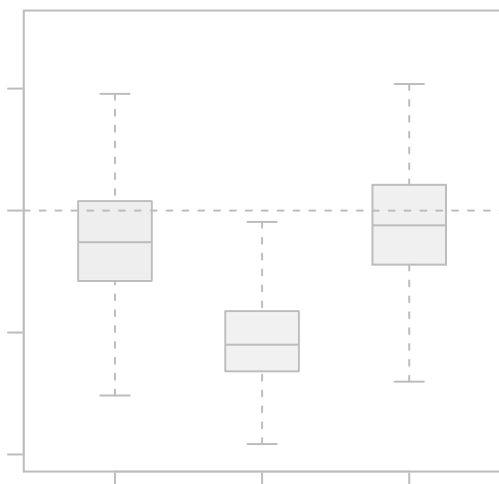
In pharmaceutical industry, translational research refers to those activities conducted to bridge the gap between drug discovery in animals and drug development in human patients (1). Translational research activities, in a pharmaceutical industry context, aim to predict the biomarker or drug effects in clinical situations based on *in vitro* or preclinical information. In this thesis we aimed to develop a translational pharmacokinetic and pharmacodynamic (PKPD) modeling framework by integrating *in vitro*, and *in vivo* preclinical data with mechanism-based models to predict the effects of drugs in humans. In this thesis, the translational PKPD models are developed specifically to the schizophrenia indication.

Schizophrenia is a severe and disabling mental disorder, associated with dopamine dysregulation in brain and the blockade of D_2 receptors is the key to the antipsychotic efficacy (2, 3). Hence, dopamine D_2 receptor occupancy (D_2RO) is considered as a potential biomarker in antipsychotic treatment (4). We aimed to build a translational framework to predict D_2RO in human using *in vitro* and preclinical information.

Even though it is evident that D_2 receptor blockade is crucial for antipsychotic efficacy, the degree and duration of D_2 antagonism required for effective treatment is not clear. Several studies suggested that blockade of 65% to 80% of D_2 receptors is the key to antipsychotic efficacy (2, 3, 5). Some antipsychotics, for example clozapine, show antipsychotic activity at a lower receptor blockade (20-67%) than other antipsychotics (6). Aripiprazole, an atypical antipsychotic, has been shown to be a partial agonist on the D_2 receptors, suggesting that for this drug even high receptor occupancy may be optimal (7). Kapur *et al* (8) reported that the rate of dissociation of antipsychotics from the D_2 receptors drives their efficacy and safety. These studies show that little is known about the degree of target occupancy and the role of the dynamic interactions between the drugs and the D_2 receptor in schizophrenia treatment. In addition, one of the other challenges in this translation process is the lack of proper understanding of the passive and active drug transport into the brain and the influence of drug distribution to the target site on the receptor binding.

In translational drug research, understanding and learning the physiology and the mechanisms involved in drug distribution and drug-receptor binding processes at a preclinical level are helpful to scale those processes to human. In recent years, mechanism-based PKPD models are increasingly used to understand drug distribution and binding processes (9). Moreover, these models explicitly express and separate the drug- and system- specific components contributing to the drug effects and thereby provide an opportunity to scale parameters between species (10).

Hence, we aimed to build a translational framework using mechanism-based PKPD modeling tools with a physiological basis. This framework would help to scale information from *in vitro* binding studies and preclinical receptor occupancy studies to predict human D_2RO.

PKPD Modeling and Target Site Distribution

The distribution of drug to the site of action is an important determinant of the time course and intensity of drug effects in CNS drug therapy. The drug distribution at the site of action may be different from the distribution in the plasma compartment, because of the passive permeability process and the efflux transporters present at the luminal surface of the blood-brain barrier (BBB). In drug development, free plasma concentration and cerebrospinal fluid (CSF) concentrations may be used as a reflection of the target site (brain) concentration to predict the effect of a drug. However, for drugs that show a heterogeneous distribution due to active transport, it was concluded that the value of CSF concentrations in predicting the effect of drug acting on central nervous system (CNS) is limited (11). Hence, it is necessary to know the drug exposure in the brain.

Brain drug concentrations are seldom measured in humans. Hence, it is not possible to study the drug exposure in brain and its relationship with effects in humans. However, understanding the exposure-effect relationship in animals using PKPD modeling tools will allow translating this relationship from one species to other species.

A number of PKPD models developed to study the drug distribution to the brain using empirical and mechanistic approaches have been reported in literature. PKPD modeling for oxycodone was performed using compartmental modeling approaches. The transport across the BBB was modeled as an active influx process to explain the higher unbound concentrations in brain compared to that in blood (12). This active influx phenomenon of oxycodone was important to interpret the pharmacodynamic data and facilitated to explain discrepancies in the *in vivo* potencies between oxycodone and morphine (13).

Groenendaal *et al* (14) explained the influence of biophase distribution and P-glycoprotein (P-gp) on drug distribution and effect using an extended catenary biophase distribution model. The influence of active transport was studied using the co-administration of a P-gp inhibitor. The brain distribution of morphine and its metabolites to brain was studied by fitting compartmental models to the free drug concentration in brain and extracellular fluid (ECF) obtained using the microdialysis technique in rats. A mechanistic model including passive diffusion, active influx and efflux transport was also applied to describe non-linear distribution of morphine and fluvoxamine (15, 16). These mechanistic models explain the drug distribution to brain in a quantitative manner. However, the translatability of these models to the human system has not yet been elucidated.

Physiology-based pharmacokinetic (PBPK) models have been used to explain the drug distribution to brain. Liu *et al* (17) proposed a hybrid PBPK model with passive

drug transport across the BBB to explain the time to reach equilibrium between brain and plasma. This PBPK model was extended to explain the drug distribution to the site of action and receptor binding while retaining the physiological basis (18, 19). An important feature of a PBPK modeling approach is that allows using species-specific data on tissue structure, volume and blood flows for the extrapolation from pre-clinical animal models to humans. Moreover, for drug transport involving active transporters, a physiological basis allows to account for the interspecies differences in the expression and function of these transporters (10). It has been reported that drugs that are P-gp substrates in rats are likely to also be P-gp substrates in higher species (20). Hence, considering differential expression and functionality of drug transporters (21) and structural differences of the BBB between species (11) will be helpful to translate target site kinetics from rat to human. Thus, a translation of the target site kinetics for CNS active drugs from rat to human would require a proper understanding of drug transport at the BBB.

PKPD Modeling and Target Binding

PKPD models utilize non-linear mathematical expressions, often a hyperbolic function, to explain the *in vivo* plasma drug concentration (C) and receptor occupancy (RO) relationship (22-24).

$$RO = RO_{max} * C / (RC_{50} + C)$$

RO_{max} represents the maximum receptor occupancy. RO_{max} is expected to be 100%. However, due to experimental constraints and inevitable measurement errors in receptor occupancy measurements, RO_{max} is estimated as less than 100% and varies between drugs (4, 22, 24). This makes this parameter dependent on data and lacks the translatability of this parameter from one species to other species.

In addition, RC_{50} represent the plasma drug concentration required to obtain 50% of RO_{max}. For translational research purposes, RC_{50} derived based on the unbound plasma drug concentration may be considered as equivalent to drug-specific *in vitro* Ki values obtained from binding assays. However, for drugs acting on CNS, drug distribution to the site of action involves complex transport mechanisms at BBB. Hence, the unbound drug concentration at the site of action may be different from the unbound drug plasma concentration. So, the RC_{50} obtained by fitting this empirical model to drug plasma concentration may not represent the drug affinity (i.e. Ki) to the receptor.

Moreover, *in vivo* drug-receptor interaction is a dynamic process, which involves association and dissociation processes that are governed by the drug-specific

properties. Hence, it is appropriate to describe the time course of receptor occupancy data using association and dissociation constants as explained in the equation:

$$d(RO/dt) = k_{on}*C_{free}*(B_{max} - C_{bound}) - k_{off}*C_{bound}$$

This approach utilizes second order association (k_{on}) and first order dissociation (k_{off}) rate constants for the binding of the drug to the receptor and the receptor density (B_{max}) to explain the *in vivo* drug brain concentration (C_{free}) and receptor occupancy (RO) relationship. It has been proposed that drug specific parameters like k_{on}, k_{off} and target affinity ($Kd = k_{off}/k_{on}$) are species independent and thus, identical drug specific parameters can be used for rat and human (10).

Hence, a mechanistic understanding of target binding is a prerequisite to build a translational framework.

Translational PKPD Modeling

Mechanism-based PKPD modeling in rats

In **chapters 3 & 4**, we started building the translational framework with the development of a mechanism-based pharmacokinetic-pharmacodynamic model to predict the time course of receptor occupancy following administration of antipsychotic drugs in rats. Mechanism-based PKPD models combined with physiological parameters have the ability to predict human PKPD properties using prior information from *in vitro* and preclinical studies. So, we aimed at a physiology-based model to explain the drug transport at the BBB. Moreover, it is essential to have sufficient information about the cascade of processes (distribution to and in the brain, receptor occupancy as a net result of association and dissociation) to develop a PKPD model. In schizophrenia drug discovery research, the information on drug distribution into brain and the time course of receptor occupancy is rather sparse. So, a population-based approach was utilized to integrate information from different sources. We used a hybrid (7) approach to combine a classical compartmental model for plasma pharmacokinetics and a physiology-based model to describe the drug disposition and receptor binding in the brain.

In chapter 3, a hybrid physiology-based pharmacokinetic and pharmacodynamic (PBPKPD) model was developed to characterize the D_2 receptor binding of the atypical antipsychotic drug olanzapine in the striatum in rats. We found a good agreement between the estimated association and dissociation rate constants and the in vitro values reported in literature (25).

Drug transport to brain is a complex process involving both passive and active transport. So, we extended this PBPKPD model to account for drug distribution

involving both passive permeability and active efflux transport mechanisms at the BBB. Risperidone and its active metabolite paliperidone were used in this model extension. Risperidone and paliperidone show similar binding properties and also a similar clinical profile. Therefore, to properly describe the D_2 receptor occupancy of risperidone, it is necessary to take into account the formation of paliperidone and its distribution to brain and its binding to receptors. In addition, risperidone and paliperidone have affinity for the serotonin 5-HT_{2A} receptor (and for other receptors) and demonstrated antipsychotic efficacy with less affinity towards D_2 receptors than 5-HT_{2A} receptors. So, we extended this PBPKPD model to predict the time course of the brain concentration and the D_2 and 5-HT_{2A} receptor occupancy in rats. In Chapter 4, the PBPKPD model was expanded by including metabolite kinetics, active efflux from brain and binding to 5-HT_{2A} receptors in frontal cortex. The extended PBPKPD model described 5-HT_{2A} RO well. Inclusion of binding to 5-HT_{2A} receptors was necessary to describe the observed brain-to-plasma ratios accurately. Simulations showed that the receptor affinity strongly influences the brain-to-plasma ratio pattern. We concluded that binding to both D_2 and 5-HT_{2A} receptors influences brain distribution of risperidone and paliperidone. This may stem from their high affinity for D_2 and 5-HT_{2A} receptors.

In conclusion, we have developed PBPKPD models to explain the time course of RO in rats. The distribution of drug to brain was described using passive and active transport processes in a physiological manner and a mechanistic approach was used to explain the dynamic drug-receptor binding process by means of association and dissociation constants of the drugs to the receptor.

Translation of RO: Concepts
The main objective of our translational framework was to assess the ability of the PBPKPD model to predict the receptor occupancy in humans following administration of antipsychotic drugs. In **chapter 5,** three different approaches were used to predict the drug transport across the human blood brain barrier (BBB) and the binding to D_2 receptors in striatum.

In Approach A, we used the minimal *in vitro* binding assay information to predict human D_2RO. Apparent permeability values were scaled based on human brain endothelial surface area to predict the passive drug transport across BBB and active efflux clearance was scaled from *in vitro* system to *in vivo* human based on their expression in *in vitro* assay systems and in human brain. *In vitro* Ki values and *in vitro* k_{off} values for binding at the dopamine D_2 receptor were used to predict the human D_2RO in striatum.

In Approach B, PBPKPD model estimates (based on preclinical *in vivo* information) describing drug distribution to the brain and binding to receptors in the brain were utilized to translate D_2RO from rat to human. The parameter describing the

passive drug transport across the BBB in rats was normalized to rat brain endothelial surface area to obtain apparent permeability values and these values were used in a similar fashion to approach A to obtain human CL_{bev} values, which characterize the passive drug transport across the BBB in human. Active efflux transport was scaled from rat to human based on the MDR1 expression in both the species. *In vivo* (model estimated) Kd and k_{off} values were used to predict human D_2RO in striatum.

Finally, in the exploration of the minimal information required to be used in this translational model, we derived approach C. This approach uses the methods of approach A to scale information regarding drug transport across the BBB. It has been suggested that the drug specific parameters (target affinity – Ki or Kd) may be considered identical between different systems (*in vitro*, rat and human). However, we observed differences in the target affinity between *in vitro* and *in vivo* systems. This difference between the *in vivo* and *in vitro* scenarios could arise from the assumptions used in both *in vitro* calculations and model estimations. Additionally, radioligand selection and disturbances in assumed equilibrium conditions in *in vitro* and *in vivo* systems could lead to biased or inappropriate Ki calculations (26). Hence, in approach C, we applied a correction between systems to obtain *in vivo* Kd_{human} values.

The predictive power of this physiology-based approach was determined by comparing the D_2RO predictions with the observed human D_2RO of seven antipsychotics at clinically relevant doses. In general, human D_2RO was predicted well, when only *in vitro* information (Approach A) was used in the simulations. The correction as applied in approach C might help with the normalization of the scaling from an *in vitro* to an *in vivo* system for different species. Finally, this model was extended to successfully predict $5\text{-HT}_{2A}RO$ in human cortex.

Translation of RO: Challenges

Physiology-based modeling unwraps ways to translate drug distribution and binding in rat brain to human conditions. However, difference in rat and human brain in terms of anatomy and physiology, and differential expression of transporters at the BBB, make this task challenging. The uncertainty in the available physiological values, pathological conditions, and different experimental conditions for D_2RO measurements are complementing to this challenge.

Physiological differences

Westerhout *et al* (11) reviewed the physiological and anatomical differences between rat and human BBB. The endothelial surface area of human BBB was estimated to be 20 m^2 (27), which is approximately 100 times larger than that of rat BBB. In addition, it has been reported that the contribution of brain-cerebrospinal fluid-barrier (BCSFB) to drug transport to brain is relatively larger in rats than in human (11).

Furthermore, with the evident P-gp function in BSCFB as both efflux and influx transporter, BSCFB might play different roles in rat than in human in relation to drug distribution to brain (11). These differences between rat and human BBB should be considered while translating brain distribution of antipsychotics from rat to human.

Occupancy measurement
Receptor occupancy in human brain is measured using imaging techniques like positron emission tomography (PET) and single-photon emission computed tomography. Measuring drug-related receptor occupancy using these techniques is discussed elsewhere (28). Briefly, receptor occupancy is calculated based on the binding potential (BP) of the drug to the receptor which is defined as B_{max}/Kd, where B_{max} is the receptor density and Kd is the drug concentration required to occupy 50% of the maximum available receptors (29). PET scans of the brain are obtained, at baseline and after treatment with a drug, by injecting a radioligand (for e.g. [^{11}C]raclopride). Time activity curves are obtained for the region of interest (high expression of receptor) and a region of reference (no receptors present). PET kinetic modeling is used to calculate the binding potential of the region of interest. Receptor occupancy is then calculated as the percentage reduction of receptor binding potential with drug treatment relative to baseline.

$$\% \text{ Receptor Occupancy} = 100 * \frac{BP_{baseline} - BP_{aftertreatment}}{BP_{baseline}}$$

It is not possible to obtain a true estimate of $BP_{baseline}$ (binding potential before drug treatment) from all individual patients due to the procedural constraints and due to the fact that all patients are treated previously with antipsychotics (30). Hence, most human occupancy measurement studies used a baseline reference value obtained from other subjects. It has been reported that the lack of patients with individual baseline introduces a random error which varies from 3-12% depending on the measured occupancy (30).

D_2 dopamine receptor density varies several folds between individuals (31). Seeman et al. (32) have reported that estimates of D_2 receptor density were dependent on the brain region (cerebellum or basal ganglia) used for normalization of nonspecific binding. Both these individual and measurement levels differences could change the BP and thereby RO to a great extent.

It is usually assumed that RO is measured at equilibration conditions when the elevations of endogenous dopamine levels are stable rather than dynamic. It has been reported that administration of 0.2 mg/kg amphetamine elevated the endogenous dopamine levels 5 times and reduced radioligand (tracer) binding to approximately 10% (33).

Hence, these measurement errors can lead to discrepancies between the observed and predicted human D_2RO.

Drug-specific properties
Danhof *et al* (9) proposed that the values of drug-specific parameters such as target affinity are likely to be identical between species and individuals. Yassen *et al* (34) extrapolated pharmacodynamic effects of buprenorphine from rats to humans by using identical drug-specific parameters between species. This would imply that the binding rate constants estimated in rats could be used in extrapolation from rat to human. However, several other studies showed differences in receptor affinity between species (35). Notwithstanding divergent reports on the species independence of drug-specific parameters, an integration of allometric principles (36-38), *in vitro* information, and a physiological basis to PKPD modeling would increase the prospective of translating effects. We also suggest that normalization of *in vitro* Ki for *in vivo* conditions in lower species, and applying this correction to *in vitro* human Ki would improve the prediction of receptor occupancy.

PKPD modeling helps to understand the different processes involved in drug distribution and effects. In addition, PKPD modeling also brings forth drug-specific transport process (15). Despite of this usefulness of PKPD models, unique transport property like active influx are not translatable in a quantitative manner till date because of lack of information on this unique process. For example, D_2RO predictions of haloperidol (HAL) were lower than the observations. This may be related to the high ratio of unbound concentrations of HAL in brain and plasma, which is close to 4 in rats (39). This high brain to plasma ratio may indicate a unique active influx transport to the brain. In addition, it has been documented that the metabolism of HAL involves a conversion of HAL to reduced haloperidol, and back-conversion of reduced haloperidol to HAL (40) in the brain of guinea pigs. Accounting for this metabolism and/or active influx transport may help to improve predictions. However, due to the lack of relevant quantitative data describing these processes, we did not include these components in the translational model.

Uncertainty in parameter estimates
In translational PKPD modeling, the PKPD model structure developed for preclinical species is used to predict the PKPD relationship in human. The precision of the parameter estimates (regarding drug distribution and receptor binding) obtained from the rat PKPD model might also play a role in the accuracy of the predictions of effects in human. Hence, it is suggested to use optimally designed studies in the preclinical level for precise parameter estimation to allow appropriate predictions in human.

Uncertainty in physiological values

We proposed to translate the passive permeability from rat to human by normalizing the drug distribution to the brain-endothelial surface area (BES). Hence, BES values play a role in the translation of drug transport from rat to human. However, rat BES values reported in literature range from 100 to 240 cm² per g brain tissue (41, 42). The choice of these values for the calculation of passive transport across the BBB might play a role in the accuracy of predictions.

Hence, we proposed to use *in vitro* apparent permeability (P_{app}) values to predict the passive permeability across the BBB by taking the product of P_{app} and human brain endothelial surface area (18). *In vitro* effective permeability of compounds with various characteristics across human primary brain endothelial cells was comparable to those obtained with bovine and rat capillary endothelial cells (43). Hence, it is expected that ability to passively cross the BBB could be similar between species. This approach has the advantage of using *in vitro* values to predict the pharmacokinetics in brain and consequently reduce the need of animal experiments to measure brain concentrations. Hence, we suggest using P_{app} values to predict passive permeability of drug across the BBB using this *in vitro* based approach.

Extensions to the translational framework

This translational framework has been developed based on data for antipsychotic drugs binding to the dopamine D_2 receptor and the serotonin 5-HT_{2A} receptor. We selected this specific class of drugs since it is a relatively well-developed area of research in which data are available on a range of drugs. Moreover, strong indications have been found for links between receptor occupancy and treatment effects. However, the question remains on the application of translational models developed for this class of drugs to other drugs. Grimwood *et al* (44) emphasized that similar occupancy requirements were observed for other GPCR antagonists. Hence, a similar translational approach may be also applicable for other GPCR antagonists such as neurokinin NK1 antagonists (emesis), dopamine D1 antagonists (akithisia), and mu-opiate antagonists (drug-abuse). Hence, the extension of this translational framework to other receptor types is feasible.

Catalepsy and Extrapyramidal Symptoms

In addition to the development of the predictive model, we also utilized PKPD modeling tools to scale the severity of drug-induced side effects from rat to human. In schizophrenia, extrapyramidal symptoms (EPS) in human are caused by excessive D_2RO (>80%) of antipsychotic drugs and this applies to rat catalepsy (CAT) side

effects as well (45). Although a clear relationship between D_2RO and side effects exists, quantitative information on the relationship between catalepsy and EPS is lacking. **In chapter 6,** we used PKPD modeling tools to relate CAT with D_2RO in rats and to elucidate a relationship between CAT scores in rat and EPS scores in humans, in a quantitative manner. Interestingly in humans, the probability of having EPS for 0% D_2RO is approximately 5%, which shows the effect of placebo on EPS. A risk of EPS not exceeding 10% over placebo may be predicted when 86% D_2RO results in less than 30% probability of CAT events in rats. This tool may be used in drug discovery to predict the risk of EPS in humans from D_2RO and CAT scores in rats.

Conclusion

Applications of this modeling framework as a predictive tool include predicting receptor occupancy and side effects during early drug discovery. This tool may also be applied for the selection of appropriate first-in-human doses based on pharmacodynamics. Due to the mechanism- and physiology-based approach, it is likely that this framework can be extended to other CNS indications. Nevertheless, inclusion of more mechanistic components like effect endogenous dopamine on drug binding to receptor, and correction for radio-ligand binding across species, would help to improve the predictions.

However, it is not anticipated that predictive tools will completely replace the need for clinical studies, though it is plausible that this tool can help to design more informative and more efficient clinical studies.

References

1. Hurko O, Ryan JL. Translational research in central nervous system drug discovery. NeuroRx : the journal of the American Society for Experimental NeuroTherapeutics 2005;2(4):671-82.
2. Farde L, Nordstrom AL, Wiesel FA, Pauli S, Halldin C, Sedvall G. Positron Emission Tomographic Analysis of Central D1-Dopamine and D2-Dopamine Receptor Occupancy in Patients Treated with Classical Neuroleptics and Clozapine – Relation to Extrapyramidal Side-Effects. Arch Gen Psychiatry 1992 Jul;49(7):538-44.
3. Nordstrom AL, Farde L, Wiesel FA, Forslund K, Pauli S, Halldin C, et al. Central D2-Dopamine Receptor Occupancy in Relation to Antipsychotic Drug Effects – A Double-Blind Pet Study of Schizophrenic-Patients. Biol Psychiatry 1993 Feb 15;33(4):227-35.
4. de Greef R, Maloney A, Olsson-Gisleskog P, Schoemaker J, Panagides J. Dopamine D(2) Occupancy as a Biomarker for Antipsychotics: Quantifying the Relationship with Efficacy and Extrapyramidal Symptoms. Aaps Journal 2011 Mar;13(1):121-30.

7

5. Kapur S, Remington G, Jones C, Wilson A, DaSilva J, Houle S, et al. High levels of dopamine D-2 receptor occupancy with low-dose haloperidol treatment: A PET study. American Journal of Psychiatry 1996 Jul;153(7):948-50.

6. Pickar D, Su TP, Weinberger DR, Coppola R, Malhotra AK, Knable MB, et al. Individual variation in D2 dopamine receptor occupancy in clozapine-treated patients. Am J Psychiatry 1996 Dec;153(12):1571-8.

7. Biojone C, Casarotto PC, Resstel LB, Zangrossi H, Jr., Guimares FS, Moreira FA. Anti-aversive effects of the atypical antipsychotic, aripiprazole, in animal models of anxiety. J Psychopharmacol 2010 Aug 10;Epub ahead of print Aug 10.

8. Kapur S, Seeman P. Does fast dissociation from the dopamine d(2) receptor explain the action of atypical antipsychotics?: A new hypothesis. Am J Psychiatry 2001 Mar;158(3):360-9.

9. Danhof M, de Jongh J, De Lange ECM, la Pasqua O, Ploeger BA, Voskuyl RA. Mechanism-based pharmacokinetic-pharmacodynamic modeling: Biophase distribution, receptor theory, and dynamical systems analysis. Annual Review of Pharmacology and Toxicology 2007;47:357-400.

10. Danhof M, de Lange EC, la Pasqua OE, Ploeger BA, Voskuyl RA. Mechanism-based pharmacokinetic-pharmacodynamic (PK-PD) modeling in translational drug research. Trends Pharmacol Sci 2008 Apr;29(4):186-91.

11. Westerhout J, Danhof M, de Lange EC. Preclinical prediction of human brain target site concentrations: considerations in extrapolating to the clinical setting. J Pharm Sci 2011;100(9):3577-93.

12. Bostrom E, Simonsson US, Hammarlund-Udenaes M. In vivo blood-brain barrier transport of oxycodone in the rat: indications for active influx and implications for pharmacokinetics/pharmacodynamics. Drug Metab Dispos 2006;34(9):1624-31.

13. Bostrom E, Hammarlund-Udenaes M, Simonsson US. Blood-brain barrier transport helps to explain discrepancies in in vivo potency between oxycodone and morphine. Anesthesiology 2008;108(3):495-505.

14. Groenendaal D, Freijer J, de Mik D, Bouw MR, Danhof M, De Lange ECM. Influence of biophase distribution and P-glycoprotein interaction on pharmacokinetic-pharmacodynamic modelling of the effects of morphine on the EEG. Br J Pharmacol 2007;151(5):713-20.

15. Groenendaal D, Freijer J, de Mik D, Bouw MR, Danhof M, de Lange EC. Population pharmacokinetic modelling of non-linear brain distribution of morphine: influence of active saturable influx and P-glycoprotein mediated efflux. Br J Pharmacol 2007;151(5):701-12.

16. Geldof M, Freijer J, van Beijsterveldt L, Danhof M. Pharmacokinetic modeling of non-linear brain distribution of fluvoxamine in the rat. Pharm Res 2008;25(4):792-804.

17. Liu X, Smith BJ, Chen C, Callegari E, Becker SL, Chen X, et al. Use of a physiologically based pharmacokinetic model to study the time to reach brain equilibrium: an experimental analysis of the role of blood-brain barrier permeability, plasma protein binding, and brain tissue binding. J Pharmacol Exp Ther 2005 Jun;313(3):1254-62.

18. Johnson M, Kozielska M, Reddy VP, Vermeulen A, Li C, Grimwood S, et al. Mechanism-Based Pharmacokinetic-Pharmacodynamic Modeling of the Dopamine D(2) Receptor Occupancy of Olanzapine in Rats. Pharm Res 2011 Oct;28(10):2490-504.

19. Kozielska M, Johnson M, Reddy VP, Vermeulen A, Li C, Grimwood S, et al. Pharmacokinetic-Pharmacodynamic Modeling of the D2 and 5-HT2A Receptor Occupancy of Risperidone and Paliperidone in Rats. Pharm Res 2011;Accepted.

20. Syvanen S, Lindhe O, Palner M, Kornum BR, Rahman O, Langstrom B, et al. Species Differences in Blood-Brain Barrier Transport of Three Positron Emission Tomography Radioligands with Emphasis on P-Glycoprotein Transport. Drug Metab Disposition 2009 Mar;37(3):635-43.

21. Uchida Y, Ohtsuki S, Katsukura Y, Ikeda C, Suzuki T, Kamiie J, et al. Quantitative targeted absolute proteomics of human blood-brain barrier transporters and receptors. J Neurochem 2011 Apr;117(2):333-45.

22. Nucci G, Gomeni R, Poggesi I. Model-based approaches to increase efficiency of drug development in schizophrenia: a can't miss opportunity. Expert Opinion on Drug Discovery 2009;4(8):837-56.

23. Olsen CK, Brennum LT, Kreilgaard M. Using pharmacokinetic-pharmacodynamic modelling as a tool for prediction of therapeutic effective plasma levels of antipsychotics. Eur J Pharmacol 2008 Apr 28;584(2-3):318-27.

24. Uchida H, Takeuchi H, Graff-Guerrero A, Suzuki T, Watanabe K, Mamo DC. Predicting Dopamine D2 Receptor Occupancy From Plasma Levels of Antipsychotic Drugs: A Systematic Review and Pooled Analysis. J Clin Psychopharmacol 2011;31(3).

25. Kapur S, Seeman P. Antipsychotic agents differ in how fast they come off the dopamine D2 receptors. Implications for atypical antipsychotic action. J Psychiatry Neurosci 2000 Mar;25(2):161-6.

26. Hulme EC, Trevethick MA. Ligand binding assays at equilibrium: validation and interpretation. Br J Pharmacol 2010 Nov;161(6):1219-37.

27. Fagerholm U. The highly permeable blood-brain barrier: an evaluation of current opinions about brain uptake capacity. Drug Discov Today 2007 Dec;12(23-24):1076-82.

28. Passchier J, Gee A, Willemsen A, Vaalburg W, van Waarde A. Measuring drug-related receptor occupancy with positron emission tomography. Methods 2002 Jul;27(3):278-86.

29. Kapur S. Receptor Occupancy by Antipsychotics – Concepts and Findings. Neurotransmitter Receptors in Actions of Antipsychotic Medications. CRC Press; 2000. p. 163-76.

30. Shitij K. Receptor Occupancy by Antipsychotics – Concepts and Findings. Neurotransmitter Receptors in Actions of Antipsychotic Medications. CRC Press; 2000. p. 163-76.

31. Farde L, Hall H, Pauli S, Halldin C. Variability in D-2-Dopamine Receptor Density and Affinity – A Pet Study with [C-11] Raclopride in Man. Synapse 1995 Jul;20(3):200-8.

32. Seeman P, Niznik HB, Guan HC. Elevation of Dopamine-D2 Receptors in Schizophrenia Is Underestimated by Radioactive Raclopride. Arch Gen Psychiatry 1990 Dec;47(12):1170-2.

33. Strange PG. Antipsychotic drugs: importance of dopamine receptors for mechanisms of therapeutic actions and side effects. Pharmacol Rev 2001;53(1):119-33.

7

34. Yassen A, Olofsen E, Kan J, Dahan A, Danhof M. Animal-to-human extrapolation of the pharmacokinetic and pharmacodynamic properties of buprenorphine. Clin Pharmacokinet 2007;46(5):433-47.

35. Chien JY, Friedrich S, Heathman MA, de Alwis DP, Sinha V. Pharmacokinetics/Pharmacodynamics and the stages of drug development: role of modeling and simulation. AAPS J 2005 Oct 7;7(3):E544-E559.

36. Zuideveld KP, Van der Graaf PH, Peletier LA, Danhof M. Allometric scaling of pharmacodynamic responses: application to 5-Ht1A receptor mediated responses from rat to man. Pharm Res 2007 Nov;24(11):2031-9.

37. Woo S, Jusko WJ. Interspecies comparisons of pharmacokinetics and pharmacodynamics of recombinant human erythropoietin. Drug Metab Dispos 2007 Sep;35(9):1672-8.

38. Agoram BM, Martin SW, Van der Graaf PH. The role of mechanism-based pharmacokinetic-pharmacodynamic (PK-PD) modelling in translational research of biologics. Drug Discov Today 2007 Dec;12(23-24):1018-24.

39. Zhang G, Terry AV, Bartlett MG. Sensitive liquid chromatography/tandem mass spectrometry method for the simultaneous determination of olanzapine, risperidone, 9-hydroxyrisperidone,, clozapine, haloperidol and ziprasidone in rat brain tissue. Journal of Chromatography B-Analytical Technologies in the Biomedical and Life Sciences 2007 Oct 15;858(1-2):276-81.

40. Chang WH, Jaw SS, Wu HS, Tsay L, Yeh EK. Pharmacodynamics and Pharmacokinetics of Haloperidol and Reduced Haloperidol in Guinea-Pigs. Psychopharmacology (Berl) 1988;96(3):285-8.

41. Hammarlund-Udenaes M, Friden M, Syvanen S, Gupta A. On the rate and extent of drug delivery to the brain. Pharm Res 2008 Aug;25(8):1737-50.

42. Avdeef A. How well can in vitro brain microcapillary endothelial cell models predict rodent in vivo blood-brain barrier permeability? European Journal of Pharmaceutical Sciences 2011 Jun 14;43(3):109-24.

43. Garberg P, Ball M, Borg N, Cecchelli R, Fenart L, Hurst RD, et al. In vitro models for the blood-brain barrier. Toxicology in Vitro 2005 Apr;19(3):299-334.

44. Grimwood S, Hartig PR. Target site occupancy: emerging generalizations from clinical and preclinical studies. Pharmacol Ther 2009 Jun;122(3):281-301.

45. Kapur S, Remington G, Jones C, Wilson A, DaSilva J, Houle S, et al. High levels of dopamine D2 receptor occupancy with low-dose haloperidol treatment: a PET study. Am J Psychiatry 1996;153(7):948-50.

Summary of the Thesis
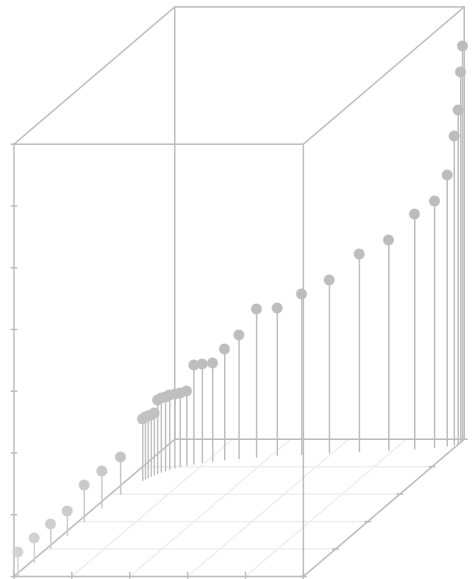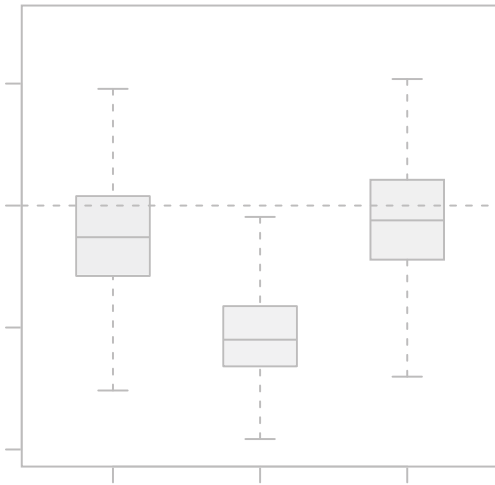
Translational research, in a pharmaceutical industry context, aims to predict drug effects in clinical situations based on *in vitro* and preclinical information from studies in laboratory animals. In this thesis we aimed to develop a translational pharmacokinetic and pharmacodynamic (PKPD) modeling framework for the prediction of drug effects in schizophrenia. This was pursued by integrating *in vitro* and *in vivo* preclinical data with mechanism-based PKPD models to predict the target occupancy of antipsychotic drugs in humans. The prediction of extrapyramidal side effects on the basis of preclinical *in vivo* information was an additional objective.

Schizophrenia is a severe and disabling disorder, associated with a marked social and occupational dysfunction, a tenfold increase in suicidal risk, an intensive use of healthcare resources, and a poor prognosis. It is now widely accepted that excessive dopamine release in the striatum plays a central role in the pathophysiology of schizophrenia. Several studies suggest that blockade of D_2 receptors is the key to antipsychotic efficacy for both conventional neuroleptics and novel antipsychotics. Hence, dopamine D_2 receptor occupancy (D_2RO) is considered as a potential biomarker for anti-schizophrenic treatment. Estimation of target occupancy is important both in early drug discovery, where accurate knowledge of the degree of occupancy could help to determine the suitability of a drug candidate for further development, as well as later in the drug development process, where target site occupancy measurements can guide dose selection. The development of a translational tool to predict human D_2RO (based on PKPD models) involves scaling of information from rat to human. Drug distribution to brain is a key factor in this respect. Drug distribution to the brain involves complex passive and active transport processes and drug binding to receptor is also a dynamic mechanism. Hence, we used mechanism-based PKPD models to predict the time course of target occupancy and pharmacodynamic responses in rats and human. These models contain separate expressions to parameterize biophase kinetics and receptor association–dissociation kinetics to describe the drug binding to receptors. The important feature of these mechanistic models is their ability to distinguish the system- and drug- specific parameters, which has been proven to be useful in the extrapolation of treatment effects from rat to human.

In **chapters 3 & 4**, we started building the translational framework with the development of a mechanism-based PKPD model to predict the time course of receptor occupancy following administration of antipsychotic drugs in rats. In this regard we aimed at developing a physiology-based model to explain the drug transport at the blood-brain barrier (BBB) in conjunction with a receptor model to describe the kinetics of association and dissociation at the dopamine D_2 receptor. In the development of antipsychotic drugs, the information on drug distribution into brain and the time course of receptor occupancy is rather sparse. So, a population-based approach was utilized to integrate information from different sources.

In **chapter 3**, a hybrid physiology-based pharmacokinetic-pharmacodynamic (PBPKPD) model was developed to characterize the D_2 receptor binding of the atypical antipsychotic drug olanzapine in the striatum of rats. To this end, data on the time course of the olanzapine plasma concentration, brain concentration and the D_2 receptor occupancy following different routes of administration in rats was analyzed. In this model the distribution to the brain was described as a simple passive diffusion process. In addition drug association to the D_2 receptor was described as a second-order process and drug dissociation from the D_2 receptor was described as a first-order process. We found a good agreement between the estimated association (k_{on}) and dissociation (k_{off}) rate constants, and the *in vitro* values reported in literature.

In **chapter 4** the modeling of the time course of dopamine D_2 receptor occupancy in rats was extended to the atypical antipsychotics risperidone and its metabolite paliperidone. Specific features of this modeling were i) the modeling of complex non-linear brain distribution kinetics, ii) the competitive interaction of the binding of risperidone and its active metabolite paliperidone and iii) the modeling of the binding at two receptor subtypes (i.e. the dopamine D_2 and the serotonin 5-HT_{2A} receptor). Risperidone is metabolized to paliperidone and both compounds show similar binding properties and clinical profile. Therefore, to properly describe receptor occupancy of risperidone, it is necessary to take into account the formation of paliperidone, and its distribution to brain and binding to receptors.

A pertinent feature of both risperidone and paliperidone is that active efflux mechanisms govern, at least in part, the distribution to the brain. To account for this, the PBPKPD model was expanded by including active efflux from brain. In addition, risperidone and paliperidone have shown affinity for the serotonin 5-HT_{2A} receptor (and other receptors) and demonstrated antipsychotic efficacy with less affinity towards D_2 receptors than towards 5-HT_{2A} receptors. So, risperidone and paliperidone binding to 5-HT_{2A} receptors in frontal cortex was described using association and dissociation processes. The extended PBPKPD model described the observed brain concentrations and D_2RO and 5-$HT_{2A}RO$ well. Inclusion of binding to 5-HT_{2A} receptors was necessary to describe the observed brain-to-plasma ratios accurately. Simulations showed that the receptor affinity (Kd or Ki) strongly influences brain-to-plasma ratio pattern. Hence, **chapter 4** concluded that binding to both D_2 and 5-HT_{2A} receptors influences brain distribution of risperidone and paliperidone. This may stem from their high affinity for D_2 and 5-HT_{2A} receptors. Receptor affinities and brain-to-plasma ratios may need to be considered before choosing the best PKPD model for centrally active drugs.

The main objective of this translational framework is to assess the ability of the PBPKPD model to predict the receptor occupancy in humans following administration of antipsychotic drugs. In **chapter 5**, three different approaches were used to

8

predict the drug transport across the human blood brain barrier (BBB) and the binding to D_2 receptors in striatum.

In Approach A, we used the minimally required *in vitro* assay information to predict human D_2RO. Apparent permeability values (P_{app}) were scaled based on human brain endothelial surface area to predict the passive drug transport across BBB. Active efflux clearance was scaled from *in vitro* system to *in vivo* human based on expression of drug transporters in *in vitro* assay systems and in human brain. *In vitro* Ki_{human} values and *in vitro* $k_{off-rat}$ values were used to predict the human D_2RO in striatum.

In Approach B, the PBPKPD model estimates which were parameterized to describe drug distribution and binding to receptor in rat brain were utilized to translate D_2RO from rat to human. The parameter describing the passive drug transport across the BBB in rats (rCL_{bev}) was normalized to rat brain endothelial surface area to obtain apparent permeability values and these values were used in a similar fashion to approach A to obtain human CL_{bev} values, which characterize the passive drug transport across the BBB in human. Active efflux transport was scaled from rat to human based on the MDR1 expression in both species. *In vivo* (model estimated) Kd_{rat} and $k_{off-rat}$ values were used to predict human D_2RO in striatum.

Further, in the exploration of the minimal information required to be used in this translational model, we derived approach C. Basically, approach C uses the methods of approach A to scale information regarding drug transport across the BBB. Danhof *et al* proposed that the drug specific parameters (target affinity – Kd or Ki) may be considered identical between different systems (*in vitro*, rat and human). However, we observed differences in the target affinity between *in vitro* and *in vivo* systems. This difference between the *in vivo* and *in vitro* scenarios could arise from the assumptions used in both *in vitro* calculations and model estimations. Additionally, radio-ligand selection and disturbances in assumed equilibrium conditions in *in vitro* and *in vivo* systems could lead to biased or inappropriate Ki calculations. Hence, in approach C, *in vivo* Kd_{human} parameters were corrected for the differences between *in vitro* and *in vivo* scenarios by normalizing model estimated *in vivo* Kd_{rat} and *in vitro* Ki values for rat and human.

The predictive power of this physiology-based approach was determined by comparing the D_2RO predictions with the observed human D_2RO of six antipsychotics at clinically relevant doses. In general, human D_2RO was predicted well, when only *in vitro* information (Approach A) was used in the simulations. The correction as applied in approach C might help with the normalization of the scaling from an *in vitro* to an *in vivo* system for different species. Finally, this model was extended to successfully predict 5-HT_{2A}RO in human cortex.

Several aspects of this translational modeling are discussed in **chapter 7**. The list of challenges includes the physiological differences between rat and human,

methodological issues in receptor occupancy measurements, uncertainty in preclinical PKPD parameters estimates and lack of information on drug-specific parameters. For example, D_2RO predictions of haloperidol were lower than the observations. Drug-specific parameters like metabolism and active influx transport at BBB may play a role in the under predictions of D_2RO for haloperidol. However, due to the lack of information related to these processes, we did not include these components in the translational model. Notwithstanding to limitations and challenges, a general translational framework was developed which is based on a mechanism-based approach and accounts for the different processes involved in the transport of drug to the brain.

In schizophrenia, extrapyramidal symptoms (EPS) are caused by excessive D_2RO (>80%) of antipsychotic drugs and this applies to rat catalepsy (CAT) side effects as well. Even though a clear relationship between D_2RO and side effects exists, the relationship between catalepsy and EPS is lacking. In **chapter 6**, the relationship between CAT scores in rat and EPS scores in humans was elucidated in a quantitative manner. Interestingly in humans, the probability of having EPS for 0% D_2RO is approximately 5%, which shows the effect of placebo on EPS. A risk of EPS not exceeding 10% over placebo, may be predicted when 86% D_2RO results in less than 30% probability of CAT events in rats. This tool may be used in drug discovery to predict the risk of EPS in humans from D_2RO and CAT scores in rats.

Concluding remarks

Applications of this modeling framework as a predictive tool include predicting receptor occupancy and side effects during early drug discovery. This tool may also be applied for the selection of appropriate first-in-human doses based on pharmacokinetics and pharmacodynamics. Due to the mechanism- and physiology-based approach, it is likely that this framework can be extended to other indications in the central nervous system. Nevertheless, inclusion of more mechanistic components like effect of endogenous dopamine on drug binding to receptors, and a correction for radio-ligand binding across species, would help to improve the predictions.

However, it is not anticipated that predictive tools will completely replace the need for clinical studies, though it is plausible that this tool can help to design more informative and more efficient clinical studies.

Samenvatting
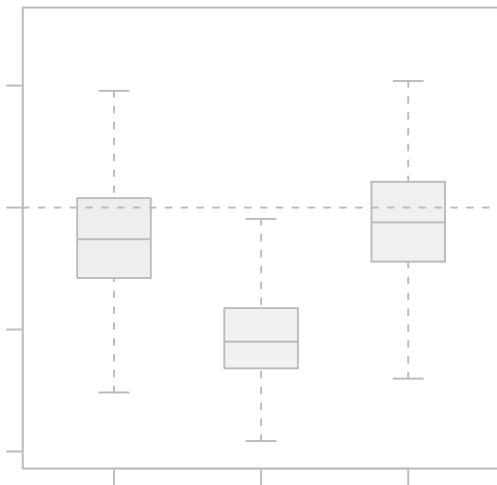
Translationeel onderzoek in de farmaceutische industrie is gericht op het voorspellen van de effecten van geneesmiddelen in klinische situaties, gebaseerd op *in vitro* metingen en preklinische gegevens uit studies bij proefdieren. Het doel van het onderzoek beschreven in dit proefschrift was om een translationeel farmacokinetisch-farmacodynamisch (PKPD) model voor het voorspellen van de effecten van geneesmiddelen bij schizofrenie te ontwikkelen. Dit doel werd bereikt door de integratie van *in vitro* en *in vivo* preklinische gegevens met mechanistische PKPD modellen om de receptorbezetting van antipsychotica bij de mens te voorspellen. Een tweede doelstelling was het voorspellen van extrapiramidale bijwerkingen op basis van preklinische *in vivo* informatie.

Schizofrenie is een ernstige en invaliderende aandoening, die gepaard gaat met een duidelijke sociale en beroepsmatige dysfunctie, een vertienvoudiging van het suicidale risico, een intensieve aanspraak op de beschikbare middelen in de gezondheidszorg en een slechte prognose. Het is nu algemeen aanvaard dat overmatige dopamine-afgifte in het striatum een centrale rol speelt in de pathofysiologie van schizofrenie. Verschillende studies suggereren dat blokkade van D_2-receptoren de sleutel is tot de antipsychotische werking van conventionele neuroleptica en nieuwe antipsychotica. Daarom wordt de dopamine D_2-receptor bezetting (D_2RO) beschouwd als een potentiële biomarker voor het succes van een anti-schizofrenie behandeling. Het bepalen van de receptorbezetting is belangrijk, zowel in de beginfase van de ontdekking van geneesmiddelen, waar nauwkeurige kennis van de bezettingsgraad zou kunnen helpen om de geschiktheid van een kandidaat-geneesmiddel voor verdere ontwikkeling te bepalen, maar ook later in het ontwikkelingsproces, waar metingen van de receptorbezetting kunnen helpen bij de keuze van de dosering. De ontwikkeling van een translationele methode om de D_2RO in de mens te voorspellen op basis van PKPD modellen impliceert het vertalen van informatie van de rat naar de mens. De verdeling van het geneesmiddel naar de hersenen is in dit opzicht een belangrijke factor. Deze verdeling wordt bepaald door complexe passieve en actieve transportprocessen. Daarnaast is de binding van het geneesmiddel aan de receptor ook een dynamisch proces. Daarom hebben we mechanistische PKPD modellen gebruikt om het tijdsverloop van de receptorbezetting en de farmacodynamische respons bij de rat en de mens te voorspellen. Deze modellen bevatten afzonderlijke vergelijkingen voor de biofase-kinetiek, de kinetiek van associatie aan en dissociatie van de receptor om de binding van geneesmiddelen aan receptoren te beschrijven. Het belangrijkste kenmerk van deze mechanistische modellen is hun vermogen om de systeem- en geneesmiddel-specifieke parameters te onderscheiden, wat nuttig is gebleken bij de extrapolatie van de behandelingseffecten van de rat naar de mens.

In de hoofdstukken 3 en 4 zijn we begonnen met de bouw van het translationele kader door het ontwikkelen van een mechanistisch PKPD model om het tijdsverloop

van de receptorbezetting na toediening van antipsychotica bij ratten te voorspellen. In dit verband hebben we ons gericht op het ontwikkelen van een model gebaseerd op de fysiologie om het transport van het geneesmiddel over de bloed-hersen-barrière (BBB) te beschrijven, in combinatie met een receptormodel om de kinetiek van associatie aan en dissociatie van de dopamine D_2-receptor te beschrijven. Bij de ontwikkeling van antipsychotica is de informatie over de verdeling van geneesmiddelen in de hersenen en het tijdsverloop van de receptorbezetting vrij schaars. Dus werd een populatie-gebaseerde methode gebruikt om informatie uit verschillende bronnen te integreren.

In hoofdstuk 3 werd een hybride fysiologie-gebaseerd farmacokinetisch- farmacodynamisch (PBPKPD) model ontwikkeld om de D_2-receptor binding van het atypische antipsychoticum olanzapine in het striatum van ratten te karakteriseren. Hiertoe werden gegevens over het tijdsverloop van de plasmaconcentratie, hersenconcentratie en D_2-receptorbezetting van olanzapine via verschillende toedieningswegen in ratten geanalyseerd. In dit model werd de verdeling naar de hersenen beschreven als een eenvoudig passief diffusieproces. De associatie met de D_2-receptor werd beschreven als een tweede-orde proces en de dissociatie van de D_2-receptor werd beschreven als een eerste-orde proces. We vonden een goede overeenkomst tussen de geschatte associatie- en dissociatie-snelheidsconstanten (kon en koff) en de *in vitro* waarden in de literatuur.

In hoofdstuk 4 wordt de modellering van het tijdsverloop van de D_2-receptorbezetting bij ratten uitgebreid met de atypische antipsychotica risperidon en zijn metaboliet paliperidon. Specifieke kenmerken van deze modellen zijn: i) de modellering van complexe niet-lineaire verdeling in de hersenen, ii) de competitieve interactie van de receptorbinding van risperidon en de actieve metaboliet paliperidon, en iii) het modelleren van de binding op twee receptoren, in dit geval de dopamine D_2 en de serotonine 5-HT_{2A}-receptor. Risperidon wordt omgezet in paliperidon en beide verbindingen vertonen vergelijkbare bindingseigenschappen en klinische profiel. Daarom moet voor een goede beschrijving van de receptorbezetting van risperidon rekening worden gehouden met de vorming van paliperidon, en de verdeling in de hersenen en de binding aan receptoren.

Een relevant kenmerk van zowel risperidon als paliperidon is dat actieve effluxmechanismen, althans ten dele, de verdeling naar de hersenen bepalen. Om hiermee rekening te houden is het PBPKPD model uitgebreid met een actieve efflux vanuit de hersenen. Bovendien hebben risperidon en paliperidon affiniteit voor de serotonine 5-HT_{2A}-receptor (en andere receptoren) en hebben een antipsychotisch effect met minder affiniteit voor D_2-receptoren dan voor de 5-HT_{2A}-receptoren. Daarom werd de binding van risperidon en paliperidon aan 5-HT_{2A}-receptoren in de frontale cortex beschreven met behulp van associatie- en dissociatie-processen. Het

uitgebreide PBPKPD model beschrijft de in proefdierexperimenten waargenomen hersenconcentraties, D_2RO en $5\text{-}HT_{2A}RO$ goed. Het opnemen van de binding aan $5\text{-}HT_{2A}$-receptoren in het model was nodig om de waargenomen verhouding van de concentraties in hersenen en plasma nauwkeurig te beschrijven. Uit simulaties is gebleken dat de affiniteit voor de receptor (Kd of Ki) het patroon van de hersen-plasma-ratio sterk beïnvloedt. Daarom wordt in hoofdstuk 4 de conclusie getrokken dat de binding aan zowel de D_2 als de $5\text{-}HT_{2A}$-receptoren de verdeling van risperidon en paliperidon in de hersenen beïnvloedt. Dit kan het gevolg zijn van hun hoge affiniteit voor D_2 en $5\text{-}HT_{2A}$-receptoren. Het is dus nodig rekening te houden met de receptoraffiniteit en de hersen-plasma-ratio bij het kiezen van het beste PKPD model voor geneesmiddelen die werken op het centraal zenuwstelsel.

Het belangrijkste doel van dit translationele kader was om te beoordelen of het PBPKPD model de receptorbezetting bij de mens na toediening van antipsychotica betrouwbaar kan voorspellen. In hoofdstuk 5 worden drie verschillende methoden gebruikt om het transport van het geneesmiddel over de bloed-hersen-barrière (BBB) en de binding aan D_2-receptoren in het striatum van de mens te voorspellen.

Methode A gebruikt de minimaal vereiste *in vitro* informatie om de D_2RO in de mens te voorspellen. De waarden voor de schijnbare permeabiliteitscoëfficiënt (Papp) werden geëxtrapoleerd van proefdier naar mens op basis van het endotheliale oppervlak van de hersenen om het passieve geneesmiddeltransport over de BBB te voorspellen. De actieve effluxklaring werd geëxtrapoleerd van het *in vitro* systeem naar de mens *in vivo*, gebaseerd op de expressie van de geneesmiddel-transporters in de *in vitro* systemen en in de hersenen van de mens. Humane *in vitro* Ki waarden en *in vitro* koff waarden voor de rat werden gebruikt om de D_2RO in het striatum van de mens te voorspellen.

In methode B werden de schattingen van de parameters van het PBPKPD model voor de verdeling van geneesmiddelen en binding aan receptoren in de hersenen van de rat gebruikt om de D_2RO te vertalen van rat naar de mens. De parameter die het passieve geneesmiddeltransport over de BBB bij ratten beschrijft (rCL_{bev}) werd genormaliseerd naar het endotheliale oppervlak van de hersenen in de rat om de schijnbare permeabiliteitscoëfficiënten te berekenen en deze waarden werden gebruikt op dezelfde manier als in methode A voor berekening van de CL_{bev} waarden die het passieve geneesmiddeltransport over de BBB bij de mens karakteriseren. De actieve efflux werd geschaald van rat naar de mens op basis van de MDR1 expressie in beide soorten. De *in vivo* Kd en koff waarden voor de rat, geschat met het model, werden gebruikt om de D_2RO in het striatum van de mens te voorspellen.

In het onderzoek naar de minimale informatie die nodig is voor dit translationele model is methode C ontwikkeld. In principe maakt methode C gebruik van de methode A om informatie met betrekking tot transport over de BBB te schalen.

Danhof *et al.* hebben voorgesteld dat de geneesmiddel-specifieke parameters (receptoraffiniteit – Kd of Ki) kunnen worden beschouwd als identiek tussen verschillende systemen (*in vitro*, rat en mens). Wij hebben echter verschillen waargenomen in de receptoraffiniteit tussen *in vitro* en *in vivo* systemen. Dit verschil tussen de *in vivo* en *in vitro* scenario's zou kunnen ontstaan door de aannames die gebruikt worden in de *in vitro* berekeningen en modelschattingen. Bovendien kunnen de keuze van het radio-ligand en verstoringen in het veronderstelde evenwicht in de *in vitro* en *in vivo* systemen leiden tot onjuiste Ki berekeningen. Daarom werden in methode C de *in vivo* Kd parameters voor de mens gecorrigeerd voor het verschil tussen *in vitro* en *in vivo* scenario's door het normaliseren van de *in vivo* Kd, voor de rat, geschat door het model, en de *in vitro* Ki waarden voor de rat en de mens.

De voorspellende kracht van deze fysiologie-gebaseerde methode werd bepaald door het vergelijken van de D_2RO voorspellingen met de bij de mens waargenomen D_2RO van zes antipsychotica bij klinisch relevante doses. In het algemeen werd de D_2RO in de mens goed voorspeld, wanneer alleen *in vitro* informatie (methode A) werd gebruikt in de simulaties. De in methode C toegepaste correctie zou kunnen helpen bij de vertaling van een *in vitro* naar een *in vivo* systeem voor verschillende diersoorten. Tot slot werd dit model met succes uitgebreid om de $5\text{-}HT_{2A}RO$ in de cortex van de mens te voorspellen.

Verschillende aspecten van deze translationele modellen worden besproken in hoofdstuk 7. De lijst van problemen omvat de fysiologische verschillen tussen rat en mens, methodologische kwesties in de meting van de receptorbezetting, onzekerheid in de schattingen van de preklinische PKPD parameters en een gebrek aan informatie over geneesmiddel-specifieke parameters. Bijvoorbeeld, de voorspellingen van de D_2RO van haloperidol waren lager dan de waarnemingen. Geneesmiddel-specifieke parameters, zoals metabolisme en actieve influx over de BBB kunnen een rol spelen in de te lage voorspellingen van de D_2RO voor haloperidol. Vanwege het gebrek aan informatie over deze processen hebben we deze componenten niet in het translationele model opgenomen. Ondanks de beperkingen en problemen is een algemeen translationeel kader ontwikkeld, dat is gebaseerd op de onderliggende mechanismen en rekening houdt met de verschillende processen die betrokken zijn bij het transport van geneesmiddelen naar de hersenen.

In schizofrenie worden extrapiramidale symptomen (EPS) veroorzaakt door te hoge D_2RO (> 80%) van antipsychotica en dit geldt ook voor catalepsie (CAT) als bijwerking in de rat. Hoewel er een duidelijke relatie tussen D_2RO en bijwerkingen bestaat, is er geen relatie tussen catalepsie en EPS beschreven. In hoofdstuk 6 wordt de relatie tussen CAT scores in de rat en EPS-scores bij de mens op een kwantitatieve manier beschreven. Interessant is dat bij de mens de kans van het optreden van EPS voor 0% D_2RO ongeveer 5% is, wat het effect van placebo op de EPS laat zien. Er kan
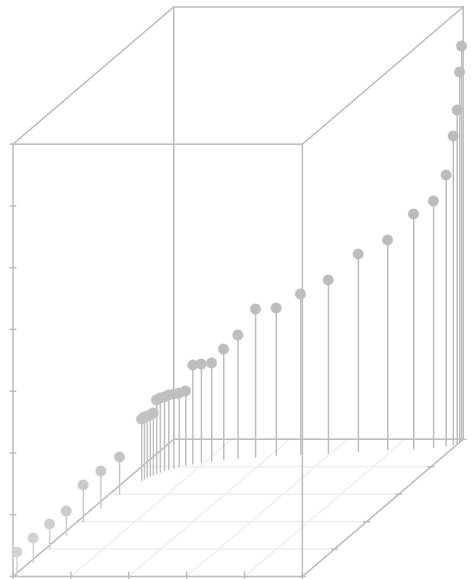
worden voorspeld dat het risico op het optreden van EPS niet meer dan 10% hoger is dan voor placebo, wanneer 86% D_2RO resulteert in minder dan 30% kans op CAT in ratten. Deze methode kan worden gebruikt bij de ontwikkeling van geneesmiddelen om het risico van EPS bij mensen te voorspellen op basis van D_2RO en CAT scores in ratten.

Slotopmerkingen

Toepassingen van dit kader voor modellering omvatten het voorspellen van de receptorbezetting en de bijwerkingen tijdens de beginfase in de ontdekking van geneesmiddelen. Deze methode kan ook worden toegepast voor de selectie van een geschikte eerste dosis in de mens gebaseerd op de farmacokinetiek en farmacodynamiek. Als gevolg van de mechanistische en fysiologische basis is het waarschijnlijk dat deze methode kan worden uitgebreid tot andere indicaties in het centraal zenuwstelsel. Toch zou het opnemen van meer mechanistische componenten, zoals het effect van endogeen dopamine op de binding van geneesmiddelen aan receptoren, en de correctie voor de binding van het radio-ligand tussen verschillende diersoorten, kunnen helpen om de voorspellingen te verbeteren.

Het is echter niet te verwachten dat voorspellende methoden de noodzaak van klinische studies volledig zullen vervangen, al is het aannemelijk dat deze methode kan helpen om meer informatieve en meer efficiënte klinische studies te ontwerpen.

Acknowledgement
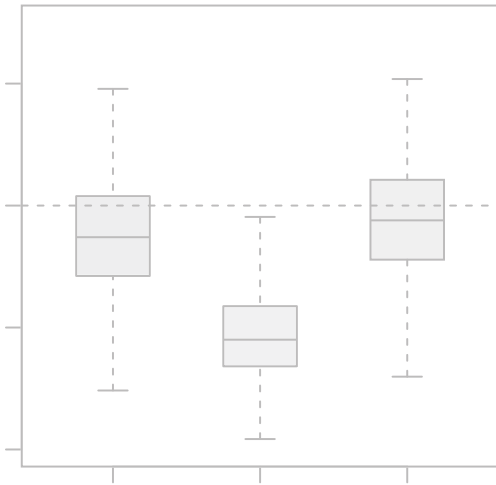
This dissertation would not have been possible without the guidance and the help of several individuals who in one way or another contributed and extended their valuable assistance in the preparation and completion of this thesis.

First and foremost, my utmost gratitude to Dr. Johannes H. Proost, my supervisor, whose sincerity, patience and enthusiasm helped in the completion of this research work.

Prof. dr. Geny M.M. Groothuis, for her unfailing support as my promotor;

Prof. dr. Meindert Danhof, Division of Pharmacology, Leiden-Amsterdam Center for Drug research, Leiden, The Netherlands, for his patience and steadfast encouragement as my promotor;

Prof. dr. A. Rostami, Prof. dr. M.M.R.F. Struys and Prof. dr. B.H.C. Westerink for taking their time to review and appraise this thesis.

Dr. Magdalena Kozielska, my post-doc colleague, for her continuous support, encouragement and for the insights she has shared in this work. I really enjoyed working with you in this project.

Dr. An Vermeulen, Director, Advanced PKPD modeling and simulation, Janssen Research and Development, Belgium, for her scientific support in this project. I admire your leadership qualities.

Mr. Rik de Greef, for his critical assessment and scientific inputs on model development process during various stages of this project.

Dr. Sarah Grimwood and Dr. Hugh A. Barton, Worldwide Research & Development, Pfizer, USA, for their continuous support on predictive modeling, despite of being miles away.

Dr. Cheryl Li, Worldwide Research & Development, Pfizer, USA, for her ideas and encouragement during the initial phase of this work. Dr. Jing Liu, Worldwide Research & Development, Pfizer, USA, for her support in PKPD model development.

Prof. dr. Klaas Poelstra, for his valuable comments and discussion during research meetings.

Prof. dr. A.J. Oldehinkel and Prof. dr. J.V.D. Born (Project management team) for the guidance to manage this project and complete this work on time in a good shape. The GUIDE team for their vision and support for PhD students.

Dr. Douglas Eleveld, for sharing his experience in NONMEM and helping to solve so many practical issues.

Mr. Fokke Dijkstra, for his support on cluster-based NONMEM executions for this project.

Dr. Margot Beukers, for organizing various courses and supporting this project very efficiently as a project manager.

Venkatesh, for the discussions, suggestions, support and especially for providing a friendly environment with kannada songs.

List of Publications

From this thesis

- Johnson M, Kozielska M, Pilla Reddy V, Vermeulen A, Li C, Grimwood S, de Greef R, Groothuis GM, Danhof M, Proost JH. Mechanism-Based Pharmacokinetic–Pharmacodynamic Modeling of the Dopamine D_2 Receptor Occupancy of Olanzapine in Rats, Pharm Res (2011) 28: 2490-2504
- Kozielska M, Johnson M, Pilla Reddy V, Vermeulen A, Li C, Grimwood S, de Greef R, Groothuis GM, Danhof M, Proost JH. Pharmacokinetic–Pharmacodynamic Modeling of the Dopamine D_2 and $5HT_{2A}$ Receptor Occupancy of Risperidone and Paliperidone in Rats, Pharm Res (2012) DOI 10.1007/s1 1095-012-0722-8
- Johnson M, Kozielska M, Pilla Reddy V, Vermeulen A, Barton HA, Grimwood S, de Greef R, Groothuis GM, Danhof M, Proost JH. Translational Modeling in Schizophrenia: Predicting Human Receptor Occupancy. (Manuscript in preparation)
- Johnson M, Kozielska M, Pilla Reddy V, Vermeulen A, Barton HA, Grimwood S, de Greef R, Groothuis GM, Danhof M, Proost JH. Pharmacokinetic-Pharmacodynamic Modeling of Catalepsy in Rats: Predicting Extra-pyramidal Side Effects in Humans. (Manuscript in preparation)

Other publications

- Pilla Reddy V, Kozielska M, Johnson M, Vermeulen A, de Greef R, Liu J, Groothuis GM, Danhof M, Proost JH. Structural models describing placebo treatment effects in schizophrenia and other neuropsychiatric disorders. Clin Pharmacokinet. 2011 Jul 1;50(7):429-50
- Pilla Reddy V, Kozielska M, Johnson M, Vermeulen A, de Greef R, Liu J, Groothuis G.M.M, Danhof M, Proost JH. Modelling and Simulation of the PANSS Time Course and Dropout Hazard in Placebo arms of Schizophrenia Clinical Trials. Clinical Pharmacokinetics 2012;51(4);261-275.
- Pilla Reddy V, Kozielska M, Johnson M, Mafirakureva N, Vermeulen A, Liu J, de Greef R, Groothuis G.M.M, Danhof M, Proost JH. Population Pharmacokinetic-pharmacodynamic modelling of haloperidol in patients with schizophrenia using Positive and Negative Syndrome rating scale (manuscript submitted to Clinical Psychopharmacology).
- Pilla Reddy V, Kozielska M, Suleiman AA, Johnson M, Vermeulen A, Liu J, de Greef R, Groothuis G.M.M, Danhof M, Proost JH. Pharmacokinetic-pharmacodynamic modelling of antipsychotic drugs in patients with schizophrenia:

Part I: the use of PANSS total score and clinical utility (manuscript submitted to Schizophrenia Research).

- Pilla Reddy V, Kozielska M, Suleiman AA, Johnson M, Vermeulen A, Liu J, de Greef R, Groothuis G.M.M, Danhof M, Proost JH. Pharmacokinetic-pharmaco-dynamic modelling of antipsychotic drugs in patients with schizophrenia: Part II: the use of subscales of the PANSS score (manuscript submitted to Schizophrenia Research).
- Pilla Reddy V, Kozielska M, Johnson M, Vermeulen A, Liu J, de Greef R, Groothuis G.M.M, Danhof M, Proost JH. Translational PKPD modelling in schizophrenia: linking receptor occupancy of antipsychotics to efficacy and safety (manuscript submitted to Pharmaceutical Research).
- Kozielska M, Pilla Reddy V, Johnson M, de Ridder F, Vermeulen A, Liu J, Groothuis G.M.M, Danhof M, Proost JH. Sensitivity of individual items of the Positive and Negative Syndrome Scale (PANSS) and items subgroups to differentiate between placebo and drug treatment in schizophrenia (manuscript submitted to Schizophrenia Research).
- Surulivelrajan M, Johnson M, Rao GP, Rajakannan T, Bathala L, Arumugam K, van Hasselt JG, Ramakrishna D. Population pharmacokinetics of Lamotrigine in Indian epileptic patients (manuscript accepted – European Journal of Clinical Pharmacology)

Curriculum Vitae

Martin Johnson was born on 4th October 1977 in Nagercoil, Tamilnadu, India. He completed his higher secondary education in 1995. Then, he started pharmacy education at JSS college of Pharmacy, Ooty, Tamilnadu, India. In 2001, he completed his pharmacy education with a master degree in the division of pharmacology. After the completion of pharmacy education, he started his pharmaceutical research career at Orchid Research Laboratories Limited, Chennai, India. He worked in the department of drug metabolism and pharmacokinetics, at different positions. In 2008 April, he started his PhD project presented in this thesis at the department of Pharmacokinetics, toxicology and Targeting, University of Groningen under the supervision of Dr. Hans Proost.

In 2012 April, he joined Merck, Sharp and Dhome in Oss, The Netherlands as a Clinical PKPD scientist.